Meereswissenschaftliche Berichte

Marine Science Reports

No 114 2020

Hydrographic-hydrochemical assessment of the Baltic Sea 2019

Michael Naumann, Ulf Gräwe, Volker Mohrholz, Joachim Kuss, Marion Kanwischer, Susanne Feistel, Ines Hand, Joanna J. Waniek, Detlef E. Schulz-Bull

"Meereswissenschaftliche Berichte" veröffentlichen Monographien und Ergebnisberichte von Mitarbeitern des Leibniz-Instituts für Ostseeforschung Warnemünde und ihren Kooperationspartnern. Die Hefte erscheinen in unregelmäßiger Folge und in fortlaufender Nummerierung. Für den Inhalt sind allein die Autoren verantwortlich.

"Marine Science Reports" publishes monographs and data reports written by scientists of the Leibniz-Institute for Baltic Sea Research Warnemünde and their co-workers. Volumes are published at irregular intervals and numbered consecutively. The content is entirely in the responsibility of the authors.

Schriftleitung: Dr. Sandra Kube
(sandra.kube@io-warnemuende.de)

Die elektronische Version ist verfügbar unter / The electronic version is available on: http://www.io-warnemuende.de/meereswissenschaftliche-berichte.html

ISSN 2195-657X

Dieser Artikel wird zitiert als /This paper should be cited as:

Michael Naumann[1], Ulf Gräwe[1], Volker Mohrholz[1], Joachim Kuss[1], Marion Kanwischer[1], Susanne Feistel[1], Ines Hand[1], Joanna J. Waniek[1], Detlef E. Schulz-Bull[1]: Hydrographic-hydrochemical assessment of the Baltic Sea 2019. Meereswiss. Ber., Warnemünde, 114 (2020), **doi:10.12754/msr-2020-0114**

Adressen der Autoren:

[1] Leibniz Institute for Baltic Sea Research (IOW), Seestraße 15, D-18119 Rostock-Warnemünde, Germany

E-mail des verantwortlichen Autors: michael.naumann@io-warnemuende.de

Content

Kurzfassung

Die Arbeit beschreibt die hydrographisch-hydrochemischen Bedingungen in der westlichen und zentralen Ostsee im Jahr 2019. Basierend auf den meteorologischen Verhältnissen werden die horizontalen und vertikalen Verteilungsmuster von Temperatur, Salzgehalt, Sauerstoff/ Schwefelwasserstoff und Nährstoffen mit saisonaler Auflösung dargestellt.

Für den südlichen Ostseeraum ergab sich im Winter 2018/2019 an der Station Warnemünde für die Lufttemperatur eine Kältesumme von 18,3 Kd. Im Vergleich belegt er damit den 7. Platz unter den wärmsten Wintern seit Beginn der Aufzeichnungen im Jahr 1948 und wird als sehr mild klassifiziert. Der Sommer 2019 nimmt mit einer Wärmesumme von 283,1 Kd den 24. Platz in der 71jährigen Datenreihe ein und liegt weit unter dem Rekordwert von 2018 (394,5 Kd). Das Langzeitmittel liegt bei 158,6 +/- 68,9 Kd.

Die Situation in den Tiefenbecken der Ostsee war weiterhin geprägt durch stagnierende Bedingungen mit ausgedehnten Sauerstoffmangelgebieten. Die baroklinen Einströme des Hitzesommers 2018 drangen bis in die zentrale Ostsee vor und erwärmten das Tiefenwasser am Gotland Tief im Dezember 2018 auf 8,6 °C, weitere Pulse warmen Wassers folgten im Februar, März und April 2019. Die Salzgehalte und Konzentrationen gelösten Sauerstoffs blieben im Bodenwasser im Wesentlichen unverändert. Im Herbst 2018 und Dezember/Januar 2019 wurden durch drei kleinere barotrope Einströme insgesamt 3.3 Gt Salz in die westliche Ostsee importiert. Im Jahresverlauf 2019 folgten weitere vier schwache Einstromereignisse (April, Juni, September, Dezember). Das letzte umfasste 1 Gt Salzimport. Diese Ereignisse beeinflussten das Tiefenwasser im Arkona Becken bis in südliche Bereiche des östlichen Gotland Beckens. Die Bodensalzgehalte in der zentralen Ostsee blieben nach den „Major Baltic Inflows“ im Zeitraum 2014-2016 auf hohem Niveau, so dass die schwächeren Einströme des Jahres 2019 den Meeresboden nicht erreichten und so auch keine Belüftung des Tiefenwassers der zentralen Ostsee bewirkten.

Die anoxischen und euxinischen Bedingungen in den Tiefengewässern verschärften sich 2019. Dies bestimmte auch die Nährstoffsituation in den Tiefenwässern des nördlichen und westlichen Gotlandbeckens. In der östlichen Gotlandsee stiegen die Phosphat- und Ammoniumkonzentrationen seit 2017 an. Im Jahr 2019 war der Sauerstoffgehalt in allen Tiefenwasser-Referenztiefen gleich Null. Eine Ausnahme bildete das zwischenzeitlich wieder mit Sauerstoff angereicherte Tiefenwasser der Bornholmsee mit etwa 3 ml/l Sauerstoff im März, was zu einem Jahresdurchschnitt von etwa 1,0 ml/l Sauerstoff führte und somit eine deutlich erhöhte Nitratkonzentration auf 6,8 µmol/l im Jahr 2019, eine relativ niedrige Ammoniumkonzentration von 1,5 µmol/l und eine Phosphatkonzentration von etwa 3,8 µmol/l im Jahresdurchschnitt zeigte.

In diesem Report sind die während der Umweltüberwachung im Januar/Februar 2019 ermittelten Konzentrationen chlorinierter und polyzyklischer aromatischer Kohlenwasserstoffe (CKW, PAK) in Gebieten des Fehmarnbeltes/Kieler Bucht bis zur Gotlandsee zusammengefasst. Konzentrationen der CKW und U.S. EPA PAK verringern sich vom Bereich der westlichen Ostsee bis zur Gotlandsee, mit der Ausnahme, dass in der Pommerschen Bucht höchste Konzentrationen für CKW und PAK nachgewiesen wurden (ΣPAH_{sum}: 15,000 pg/l, ΣCHC_{sum}: 31.5 pg/l). Für die Gruppe der CKW wurden die höchsten Konzentrationen für HCB (HCB_{sum}: 6 to 8 pg/L)

ermittelt, gefolgt von DDT/Metabolite (ΣDDT_{sum}: 3 to 7 (15)pg/L) und den PCB_{ICES} (ΣPCB_{sum}: 2 to 9 pg/L); in der Pommerschen Bucht wurden die höchsten CKW-Konzentrationen für DDT/Metabolite ermittelt. Die Daten lassen auf hohe CKW- und PAK-Belastung in den Bereichen Fehmarn Belt/Kiel Bight und der Pommerschen Bucht schließen. Mariner Schiffsverkehr und Flusseinträge von Altlasten aus dem Hinterland über die Oder sind mögliche Ursachen dieser Belastung. Die Bewertung dieser Daten auf Grundlage der UQN der Wasserrahmenrichtlinie zeigt, dass eine schädliche Wirkung auf marine Organismen durch einige der hochmolekularen PAH, insbesondere im Bereich der Pommerschen Bucht, in Betracht gezogen werden muss.

Abstract

The article summarizes the hydrographic-hydrochemical conditions in the western and central Baltic Sea in 2019. Based on the meteorological conditions, the horizontal and vertical distribution of temperature, salinity, oxygen/hydrogen sulphide and nutrients are described on a seasonal scale.

For the southern Baltic Sea area, the Warnemünde station recorded in the winter 2018/2019 a "cold sum" of the air temperature of 18.3 Kd leading to a classification of a mild winter season and a ranking as the seventh warmest winter since the beginning of the record in 1948. The summer "heat sum" of 283.1 Kd ranks on the 24th position over the past 71 years and is far below last year's record of 394.5 Kd. The long-term average is 158.6 +/- 68.9 Kd.

The situation in the deep basins of the Baltic Sea was mainly characterized by stagnation and widespread hypoxic to euxinic areas. The baroclinic inflows of the record warm summer 2018 reached the deep-water of the central Baltic Sea. The Gotland Deep showed record high 8.6 °C at the bottom. Additional inflow pulses of warm water arrived in March and April 2019, but salinity values and concentrations of dissolved oxygen stayed mainly unchanged. Three smaller barotropic inflows occurred from autumn 2018 to December /January 2019 and imported 3 Gt of salt into the western Baltic Sea. In the course of the year 2019 another four barotropic inflows of weak intensity occurred (April, June, September, December). The last one imported 1 Gt of salt. These events propagated from the Arkona Basin up to southern parts of the eastern Gotland Basin. The bottom salinity values stayed on the high level caused by the several Major Baltic Inflows in the time span 2014-2016, so that the 2019 events of weak intensity could not ventilate the bottom near water body in the central basins.

Anoxic and euxinic conditions in the deep waters intensified in 2019. This determined also the nutrient situation in the deep water of the northern and western Gotland Basin. In the eastern Gotland Sea, phosphate and ammonium concentrations were increasing since 2017. In 2019, oxygen was zero in all deep water reference depths. An exception reflected the intermittently re-oxygenated Bornholm Sea deep water with about 3 ml/l oxygen in March, leading to an annual average of about 1.0 ml/l oxygen, thus, showing a clearly increased nitrate concentration to 6.8 µmol/l in 2019, a relatively low ammonium concentration of 1.5 µmol/l, and an annual average phosphate concentration of about 3.8 µmol/l.

This report summarizes obtained data for chlorinated and polycyclic aromatic hydrocarbons (CHC, PAH) for Baltic Sea surface water from the January/February 2019 observation in areas of

the Kiel Bight/Fehmarn Belt up to the Gotland Sea. Overall, concentrations for CHC and U.S. EPA PAH decrease from areas of the western Baltic Sea to the Gotland Sea with the exception of the Pomeranian Bight. There, highest concentrations for PAH and CHC were observed (ΣPAH_{sum}: 15,000 pg/l, ΣCHC_{sum}: 31.5 pg/l). Among the analysed CHC highest concentrations were observed for HCB (HCB_{sum}: 6 to 8 pg/L) followed by DDT/metabolites (ΣDDT_{sum}: 3 to 7 (15)pg/L) and PCB_{ICES} (ΣPCB_{sum}: 2 to 9 pg/L) with the exception that at the Pomeranian Bight concentrations for DDT/metabolites were highest. The data depict high contaminant pressure for the areas Pomeranian Bight and the Kiel Bight/Fehmarn Belt, which indicates higher contaminant sources at these sites. Assessment of the results on the basis of the EQS of the Water Framework Directive shows that concentrations of a number of high molecular weight PAH might be of concern for marine organisms, particularly at the Pomeranian Bight.

1. Introduction

This assessment of hydrographic and hydrochemical conditions in the Baltic Sea in 2019 has partially been produced on the basis of the Baltic Sea Monitoring Programme that the Leibniz Institute for Baltic Sea Research Warnemünde (IOW) undertakes on behalf of the Federal Maritime and Hydrographic Agency, Hamburg and Rostock (BSH). Within the scope of an administrative agreement, the German contribution to the Helsinki Commission's (HELCOM) monitoring programme (COMBINE) for the protection of the marine environment of the Baltic Sea has been devolved to IOW. It basically covers Germany's Exclusive Economic Zone. Beyond these borders, the IOW is running an observation programme on its own account in order to obtain and maintain long-term data series and to enable analyses of the conditions in the Baltic Sea's central basins, which play a decisive role in the overall health of the sea.

The combination of both programmes leads to a yearly description of the water exchange between the North Sea and the Baltic Sea, the hydrographic and hydrochemical conditions in the study area, their temporal and spatial variations, as well as the investigation and identification of long-term trends.

Five routine monitoring cruises are undertaken each year covering all four seasons. The data obtained during these cruises, as well as results from other research activities by IOW, form the basis of this assessment. Selected data from other research institutions, especially the Swedish Meteorological and Hydrological Institute (SMHI) and the Maritime Office of the Polish Institute of Meteorology and Water Management (IMGW), are also included in the assessment.

HELCOM guidelines for monitoring in the Baltic Sea form the basis of the routine hydrographical and hydrochemical monitoring programme within its COMBINE Programme (HELCOM 2000). The five monitoring cruises in January/February, March, May, July/August and October were performed by RV *Elisabeth Mann Borgese*. Details about water sampling, investigated parameters, sampling techniques and their accuracy are given in NEHRING et al. (1993, 1995).

Ship-based investigations were supplemented by measurements at three autonomous stations within the German MARNET environmental monitoring network, the ARKONA BASIN (AB), the DARSS SILL (DS) station and the ODER BANK (OB) station. The latter was in operation from end-April to mid-November 2019 and taken out of service over the winter of 2019/2020. A second system of a new buoy construction more resistant against damages caused by ice was tested in parallel at the Oder Bank position.

Besides meteorological parameters at these stations, water temperature and salinity as well as oxygen concentrations were measured at different depths:

AB:	8 horizons T + S	+	2 horizons O_2
DS:	6 horizons T + S	+	2 horizons O_2
OB:	2 horizons T + S	+	2 horizons O_2

All data measured at the MARNET stations are transmitted via METEOSAT to the BSH database as hourly means of six measurements (KRÜGER et al. 1998, KRÜGER 2000). An acoustic doppler current profiler (ADCP) records current speeds and directions at AB and DS. The ADCP arrays are located on the seabed in some two hundred metres distance from the main stations and protected by a trawl-resistant bottom mount mooring. They are operated in real time: via an

hourly acoustic data link, they send their readings to the main station for storage and satellite transmission. For quality assurance and service purposes, data stored by the devices itself are read retrospectively during maintenance measures at the station once or twice a year.

As a general overview of the state of the Baltic Sea Figure 1 shows the recent hypoxic to euxinic conditions. Oxygen deficiency is one of the major factors influencing the Baltic Sea ecosystem. An overlay of the conditions in spring and autumn are shown in this map, visualising the development during the year 2019. A large extend of bottom water in the deep basins is influenced by hypoxia (black dotted areas) and the situation is more or less stagnant. In May, measurements at the northernmost stations failed due to bad weather. Thus, the northern extend of the hydrogen sulphide areas could not be documented by that time (see missing horizontal red lines in Fig.1).

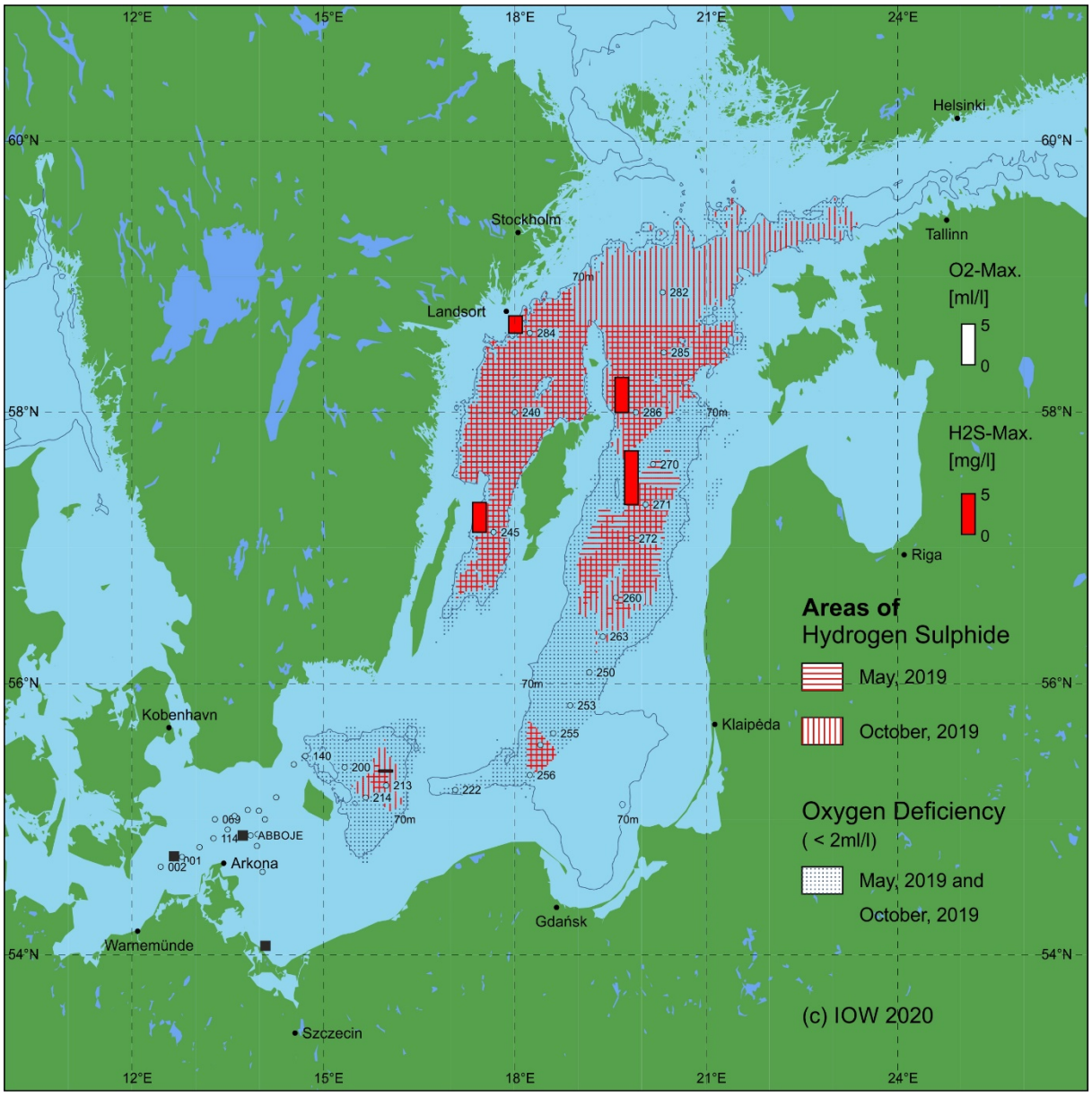

Fig. 1: Location of stations (■ MARNET- stations) and areas of oxygen deficiency and hydrogen sulphide in the near bottom layer of the Baltic Sea. Bars show the maximum oxygen and hydrogen sulphide concentrations of this layer in 2019; the figure additionally contains the 70 m -depth line.

2. General meteorological conditions

The following description of weather conditions in the southern Baltic Sea area is based on an evaluation of data from the Germany's National Meteorological Service (DWD), the Federal Maritime and Hydrographic Agency (BSH), the Swedish Meteorological and Hydrological Institute (SMHI), the Institute of Meteorology and Water Management (IMGW), Freie Universität Berlin (FU) as well as IOW itself. Table 1 gives a general outline of the year's weather with monthly mean temperature, sunshine duration, precipitation as well as the number of days of frost and ice at Arkona weather station. Solar radiation at Gdynia weather station is given in addition. The warm and cold sums at Warnemünde weather station, and in comparison with Arkona, are listed in tables 2 and 3.

According to the analysis of DWD (DWD 2019), 2019 like previous years was too warm, too dry and of a longer sunshine duration than usual. With 10.2 °C, Germany's annual mean **temperature** was 2 K warmer than those of the reference period 1961-1990. Together with 2018 (10.5 °C) and 2014 (10.3 °C), it was the third warmest year since 1881, the beginning of continuous measurements. Across Germany, 11 months showed temperatures above average. An extreme heat wave by the end of July (›40 °C at 23 stations) contributed to this result. Focussing at the Baltic Sea, the meteorological data reflect the same situation (cf. Table 1). Almost all monthly mean temperature values were above average. Only the May values lied below.

The mean amount of **precipitation** in Germany in 2019 was 730 l/m² covering 93 % of the long-term mean value (789 l/m²). In comparison, the 2018 mean value of 590 l/m² represented only 75 % of the long-term mean. The lowest precipitation with 350 l/m² was observed in the Thüringer Becken, central Germany, whereas the highest amount with 2450 l/m² was recorded in the Allgäu region close to the Alpes. In the coastal states along Germany's Baltic Sea coast precipitation ranged from 795 l/m² in Schleswig-Holstein to 595 l/m² in Mecklenburg-Vorpommern.

In Germany, the average annual sum of 1,800 **hours of sunshine** was well above the average of 1,544 hours (+18 %), but below the record-breaking values of the year 2018 with 2,020 hours of sunshine. Schleswig-Holstein showed with 1,655 hours in 2019 (long-term mean: 1,567 hours) the second lowest value of sunshine hours of all German states during 2019. Mecklenburg-Vorpommern recorded 1,795 hours (long-term mean: 1,648 hours), far below its value from 2018, when it reached the nation-wide highest value of 2,085 hours.

At Gdynia station (Gdansk Bight), an annual sum of 385,932 J/cm² of **solar radiation** was recorded. Within a data series covering 63 years back in time (first compiled by FEISTEL et al. 2008, continued to date), this value takes the 24th rank. It is much lower than the long-term maximum in 1959 with 457,751 J/cm², but slightly above the mean value of 374,979 J/cm². The sunniest month in 2019 by far was June (Table 1). With 7,1057 J/m², it takes the fifth place in the long-term comparison of monthly mean values, but still falls well short of the peak value of 80,389 J/m² in July 1994, which represents the absolute maximum of the entire series since 1956. Other top-ranked months of the year are April (on 2nd position) and July (on 4th position). The year's lowest value was 4,127 J/cm² in December, lying in 40th place in the time series and below the long-term average of 4,345 J/cm² for this month. All other months showed solar radiation monthly mean values compared to those of the last 63 years as follows: January rank 29; February rank 15, March rank 31; May rank 58; August rank 23; Sept rank 39; Oct rank 39; Nov rank 56.

Table 1: Monthly averaged weather data at Arkona station (Rügen Island, 42 m MSL) from DWD (2019). t: air temperature, Δt: air temperature anomaly, s: sunshine duration, r: precipitation, Frost: days with minimum temperature below 0 °C, Ice: days with maximum temperature below 0 °C. Solar: Solar Radiation in J/cm² at Gdynia station, 54°31‘ N, 18°33‘ O, 22 m MSL from IMGW (2020). Percentages are given with respect to the long-term mean. Maxima and minima are shown in bold.

Month	t/°C	Δt/K	s/%	r/%	Frost	Ice	Solar
January	1.8	0.6	111	100	**15**	**3**	5943
Febuary	4.1	3.0	**151**	141	3	-	13037
March	5.5	2.6	79	161	3	-	26655
April	7.3	1.3	150	45	-	-	52202
May	10.2	-0.2	84	91	-	-	46826
June	17.4	**3.2**	137	71	-	-	**71057**
July	17.5	0.4	105	43	-	-	61796
August	**18.9**	1.6	113	75	-	-	50719
September	14.9	0.8	77	**173**	-	-	30999
October	10.7	0.7	74	125	-	-	17064
November	6.8	1.3	54	138	-	-	5507
December	4.5	2.2	142	70	3	-	**4127**

Table 2: Sums of daily mean air temperatures at the weather station Warnemünde. The ‘cold sum‘ (CS) is the time integral of air temperatures below the line t = 0 °C, in Kd, the ‘heat sum’ (HS) is the corresponding integral above the line t = 16 °C. For comparison, the corresponding mean values 1948–2018 are given.

Month	CS 2018/19	Mean	Month	HS 2019	Mean
November	0	2.4 ± 6.0	April	0.4	1.0 ± 2.4
December	0.1	20.8 ± 27.8	May	0.2	6.1 ± 7.5
January	17.2	38.3 ± 39.2	June	98.9	24.8 ± 17.1
February	1	30.5 ± 37.3	July	68.1	58.6 ± 36.5
March	0	8.4 ± 12.1	August	108.8	55.3 ± 33.2
April	0	0 ± 0.2	September	6.7	12.3 ± 13.3
			October	0	0.5 ± 1.5
Σ 2018/2019	18.3	100.3 ± 84.3	Σ 2019	283.1	158.6 ± 68.9

Table 3: Sums of daily mean air temperatures at the weather station Arkona. The 'cold sum' (CS) is the time integral of air temperatures below the line t = 0 °C, in Kd, the 'heat sum' (HS) is the corresponding integral above the line t = 16 °C.

Month	CS 2018/19	Month	HS 2019
November	0	April	0
December	0	May	0
January	14.6	June	49.4
February	0	July	56.2
March	0	August	92.4
April	0	September	7.2
		October	0
Σ 2018/2019	14.6	Σ 2019	205.2

2.1 Ice winter 2018/19

For the southern Baltic Sea area, the Warnemünde station shows a **cold sum of 18.3 Kd** referring to the air temperature of the winter 2018/2019. Thus, it is classified as warm winter and ranks far below the latest winter seasons 2017/18 (67.7 Kd), 2016/17 (31.7 Kd) and 2015/2016 (63.5 Kd). Since the year 2012 all values plot below the long-term average of 100.3 Kd. In comparative data from 1948 to date, the Warnemünde winter 2018/19 ranks as the seventh warmest winter. In comparison, the cold sum at Arkona station is with 14.6 Kd (Table 3) slightly lower. Like in Warnemünde, it represents a warmer winter than the previous three winter seasons 2017/18 (53.8 Kd), 2016/17 (27.2 Kd), 2015/2016 (36.1 Kd). Within the last decade, only the winter 2014/2015 showed a lower cold sum of 8.1 Kd. Given the exposed location of the Arkona station at a headland surrounded by water masses at the northernmost coast of Rügen Island, the local air temperature development is under an even stronger influence by the water temperature of the Baltic Sea than at Warnemünde. Thus, winter values at Arkona are frequently higher, while summer values are lower.

The winter season recorded only **25 days of frost and 3 ice days** (daily mean below 0 °C), with a concentration during a cold spell in the end of January (Tab. 1). All winter months from November 2018 to April 2019 showed positive temperature anomalies between 0.6 K in January and 3 K in February at station Arkona in the western Baltic Sea (cf. NAUMANN et al. 2019: 1.3 K in November 2018, 2.1 K in December 2018). Water temperatures stayed in this region well above the freezing point in all offshore areas, only in sheltered lagoons minor icing occurred. According to SCHWEGMANN & HOLFORT (2019), this ice season in the Baltic Sea is classified as weak. Icing occurred only in a short phase from January 20th to February 6th. The **maximum ice coverage** was observed at January 27th with 106 000 km² (Figure 3). This maximum extent of ice corresponds to some 25 % of the Baltic Sea's area (415 266 km²), and was largely centred in the Bothnian Bay, the eastern part of the Gulf of Finland and smaller parts of the Estonian coast between the mainland and the isles of Hiiumaa and Saaremaa in the northern Gulf of Riga as well as the Curonian lagoon. The observed maximum ice extent is classified as mild on place 67 in a time series of 300 years (Figure 2).

The **local ice conditions at the German Baltic Sea** coast were classified as weak by SCHWEGMANN & HOLFORT (2019). A maximum of 18 days of icing was registered in sheltered lagoons (Schlei, Kappeln), starting at January 20th. Lagoons around Rügen Island and Usedom Island followed some days later, showed only 10-14 days of icing and maximum thicknesses of 10-15 cm were reached. Coastal waters remained free of ice. Another measure for the strength of an ice winter is the **accumulated areal ice volume**. Besides various other indices, this index is used to describe the extent of icing, and was introduced in 1989 to allow assessment of ice conditions in German coastal waters (KOSLOWSKI 1989, BSH 2009). The duration of icing, the extent of ice cover, and ice thickness are considered, so as to take better account of the frequent interruptions to icing during individual winters. The daily values from the 13 ice climatological stations along Germany's Baltic Sea coast are summed. The season 2018/19 showed **a very low accumulated areal ice volume** of 0.048 m (SCHWEGMANN & HOLFORT 2019), much less than in previous years like 0.49 m in 2017/18 or 0.16 m (2016/17) and 0.35 m of the season 2015/16 (SCHWEGMANN & HOLFORT 2016, 2017, 2018). It was the seventh weak ice winter in a role. Compared to long-term data the highest values yet recorded are as follows: 26.83 m in 1942; 26.71 m in 1940; 25.26 m in 1947; and 23.07 m in 1963. In all other winters, values were well below 20 m (KOSLOWSKI 1989).

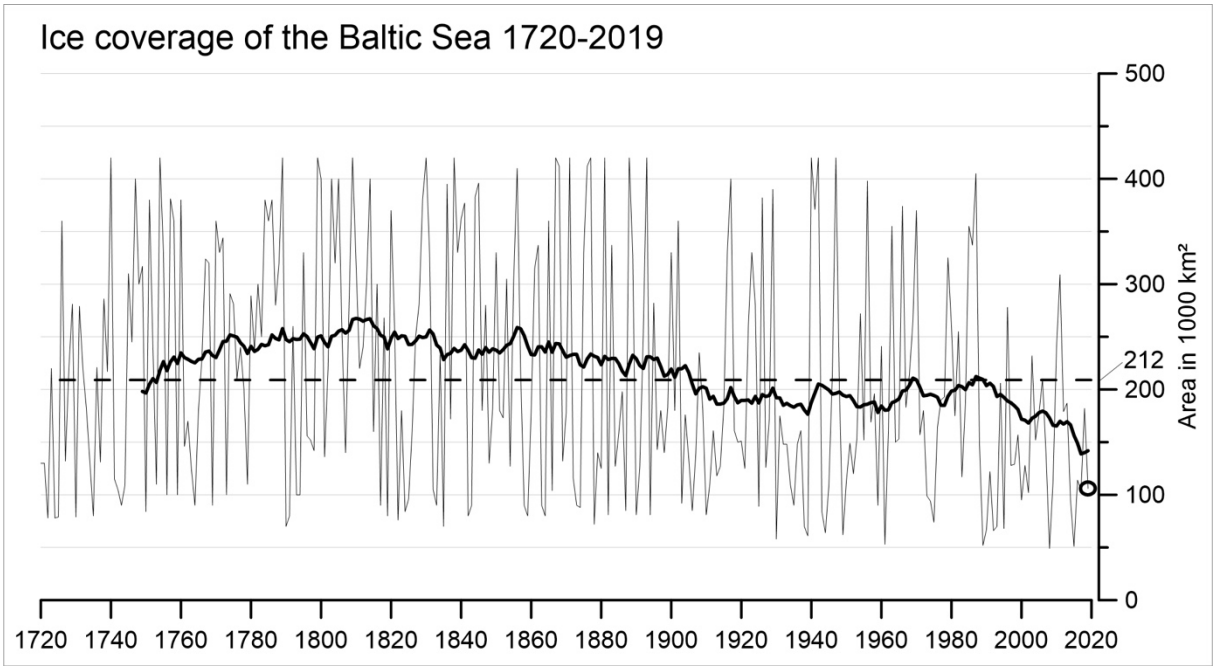

Fig. 2: Maximum ice covered area in 1.000 km² of the Baltic Sea in the years 1720 to 2019 (from data of SCHMELZER et al. 2008, SCHWEGMANN & HOLFORT 2019). The long-term average of 212 000 km² is shown as dashed line. The bold line is a running mean value over the past 30 years. The ice coverage in the winter 2018/2019 with 106 000 km² is encircled.

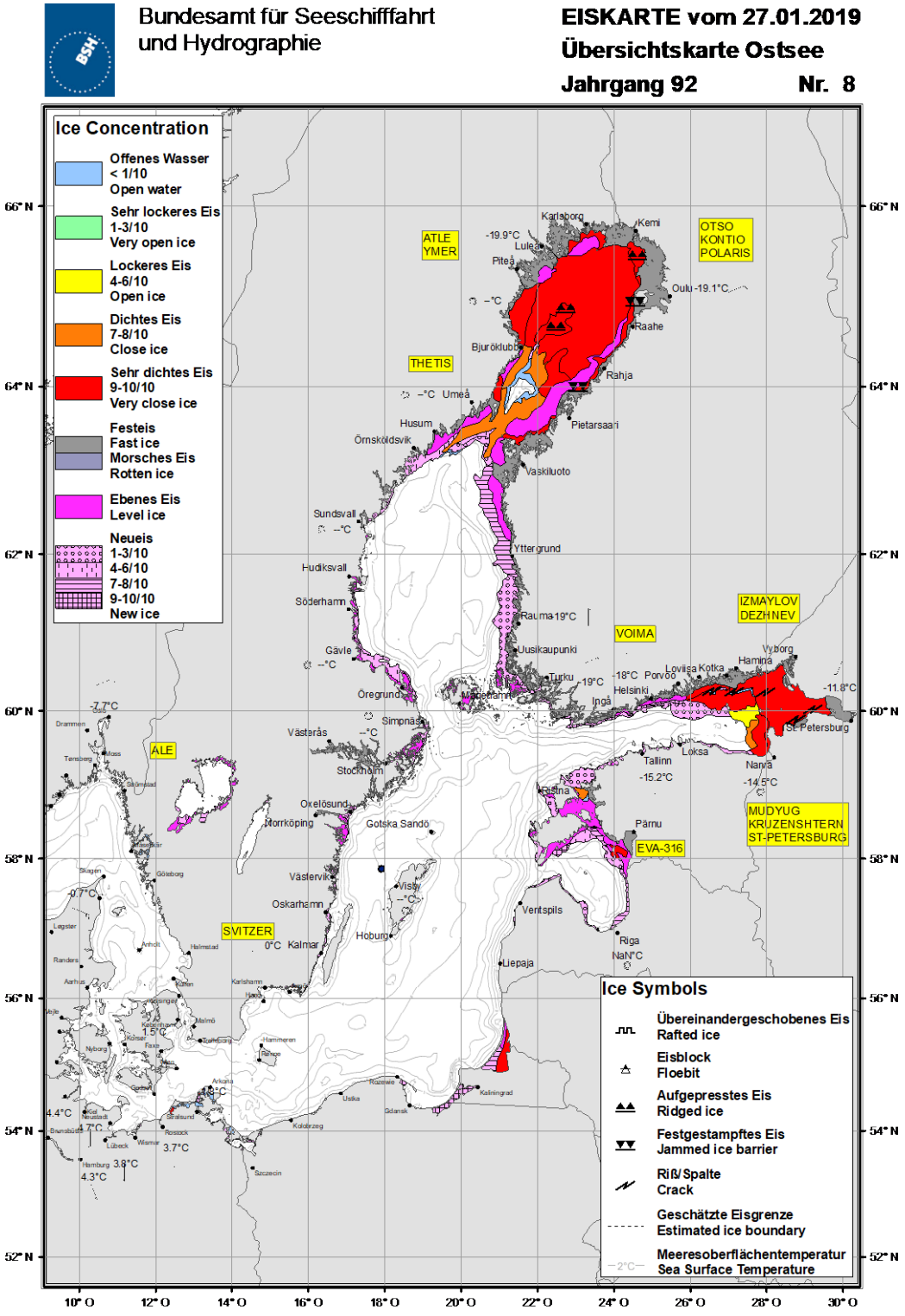

Fig. 3: Maximum ice coverage in the winter 2018/2019 on January 27th – ice concentration in colour code and ice type in symbols (SCHWEGMANN & HOLFORT 2019).

2.2 Wind conditions

During the year 2019, pressure systems and air currents changed not so often as in previous years and south-westerly to westerly **wind** directions dominated the situation, comparable to the climatic mean for this region. North-western to south-western directed winds account for about 62 % of the annual sum and easterly to north-easterly to another 22 % (Figure 5). The annual mean wind speed of 6.95 m/s (Figure 4a) is below long-term average of 7.1 m/s.

Figures 4 to 5 illustrate the **wind conditions at Arkona** throughout 2019. The **trend towards prevailing south-west winds** that began in 1981 (HAGEN & FEISTEL 2008) and continues today is evident over the year. Comparing the east component of the wind (positive westwards) with an average of 2.6 m/s (Figure 4b) with the climatic mean of 1.7 m/s (HAGEN & FEISTEL 2008), westerly winds were in 2019 much stronger than the mean. Only the months January, April and June differ from the long-term trend. In January, westerly winds dominated instead of south-westerly directions. In April, the typical westerly winds were interrupted by a long-lasting phase of easterly winds (Figure 4b). June was characterized by a strong vector compensation of western and eastern winds and generally low intensity (Figure 4a, b). All other months show their typical pattern.

According to the wind-rose diagram (Figure 5), north-western to south-western directed winds account for about 62 % of the annual sum, which is a higher percentage compared to 2018 (50 %), but lower than in 2017 (75 %). Easterly to north-easterly winds account for another 22 % in 2019. The **annual mean wind speed** of 6.95 m/s (Figure 4a) is below the average of 7.38 +/- 0.47 m/s of the last 40 years. The maximum wind speed in that period was reached with 8.41 m/s in 1990. The minimum value occurred in 2018 with 6.5 m/s (based on DWD data, 2020b). Only two high-wind days of over 15 m/s daily mean are registered at January 1st (16.5 m/s) and March 5th (15.8 m/s) of north-western and western direction. In addition to the daily means, a view at high values of hourly means and maximum gusts enables to detect short, but intensive wind events of violent character. Some storms are regionally restricted to some hours only with no significant impact on the daily mean value. However, they can lead to major damages. At March 4th, the maximum gust of the year occurred (31.6 m/s), while the maximum hourly mean of 22.2 m/s was reached at March 15th. All these 2019 maximum values are below previous peak values, for example an hourly mean of 30 m/s in 2000, 26.6 m/s in 2005; and 25.9 m/s (hurricane “Xaver”) in December 2013. This is clearly illustrated by the wind-rose diagram (Figure 6), in which orange and red colour signatures indicate values greater than 20 m/s. They did only slightly occur in 2019 (5 times an hourly mean ›20 m/s at March 15th, March 10th and March 5th all from westerly direction).

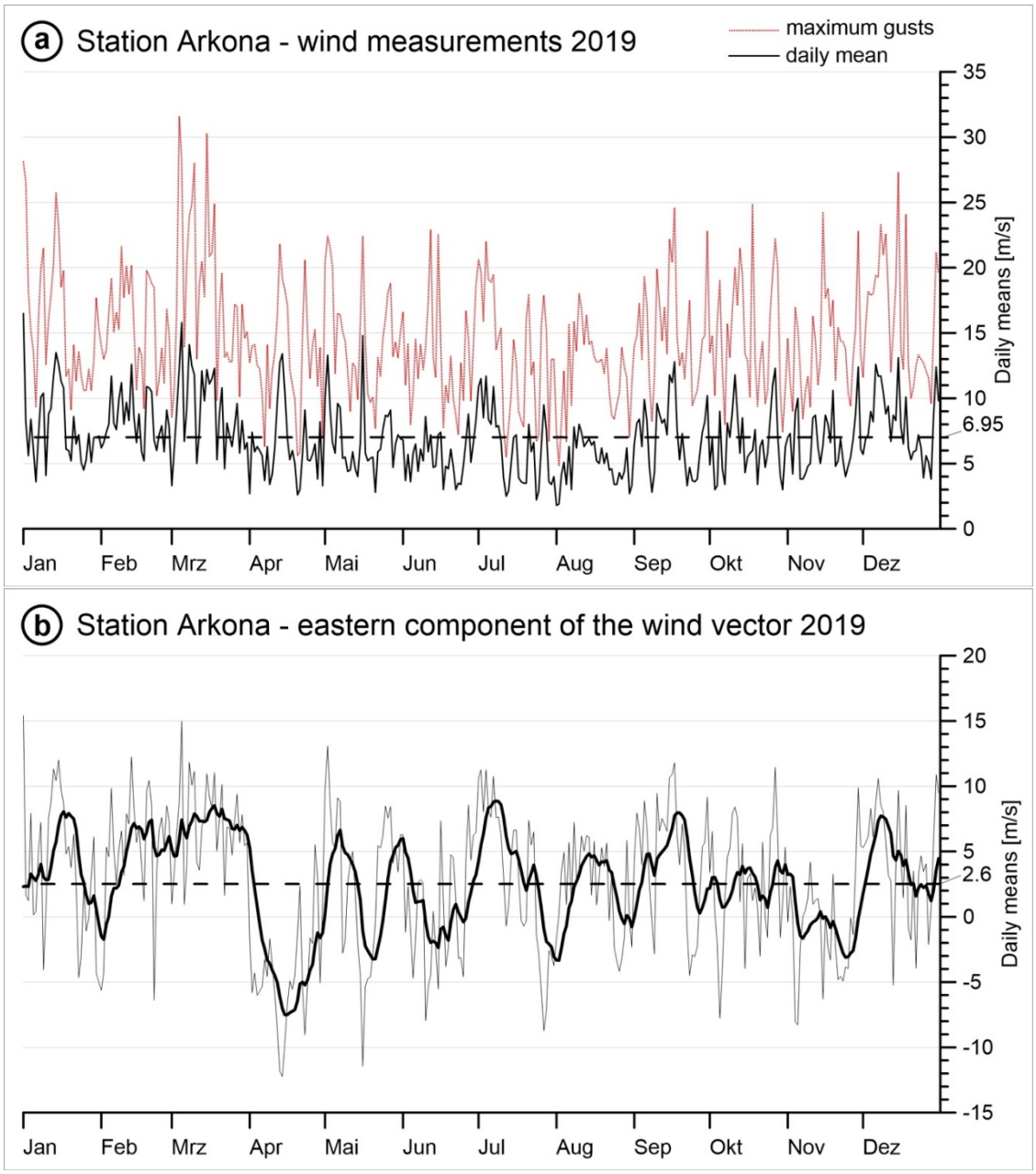

Fig. 4: Wind measurements at the weather station Arkona (from data of DWD, 2020a). a) Daily means and maximum gusts of wind speed, in m/s, the dashed black line depicts the annual average of 6.95 m/s. b) Daily means of the eastern component (westerly wind positive), the dashed line depicts the annual average of 2.6 m/s. The line in bold is filtered with a 10-days exponential memory.

Remarkable hydrographic events caused by wind drift are two storm surges in the beginning of January 2019 which occurred regional at the south-western Baltic Sea coast. Figure 6 shows the air pressure conditions across Europe /North Atlantic, tide-gauge measurements /predictions for Warnemünde and other selected stations. At January 1st, low pressure "Zeetje" (980 hPa) crossed northern Europe with gusts up to 25.8 m/s from north-western direction and the maximum daily wind speed of the year was registered. During nighttime the storm turned to northern direction, but decreased only slightly causing a strong storm surge at the southern Baltic Sea coast at January 2nd (Figure 6a). At Warnemünde a maximum sea level of +1.4 m MSL was reached. Eastwards of the nearby village Markgrafenheide the dike to the Hütelmoor broke and the planned and longtime awaited renaturation of a coastal mire by force of nature took place.

Usually during the last phase of cyclones crossing northern Europe the turn of the wind direction from north-western to northern direction lead to a dramatic decrease in windspeed (below 5 Bft). Northerly storms like “Zeetje” are really rare. One week later, a next storm surge occurred in the western Baltic. At January 9th some hours of strong north-easterly winds of up to 14.7 m/s hourly means (daily mean 10.4 m/s) pushed the water level up again to a maximum of 1.15 m MSL (Figure 6b). Low pressure “Benjamin” (995 hPa) crossed central Europe and a high pressure “Angela” (1035 hPa) across Great Britain lead to this situation. Damages were much less compared to “Zeetje”. Figure 6c shows sea level measurements of stations in the western Baltic Sea (Flensburg – Saßnitz) and additional station on the pathway to the central Baltic Sea (Simrishamn, Lanmdsort and Kronstadt) during the first two weeks of January. Maximum levels of these storm surges occurred in the western Baltic region from Flensburg to Saßnitz at the isle of Rügen.

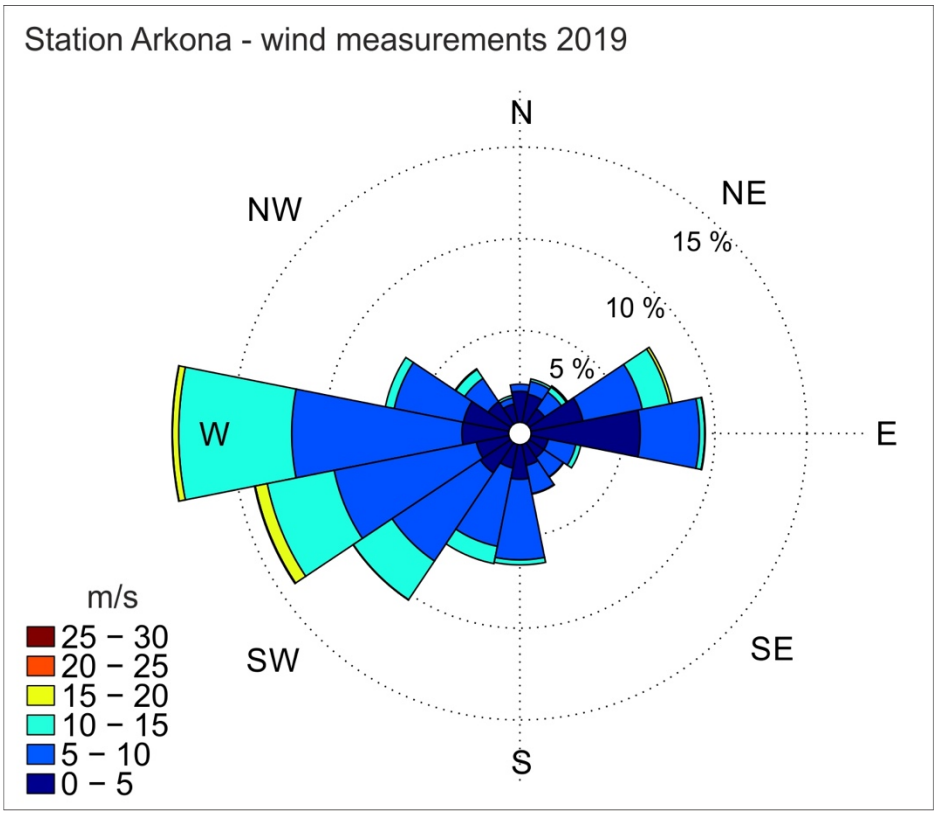

Fig. 5: Wind measurements at the weather station Arkona (from data of DWD 2020a) as windrose plot. Distribution of wind direction and strength based on hourly means of the year 2019.

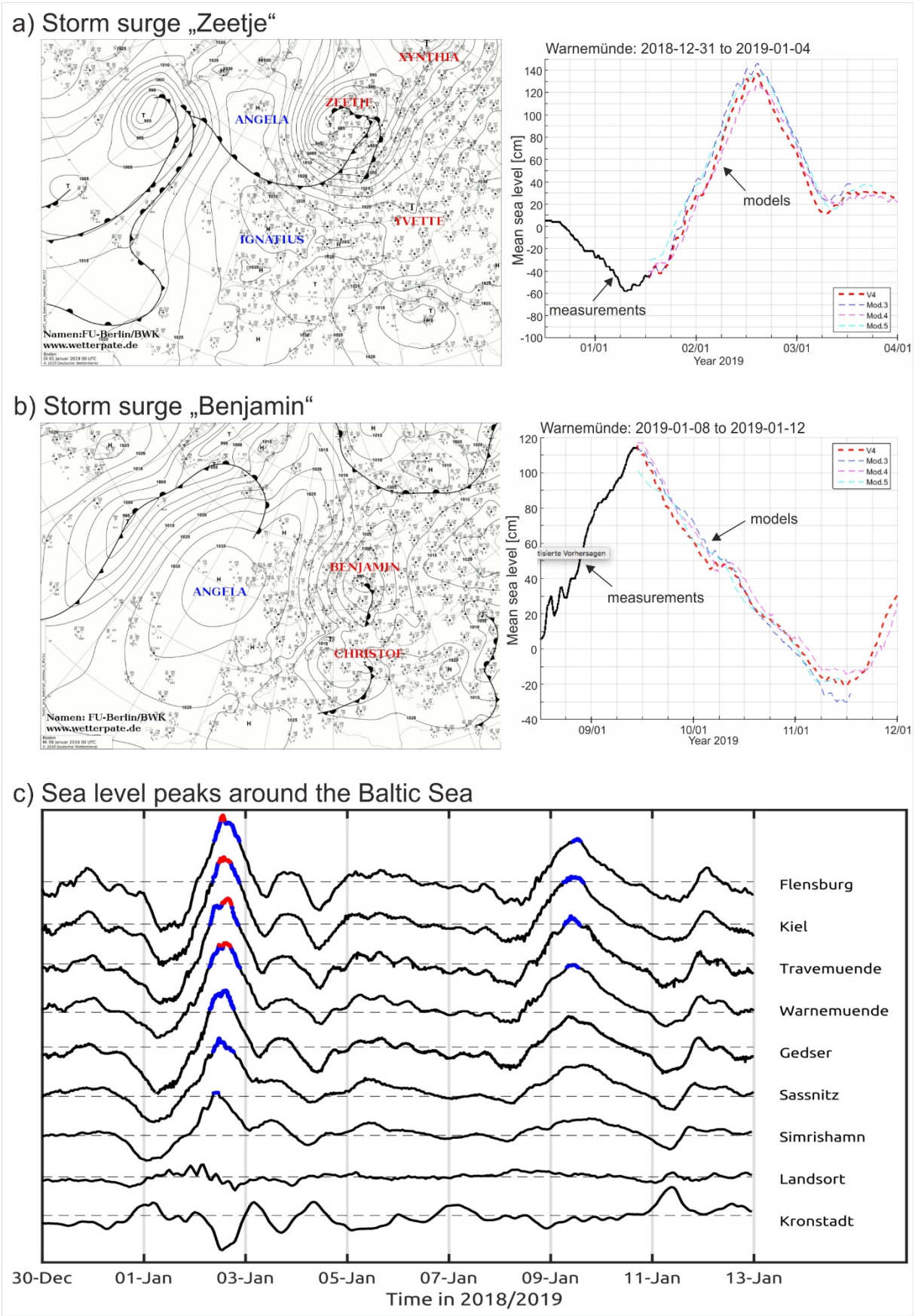

Fig. 6: Sturm surges in January 2019 - a) Storm surge "Zeetje" at 2019 January 2nd, b) Storm surge "Benjamin" at 2019 January 9th, c) sea level peaks at selected tide gauge stations around the Baltic Sea (data: FU Berlin 2020, BSH 2019, Gräwe, U. – personal communication).

3. Water exchange through the straits

3.1 Water level at Landsort

The Swedish tide gauge station at Landsort Norra, south of Stockholm, provides a good description of the mean **water level** in the Baltic Sea (Figure 7a), as it is more or less unaffected by windshift and located in the centre of the large scale seiche of the Baltic Basin (LISITZIN 1974, JACOBSEN 1980, FEISTEL et al. 2008). In the course of 2019, the Baltic Sea experienced five events of rapid sea level rises. They are the result of five barotropic inflow phases of weak category with total volumes estimated between 99 km³ and 162 km³. Rapid rises of the sea level are usually only caused by an inflow of North Sea water through the Sound and Belts. They are of special interest for the ecological conditions of the deep-water in the Baltic Sea. Such events are produced by storms from westerly to north-westerly directions, as the clear correlation between the sea level at Landsort Norra and the filtered wind curves illustrates (Figures 7b). Filtering is performed according to the following formula,

$$\bar{v}(t) = \int_0^\infty \mathrm{d}\,\tau\, v(t-\tau)\exp(-\tau/10\,\mathrm{d})$$

in which the decay time of 10 days describes the low-pass effect of the Sound and Belts (well-documented both theoretically and through observations) in relation to fluctuations of the sea level at Landsort Norra in comparison with those in the Kattegat (LASS & MATTHÄUS 2008, FEISTEL et al. 2008).

At the turn of the year 2018 /2019, the gauge at Landsort Norra recorded a stepwise but continuous increase from -14 cm MSL (December 24th) to +30 cm MSL (January 20th), which comprises a total volume of 123 km³. Calculation methods after MOHRHOLZ (2018), taking hydrographic data of the western Baltic Sea into account - MARNET autonomous stations and tide gauge stations of the Belt Sea and Landsort in the central Baltic Sea-, show a highly saline volume of 38 km³ and salt import of 0.8 Gt.

A general overview about the total import of volume can be calculated with the Landsort tide gauge data and the empirical approximation formula:

$\Delta V/\mathrm{km}^3 = 3.8 \times \Delta L/\mathrm{cm} - 1.3 \times \Delta t/\mathrm{d}$ (NAUSCH et al. 2002, FEISTEL et al. 2008).

It is possible using the values of the difference in gauge level ΔL in cm and the inflow duration Δt in days to estimate the inflow volume ΔV.

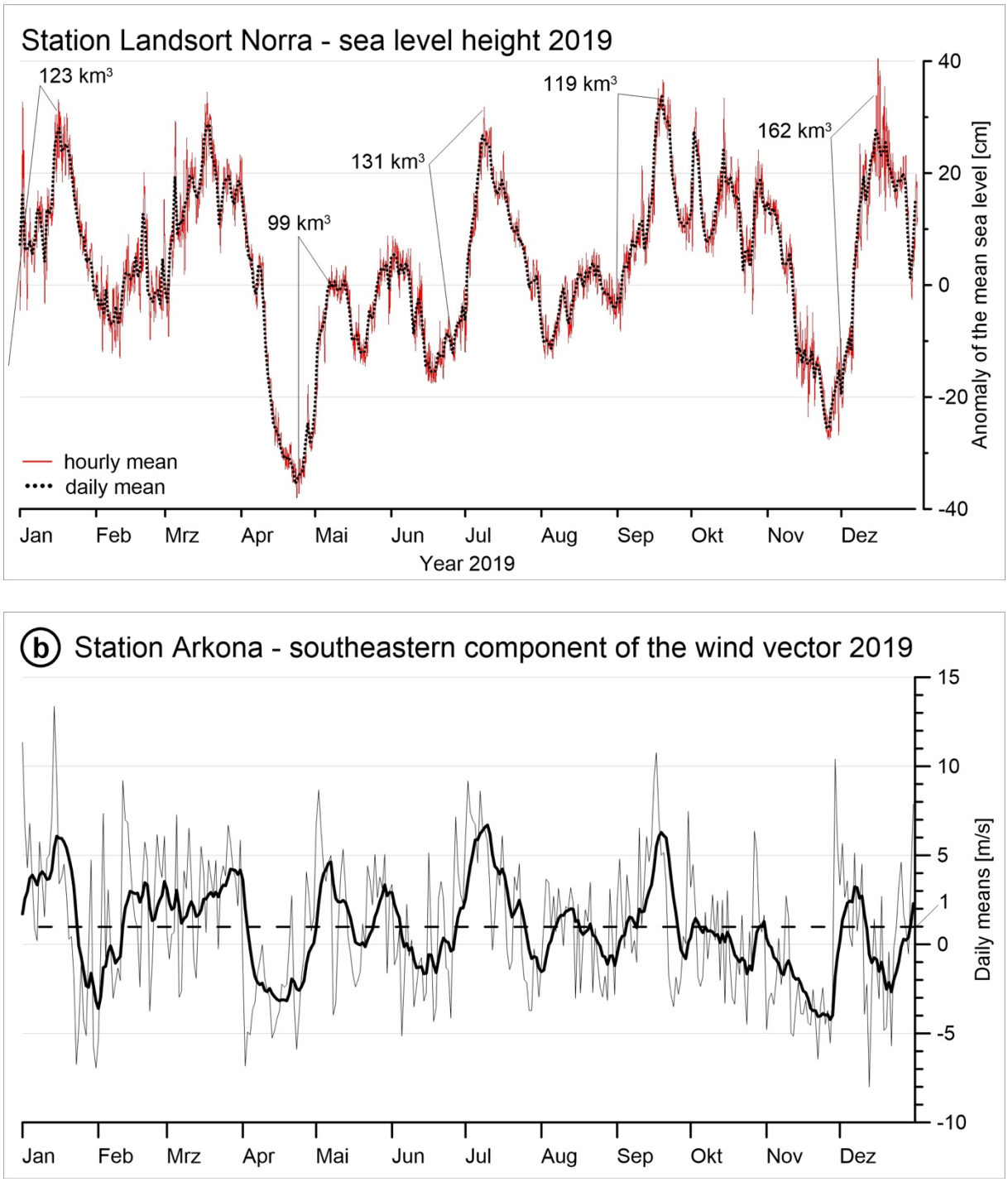

Fig. 7: above (a): Sea level at Landsort as a measure of the Baltic Sea fill factor (from data of SMHI 2020a). below (b): Strength of the southeastern component of the wind vector (northwesterly wind positive) at the weather station Arkona (from data of DWD 2020a). The bold curve appeared by filtering with an exponential 10-days memory and the dashed line depicts the annual average of 1 m/s.

A short system shift to moderate easterly winds (Figure 7b) caused a sea level drop to -12 cm (February 3rd). Afterwards, a stepwise sea level rise to +32 cm MSL (March 17th) occurred due to prevailing moderate-strong westerly winds. In total, a volume of 128 km³ was imported, but only 0.4 Gt of salt. Mid of March a longer outflow period started. At April 23rd the lowstand of the year of -38 cm MSL was reached. A shift back to westerly winds caused a rapid sea level rise up to 4cm MSL (May 7th) with a total volume import of 99 km³ and 0.3 Gt of salt. A next inflow phase

occurred from June 18th (-17 cm MSL) to July 8th (32 cm MSL), due to persistent and strong north-westerly winds in the first week of July (Figure 7b). A total volume of 131 km³ containing 20.5 km³ highly saline water and 0.5 Gt of salt entered the western Baltic Sea. Afterwards outflow conditions occurred again up to the beginning of August. A next event happened from August 30th to September 19th with a sea level rise from -7 cm MSL to 36 cm MSL. Due to a storm, the sea level rose rapidly from September 14th to 19th. This weak inflow imported a volume of 119 km³ (18 km³ highly saline water, 0.4 Gt salt). Steady easterly winds caused a longer outflow period in November, before the latest inflow period of 2019 imported 162 km³ from November 26th to December 16th (Figure 7a). A highly saline volume of 50 km³ and 1 Gt of salt was calculated. This is more or less the lower limit of a weak Major Baltic Inflow.

Compared to previous years of low inflow activity (2017-2018) the year 2019 is characterized as a moderate inflow year. This is visualized in figure 8 by the accumulated inflow volume through the Öresund (SMHI 2020b), where the inflow curve of 2019 runs around the long-term values since the year 1977. In comparison the curve of 2014 is shown, the year in which in December the latest very strong Major Baltic Inflow occurred (MOHRHOLZ et al. 2015).

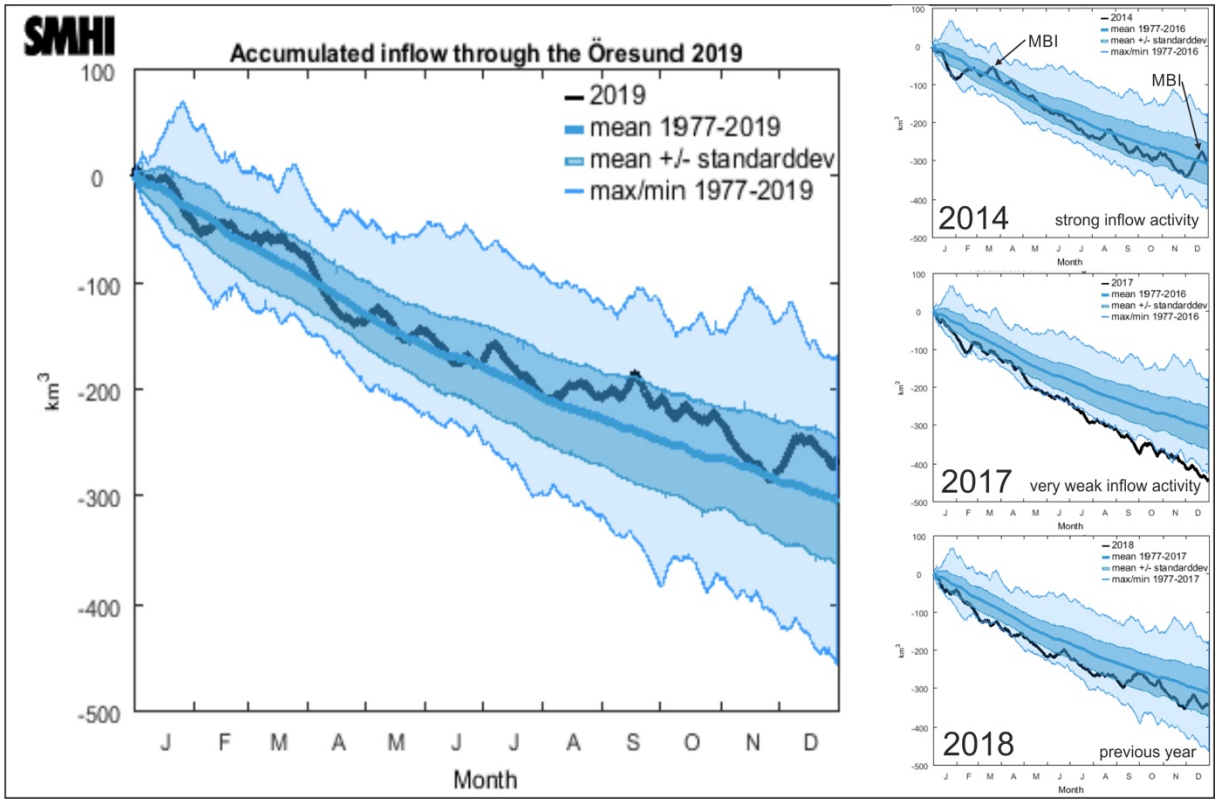

Fig. 8: Accumulated inflow (volume transport) through the Öresund during 2019 in comparison to the previous year and year 2017 of very weak inflow activity and 2014, characterized by the very strong Major Baltic Inflow in December (SMHI 2020b).

3.2 Observations at the MARNET monitoring platform "Darss Sill"

The monitoring station at the Darss Sill supplied complete records during the year 2019. [1]The ADCP provided full data records throughout the observation period. As usual, in addition to the automatic oxygen readings taken at the observation mast, discrete comparative measurements of oxygen concentrations were taken at the depths of the station's sensors using the Winkler method (cf. GRASSHOFF et al. 1983) during the regular maintenance cruises. Oxygen readings were corrected accordingly. Besides a permanent observation of meteorological and hydrographic parameters for the environmental monitoring of the Baltic Sea, the Darss Sill station provides valuable observation data on the dynamics of saltwater inflows in the western Baltic Sea at the major pathway to the deep basins. With their high temporal resolution, they enable the quantification of highly saline water volumes, salt mass and oxygen import (MATTHÄUS 2006, MOHRHOLZ et al. 2015, MOHRHOLZ 2018).

3.2.1 Statistical Evaluation

The bulk parameters defining the water mass properties at Darss Sill were determined from a statistical analysis based on the temperature and salinity time series at different depths.

The **temperature** recordings of 2019 in the surface waters of Darss Sill were close to those of the record-setting years 2014 and 2018. With 10.34 °C the yearly mean temperatures (Table 4) for the year 2019 were slightly lower than in 2014 (10.58 °C) and 2018 (10.54 °C). Annual mean surface-layer temperatures are found on rank 3 of the entire record since 1992 (i.e. in the upper quartile). The standard deviation of the surface-layer temperatures shows lower than average values. This can also be seen in Figure 9 showing the anomaly of the near surface temperature. The climatology was based on the data set of REYNOLDS et al. (2007) and covers the period 1982-2011. This period can be regarded as close to the national reference period (1981-2010). In spring and autumn, the water was up to 1 K warmer than the long-term mean. During June and August/September we see elevated water temperatures of up to 3 K above the long-term mean. However, these values are still lower than the anomalies recorded in 2018 (thin lines in Fig. 9). The temperatures in 17 m and 19 m mark 2019 as the second warmest year since 1992. Only the year 2014 was on average warmer than 2019.

The mean **salinities** and their standard deviations at the station Darss Sill are given in Table 4. The values of the lowermost two sensors reflect the near-bottom variability in salinity, and are therefore a sensitive measure for the overall inflow activity. Different from the year 2016, and the year 2014, both characterized by strong inflow activity, the year 2019 shows an average mean salinity and weak near-bottom salinity fluctuations. The variability at the 19m sensor can also be ranked as average. In contrast, the near surface salinity was well above the long-term mean and shows the fourth highest value since the start of recordings in 1992. These first findings already indicate an average barotropic inflow activity in 2019.

The amplitude and phase shift of the annual cycle were determined from a Fourier analysis of the temperature time series at 7 m depth (surface layer) and at the two lowermost sensors (17 m and

[1] The data gap in December for temperature and salinity recordings in 7 m depth is caused by a delay in data processing and validation. Although the raw data exist, the final validation is still missing. The same issue is causing the lack of oxygen data, since the salinity measurements are needed to compute the relative oxygen saturation.

19 m depth). This method finds the optimal fit of a single Fourier mode (a sinusoidal function) to the data, from which amplitude and phase can easily be inferred as the characteristic parameters of the annual cycle. The results are compiled in Table 5.

Table 4: Annual mean values and standard deviations of temperature (T) and salinity (S) at the Darss Sill. Maxima in bold face.

	7 m Depth		17 m Depth		19 m Depth	
	T	S	T	S	T	S
Year	°C	g/kg	°C	g/kg	°C	g/kg
1992	9.41 ± 5.46	9.58 ± 1.52	9.01 ± 5.04	11.01 ± 2.27	8.90 ± 4.91	11.77 ± 2.63
1993	8.05 ± 4.66	9.58 ± **2.32**	7.70 ± 4.32	11.88 ± 3.14	7.71 ± 4.27	13.36 ± 3.08
1994	8.95 ± 5.76	9.55 ± 2.01	7.94 ± 4.79	13.05 ± 3.48	7.87 ± 4.64	14.16 ± 3.36
1995	9.01 ± 5.57	9.21 ± 1.15	8.50 ± 4.78	10.71 ± 2.27	–	–
1996	7.44 ± 5.44	8.93 ± 1.85	6.86 ± 5.06	13.00 ± 3.28	6.90 ± 5.01	14.50 ± 3.14
1997	9.39 ± 6.23	9.05 ± 1.78	–	12.90 ± 2.96	8.20 ± 4.73	13.87 ± 3.26
1998	8.61 ± 4.63	9.14 ± 1.93	7.99 ± 4.07	11.90 ± 3.01	8.10 ± 3.83	12.80 ± 3.22
1999	8.83 ± 5.28	8.50 ± 1.52	7.96 ± 4.39	12.08 ± **3.97**	7.72 ± 4.22	13.64 ± **4.39**
2000	9.21 ± 4.27	9.40 ± 1.33	8.49 ± 3.82	11.87 ± 2.56	8.44 ± 3.81	13.16 ± 2.58
2001	9.06 ± 5.16	8.62 ± 1.29	8.27 ± 4.06	12.14 ± 3.10	8.22 ± 3.86	13.46 ± 3.06
2002	9.72 ± 5.69	8.93 ± 1.44	9.06 ± 5.08	11.76 ± 3.12	8.89 ± 5.04	13.11 ± 3.05
2003	9.27 ± 5.84	9.21 ± 2.00	7.46 ± 4.96	**14.71** ± 3.80	8.72 ± 5.20	15.74 ± 3.27
2004	8.95 ± 5.05	9.17 ± 1.50	8.36 ± 4.52	12.13 ± 2.92	8.37 ± 4.44	12.90 ± 2.97
2005	9.13 ± 5.01	9.20 ± 1.59	8.60 ± 4.49	12.06 ± 3.06	8.65 ± 4.50	13.21± 3.31
2006	9.47 ± 6.34	8.99 ± 1.54	8.40 ± 5.06	14.26 ± 3.92	9.42 ± 4.71	**16.05** ± 3.75
2007	9.99 ± 4.39	9.30 ± 1.28	9.66 ± 4.10	10.94 ± 1.97	9.63 ± 4.08	11.39 ± 2.00
2008	9.85 ± 5.00	9.53 ± 1.74	9.30 ± 4.60	-	9.19 ± 4.48	-
2009	9.65 ±5.43	9.39 ±1.67	9.38 ± 5.09	11.82 ± 2.47	9.35 ±5.04	12.77 ±2.52
2010	8.16 ± 5.98	8.61 ± 1.58	7.14 ± 4.82	11.48 ± 3.21	6.92 ± 4.56	13.20 ± 3.31
2011	8.46 ± 5.62	-	7.76 ± 5.18	-	7.69 ± 5.17	-
2012	-	-	-	-	-	-
2013	-	-	-	-	-	-
2014	**10.58** ± 5.58	**9.71** ± 2.27	**10.01** ± 4.96	13.75 ± 3.53	**9.99** ± 4.90	14.91 ± 3.40
2015	-	-	-	-	-	-
2016	10.23 ± 5.63	9.69 ± 1.98	9.27 ± 4.59	14.07 ± 3.53	9.11 ± 4.43	15.56 ± 3.45
2017	9.67 ± 5.05	9.40 ± 1.58	9.23 ± 4.54	11.65 ± 2.50	9.20 ± 4.45	12.39 ± 2.61
2018	10.54 ±**6.62**	8.76 ± 1.16	9.24 ± **5.41**	11.58 ±3.23	9.16 ± **5.27**	12.56 ± 3.56
2019	10.34 ±5.25	9.57 ± 1.89	9.83 ± 4.65	12.50 ±2.95	9.83 ± 4.50	13.41 ± 3.07

Table 5: Amplitude (K) and phase (converted into months) of the yearly cycle of temperature measured at the Darss Sill in different depths. Phase corresponds to the time lag between temperature maximum in summer and the end of the year. Maxima in bold face.

	7 m Depth		17 m Depth		19 m Depth	
	Amplitude	Phase	Amplitude	Phase	Amplitude	Phase
Year	K	Month	K	Month	K	Month
1992	7.43	4.65	6.84	4.44	6.66	4.37
1993	6.48	4.79	5.88	**4.54**	5.84	**4.41**
1994	7.87	4.42	6.55	4.06	6.32	4.00
1995	7.46	4.36	6.36	4.12	–	–
1996	7.54	4.17	6.97	3.89	6.96	3.85
1997	8.60	**4.83**	–	–	6.42	3.95
1998	6.39	4.79	5.52	4.46	–	–
1999	7.19	4.52	5.93	4.00	5.70	3.83
2000	5.72	4.50	5.02	4.11	5.09	4.01
2001	6.96	4.46	5.35	4.01	5.11	3.94
2002	7.87	4.53	6.91	4.32	6.80	4.27
2003	8.09	4.56	7.06	4.30	**7.24**	4.19
2004	7.11	4.48	6.01	4.21	5.90	4.18
2005	6.94	4.40	6.23	4.03	6.21	3.93
2006	**8.92**	4.32	7.02	3.80	6.75	3.72
2007	6.01	4.69	5.53	4.40	5.51	4.36
2008	6.84	4.60	6.23	4.31	6.08	4.24
2009	7.55	4.57	7.09	4.37	7.03	4.32
2010	8.20	4.52	6.54	4.20	6.19	4.08
2011	7.70	4.64	6.98	4.21	7.04	4.14
2012	–	–	–	–	–	–
2013	–	–	–	–	–	–
2014	7.72	4.43	6.86	4.17	6.77	4.13
2015	–	–	–	–	–	–
2016	7.79	4.65	6.33	4.33	6.11	4.23
2017	7.00	4.56	6.20	4.31	6.15	4.28
2018	8.82	4.53	**7.31**	4.08	7.18	4.01
2019	7.29	4.47	6.42	4.21	6.22	4.18

Similar to the elevated mean temperatures and lower than average variability in 2019, discussed above, Table 5 shows that also the **amplitudes of the annual cycle** at different depths are close to the long-term average. Thus, 2019 was characterised by high mean temperature but weak annual cycle. Compared to the pronounced phase lag of approximately 0.5 months between the surface and near-bottom temperatures in 2018, the near bottom water temperature follows closely the onset of surface warming. The near bottom temperature at 19 m depth also shows a weak annual cycle.

Table 6: Listing of the minimum and maximum temperature measured at 7m water depth at Darss Sill. Time indicates the date of occurrence. The column Range provides the difference between minimum and maximum temperature. Minima and maxima are highlighted in bold face. For the occurrence of the annual maximum, we indicated in bold face the first ever recording.

Year	Minimum Temperature °C	Time	Maximum Temperature °C	Time	Range °C
1995	0.98	30.12	20.54	05.08	19.56
1996	0.37	27.01	17.65	09.08	17.28
1997	0.16	21.01	22.50	19.08	22.34
1998	2.59	16.12	16.61	10.08	14.02
1999	1.55	18.02	19.84	31.07	18.29
2000	2.65	25.01	17.87	14.08	15.22
2001	2.33	28.03	20.65	29.07	18.32
2002	2.03	13.01	20.24	30.08	18.21
2003	0.09	11.01	21.92	13.08	21.83
2004	1.45	28.02	19.11	20.08	17.66
2005	1.50	13.03	19.79	13.07	18.29
2006	0.40	30.01	22.80	21.07	**22.40**
2007	3.36	25.02	18.70	14.08	15.34
2008	3.12	17.02	19.67	29.07	16.55
2009	1.65	25.02	19.62	10.08	17.97
2010	**-0.44**	05.02	20.33	21.07	20.77
2011	-0.12	05.01	17.94	12.07	18.06
2012	–	–	–	–	-
2013	–	–	–	–	
2014	1.54	09.02	21.61	09.08	20.07
2015	2.95	04.02	18.14	13.08	15.19
2016	1.81	23.01	20.42	28.07	18.61
2017	2.09	19.02	18.61	30.08	16.52
2018	1.11	18.03	**23.10**	04.08	21.99
2019	2.82	26.01	20.91	01.09	18.09

To provide a final statistical measure, we evaluated the minimum and maximum temperatures recorded at 7m water depth at Darss Sill. Table 6 indicates that we recorded in 2019 the 4th warmest winter since 1995. Compared to 2018, the winter minimum temperature was 1.7 K higher (2.82 °C). As already indicated in Tab.4, the year 2019 was one of the warmest, but showed only a weak annual cycle (Tab. 5). The maximum value, recorded in mid-August, was with 18.14 °C well below the high values in 2018. Additionally, the temperature range in 2019 was below the long-term mean.

3.2.2 Temporal development at Darss Sill

Fig. 9 shows the development of water temperature and salinity in 2019 in the surface layer (7 m depth) and the near-bottom region (19 m depth). As in the previous years, the currents observed by the bottom-mounted ADCP in the surface and bottom layers were integrated in time, respectively, in order to emphasize the low-frequency baroclinic (depth-variable) component, plotted in Fig. 11 as a 'progressive vector diagram' (pseudo-trajectory). This integrated view of the velocity data filters short-term fluctuations, and allows long-term phenomena such as inflow and outflow events to be identified more clearly. According to this definition, the average current velocity corresponds to the slope of the curves shown in Fig. 11, using the convention that positive slopes reflect inflow events.

The year 2019 started with well-mixed conditions in temperature and weak stratification in salinity that lasted until mid of April. The lowest temperature of 2.82°C at Darss Sill was recorded on **January** 26 (Table 6). In **mid-April**, easterly winds of up to 15 m/s homogenised the water column at Darss Sill and removed any stratification in temperature and salinity (Fig. 9). The stratification measure, according to MATTHÄUS & FRANK (1992) (Fig. 9 lower panel), was close to zero, indicating the lack of stratification. The outflow of Baltic Sea water further suppressed the build-up of stratification (Fig. 11). At the end of April, the easterly winds weakened and turned to westerly directions. This lead to a reestablishment of the two-layer exchange flow at Darss Sill. For the first time of the year 2019, the near bottom salinities reached 17 g/kg. With the start of **May**, the westerly winds increased to 15 m/s and mixed the entire water column. After this event, the wind calmed down. Until the end of **June**, a thermal stratification could build up with a maximum temperature difference between surface and bottom of 5 K. The two layer flow lead to a decoupling of well oxygenised surface waters from the stagnant bottom waters. End of June, the near bottom oxygen saturation dropped to 60% (Fig. 12).

At the beginning of **July**, the westerly winds increased again to 15 m/s, leading to a collapse of the thermal and haline stratification at Darss Sill. The strong westerly winds caused an inflow over the entire water column (Fig. 11). At the same time, the near bottom salinity increased to 18 g/kg. For the remaining July the inflow conditions persisted. However, stratification at Darss Sill was still present (Fig. 9). Thus, the criteria for a barotropic inflow were not satisfied. The haline stratification was also mirrored in the temperature: inflow of colder and saline bottom water and outflow of warm and brackish surface water. The stratification, at Darss Sill and in the Belt Sea, had negative consequence for the oxygen dynamics. The ongoing bloom in the surface layers, the sinking of organic material to the bottom causing a strong oxygen demand due to remineralisation in the near bottom layers, and the haline and thermal stratification lead to a further lowering of the near bottom oxygen levels. At the end of **August**, values lower than 40% were reached (Fig. 12). The sporadic inflows (MOHRHOLZ et al. 2015) lasted until mid of **October**. Although the bottom salinity reached peak values of 20 g/kg, stratification was still present at Darss Sill. The strong stratification further enhanced and maintained the estuarine circulation: inflow of saline water at the bottom and outflow of low saline water at the surface.

The heat anomaly at the beginning of **September** (Fig. 10), with surface temperatures 4K higher than the long-term mean, further increased the thermal stratification. A bloom at the surface lead to an oversaturation with oxygen (Fig. 12). At the same time, the oxygen saturation in the lower

half of the water column dropped below 20%, due to the shielding effect of the double stratification (halocline and thermocline). At the 10th September, a wind event with 15 m/s again homogenised the water column. Until the end of the year, no significant thermal stratification could build up.

During **November**, easterly winds caused an outflow and a lowering of the filling state of the Baltic Sea. The integrated velocities (Fig. 10) indicate a barotropic outflow over the entire water column. The situation lasted until and of November and lead to a homogeneous water column at Darss Sill, with only brackish water at the measuring station. With the start of **December**, the westerly winds kicked back in and caused a weak barotropic inflow. The near bottom salinities reached peak values of 18 g/kg. The exact classification of this event is still ongoing, since some validated measurements are missing.

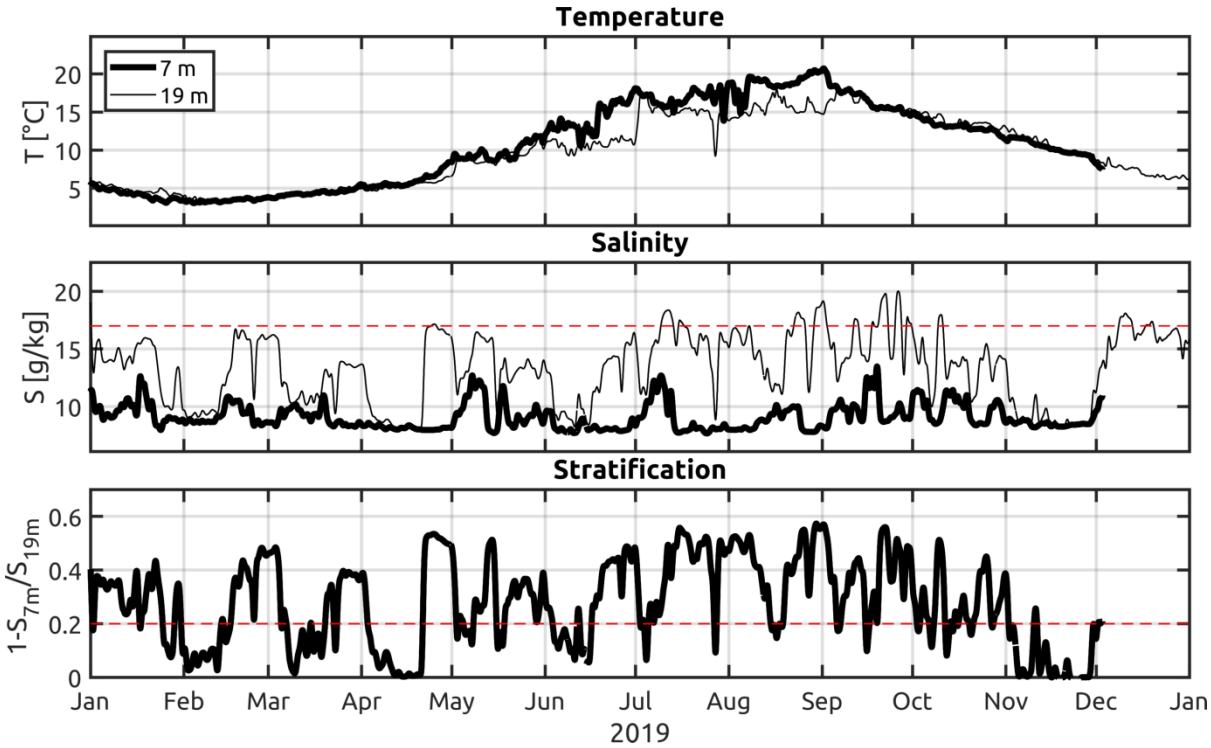

Fig. 9: Water temperature (upper panel) and salinity (middle panel) measured in the surface layer and the near bottom layer at Darss Sill in 2019. The red dashed line indicates the salinity threshold of 17 g/kg.). In the lower panel we show a stratification measure according to MATTHÄUS & FRANK (1992). Here the red dashed line marks the stratification threshold of 0.2.

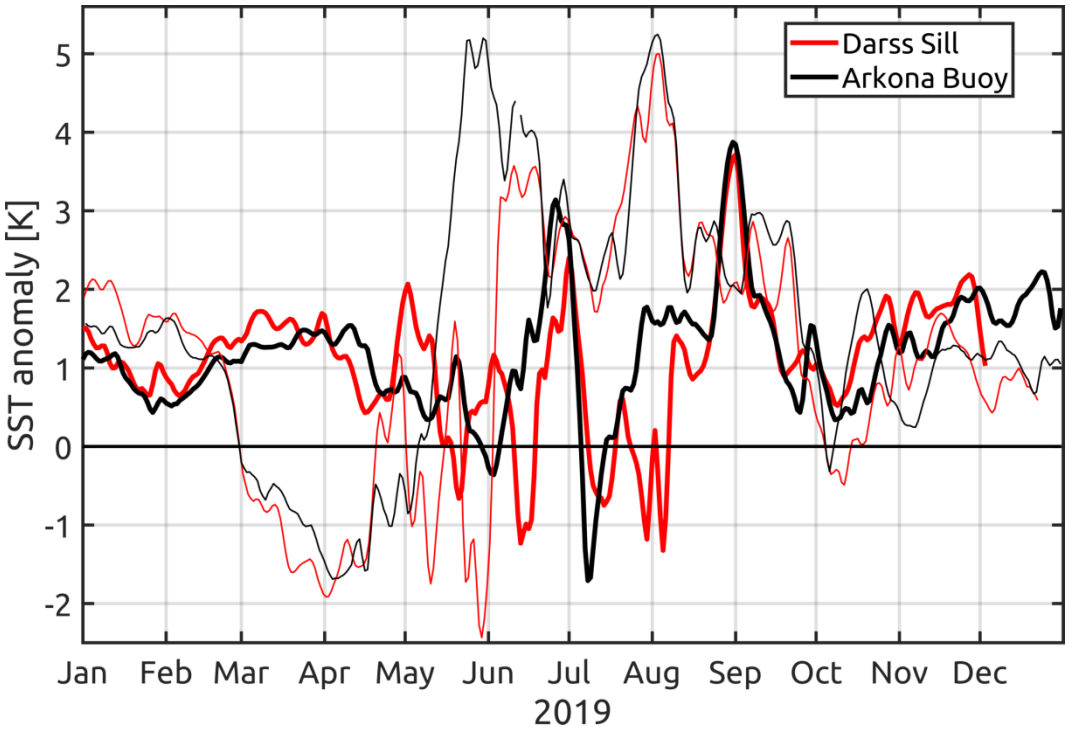

Fig. 10: Deviation of near surface temperature from the climatology at Darss Sill and Arkona Buoy in 2019. The climatology was built for the national reference period 1981-2010 and is based on the dataset of REYNOLDS *et al. (2007). The thin lines show the anomaly from 2018.*

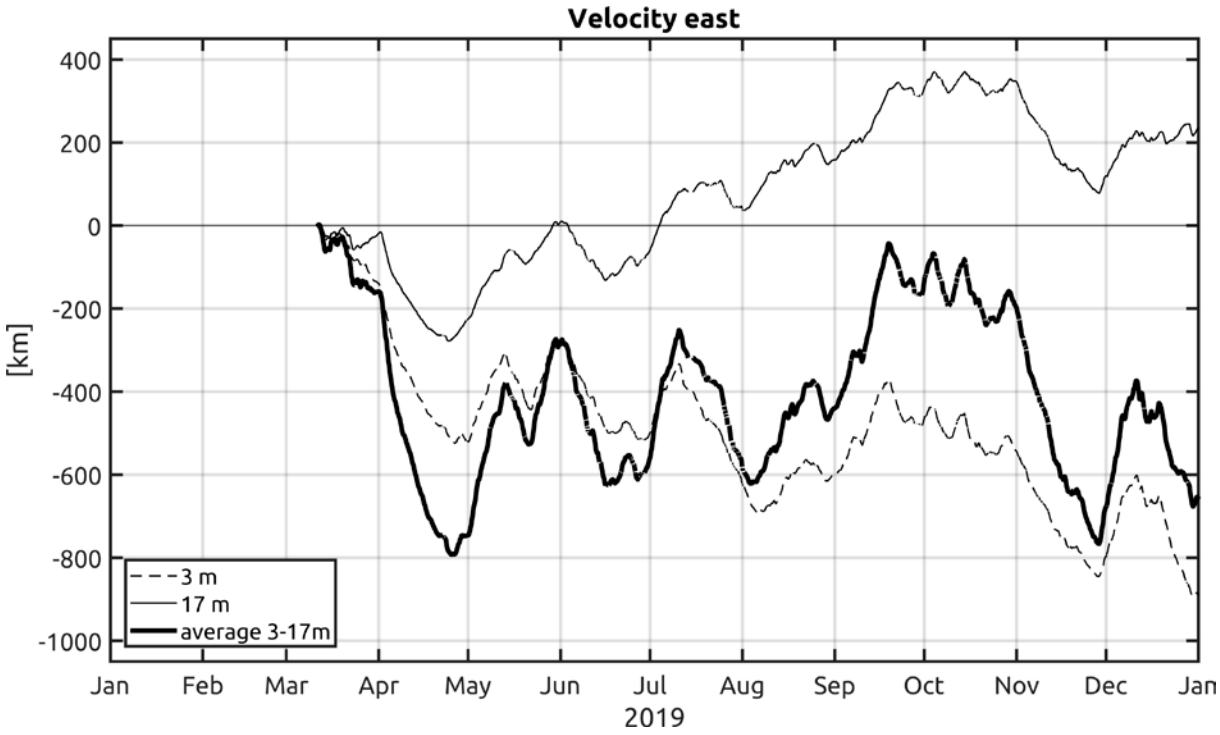

Fig. 11: East component of the progressive vector diagrams of the current in 3 m depth (solid line), the vertical averaged current (thick line) and the current in 17 m depth (dashed line) at the Darss Sill in 2019.

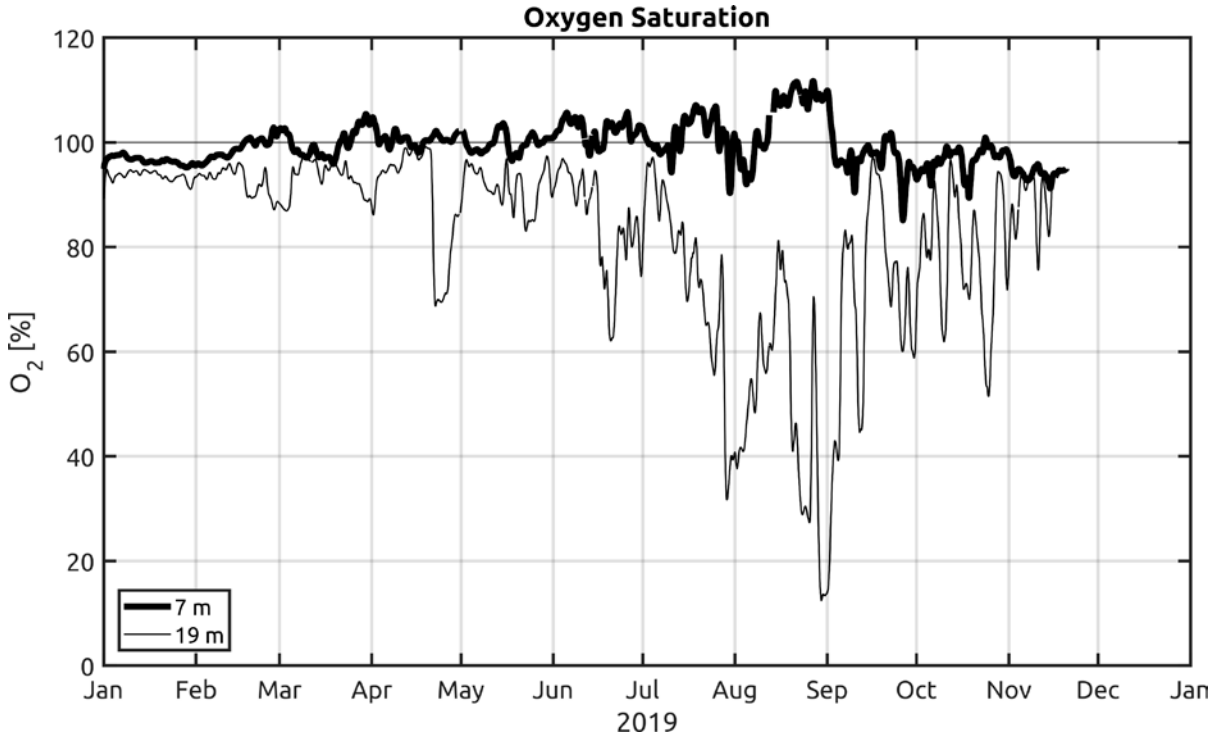

Fig. 12: Oxygen saturation measured in the surface and bottom layer at the Darss Sill in 2018.

3.3 Observations at the MARNET monitoring buoy "Arkona Basin"

3.3.1 Temporal development until summer

The dynamics of saline bottom currents in the Arkona Basin were investigated in detail in the projects "QuantAS-Nat" and "QuantAS-Off" (Quantification of water mass transformation in the Arkona Sea), funded by the German Research Foundation (DFG) and the Federal Ministry for the Environment (BMU). Data from these projects included the first detailed and synoptic turbulence and velocity transects across bottom gravity currents passing through a channel north of Kriegers Flak during a number of medium-strength inflow events (ARNEBORG et al. 2007, UMLAUF et al. 2007, SELLSCHOPP et al. 2006). In a pilot study, BURCHARD et al. (2009) investigated the pathways of these haline intrusions into the Arkona Basin in 2003 and 2004. They identified the channels north of Kriegers Flak and the Bornholm Channel as zones of greatly intensified mixing, and validated their model results using data from the MARNET monitoring network as published in this report series every year. The theoretical analysis of these data revealed a surprisingly strong influence of Earth's rotation on turbulent entrainment in dense bottom currents, leading to the development of new theoretical model that take rotation into account (UMLAUF & ARNEBORG 2009a, b, UMLAUF et al. 2010). The correct representation of the turbulent entrainment rates in numerical models of the Baltic Sea is known to be essential to predict the final interleaving depth and ecosystem impact of the inflowing bottom gravity currents in the deeper basins of the central Baltic Sea. Recently, a comparison of MARNET data with the results of new generation of three-dimensional models with adaptive, topography-following numerical grids has shown that the model was able to provide an excellent representation of the processes in the Western Baltic Sea also during MBIs, taking the record-setting MBI 2014 as an example (GRÄWE et al. 2015).

The Arkona Basin MARNET station is located almost 20 nm north-east of Arkona in 46 m water depth. It supplied complete records during the year 2019. As described in chapter 3.2 for the Darss Sill station, the optode-based oxygen measurements were corrected with the help of the Winkler method, using water samples collected and analysed during the regular MARNET maintenance cruises. Due to some ongoing validation, the oxygen data for December are still missing. Figure 13 shows the time series of water temperature and salinity at depths of 7 m and 40 m, representing the surface and bottom layer properties. Corresponding oxygen concentrations, plotted as saturation values as explained in the previous chapter, are shown in Fig. 14.

Similar to the measurements at the Darss Sill, also at station AB, the first weeks of the year were characterized by a cooling phase that induced gradually decreasing temperatures in the surface layer. The lowest daily mean temperatures of the year, approximately 2.7 °C, were reached on February 02. (Fig. 13), approximately 0.1 K lower than the minimum temperatures measured 7 days earlier at the Darss Sill. While the surface temperatures in the Arkona Basin are largely determined by the local atmospheric fluxes, those at the Darss Sill are more strongly affected by lateral advection, which may explain the observed differences.

The water mass properties in the bottom layer, during the first two weeks of 2019, were determined by the aftermath of small inflow events that had occurred in the second half of December 2018. Peak salinities in the bottom waters reached 21 g/kg. Since the maximum salinities at Darss Sill were below 17 g/kg, during the end of 2018, the water masses must originated from Drogden Sill. Nearly stagnant temperatures around 6 °C suggest that the near-bottom region was decoupled from direct atmospheric cooling. The slowly decaying salinities indicate the draining of the bottom pool of salty and dense inflow waters through the Bornholm Channel (Fig. 13). The oxygen demand due to respiration is usually small during this time of the year due to low water temperatures, and oxygen concentrations therefore did not fall below approximately 80% of the saturation threshold (Fig. 14).

During March, the entire water column was homogeneous in temperature, only a haline stratification existed. With the start of May and an increase in westerly winds up to 15 m/s, some mixing happened in the Arkona Basin. The slight thermal stratification collapsed. Additionally, the bottom salinity dropped to values of 9 g/kg in the bottom waters, which was close to the near surface values. Although it looked like an effect of wind mixing, the drop in bottom salinity was caused by several effects.

To gain some insights in the near bottom dynamics in the Arkona Basin in 2019, we applied the numerical model of GRÄWE et al. (2015), and extended the simulation to the year 2019. The model results suggest three main mechanisms. At first, during April we had mainly easterly winds over the Arkona Basin. At the end of April, the wind turned to westerly directions and increased in wind speed. Thus, during April a permanent outflow was recorded at Darss Sill (Fig. 11). Hence, the supply of saline water was low. Secondly, due to the weak thermal stratification, the wind could effectively erode the halocline. Due to alternations of the wind direction between easterly and westerly winds, at the end of April, some internal oscillations of the halocline were forced. The oscillations had a period of approx. 9 days. In combination, at the last days of April, the

filling of the saline bottom pool was low and the halocline was high on the Swedish side and low on the Rügen side.

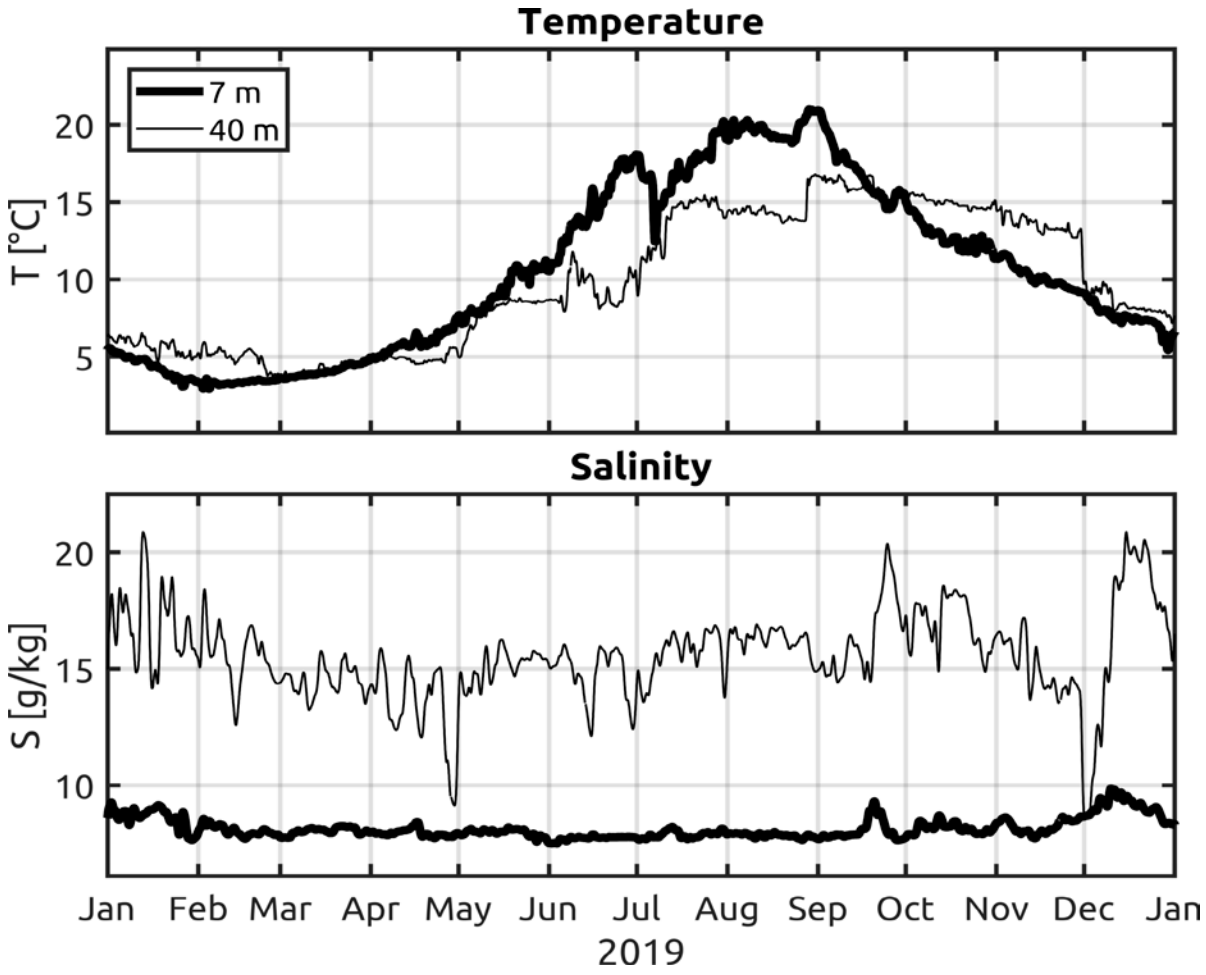

Fig. 13: Water temperature (above) and salinity (below) measured in the surface layer and near bottom layer at the station AB in the Arkona Basin in 2019.

After this event, the wind calmed down. Until the end of **June**, a thermal stratification could build up with a maximum temperature difference between surface and bottom of 10 K. The two layer flow lead to a decoupling of well oxygenised surface waters from the stagnant bottom waters. End of June, the near bottom oxygen saturation dropped to 50% (Fig. 14).

At the beginning of **July**, the near surface temperature dropped from 17 °C to 13 °C (Fig. 13). Since this sudden cooling was not visible at Darss Sill (Fig. 9), atmospheric cooling could be excluded. To get a spatial impression of the western Baltic Sea, we analysed model results of GRÄWE et al. (2015), and satellite derived surface temperature fields. A snapshot of the surface temperature is shown in Fig. 15. Here, we present the conditions at the 9th July. From the 27th June until the 18th July a nearly persistent northwesterly wind, with average wind speeds of 10 m/s was measured. This caused **a massive upwelling** at the southern coast of Sweden. The temperature dropped to 10 °C, the near bottom values at Arkona Buoy. The cold upwelled water reached finally Arkona Buoy, leading to the measured drop in near surface temperature (Fig. 13). Besides occupying

large parts of the Arkona Basin, the upwelling also affected Hanöbukten. We could also detect upwelling filaments at the southern tip of Öland and at the southwestern coast of Bornholm. The upwelling lasted from the 1st of July until the 20th July. During that episode, the temperature difference between the Polish coast (20 °C) and the Swedish coast (10 °C) reached peak values of 11 K.

During the upwelling, the bottom oxygen conditions slightly improved. The upwelled water, with oxygen saturation of 70% (Fig. 14), could be oxygenised at the surface. During the recovery, these water masses sank again to the sea floor and increased the near bottom oxygen saturation to 90%.

The ongoing warming in **August** at a heat anomaly at the start of **September** (Fig. 10) lead to a fast equilibration of the upwelled water with the much warmer air. Finally, on 28th August the annual maximum temperature of 21.14 °C was reached.

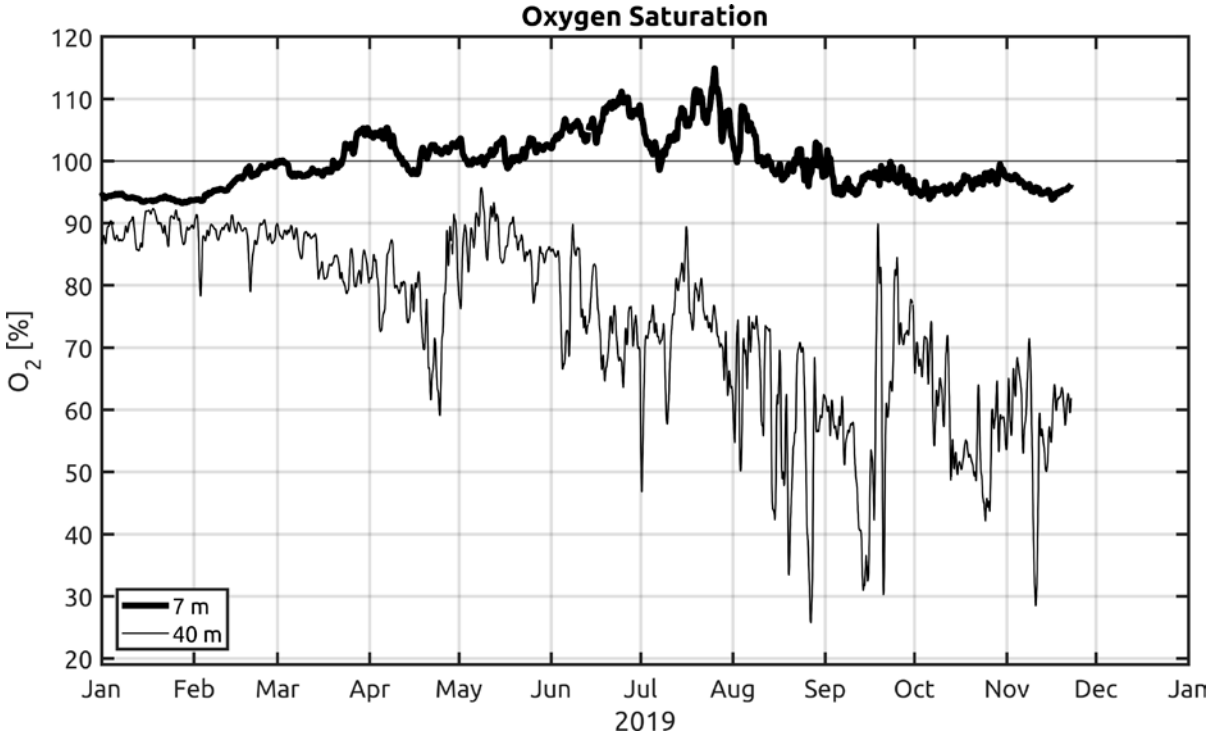

Fig. 14: Oxygen saturation measured in the surface and bottom layer at the station AB in the Arkona Basin in 2019.

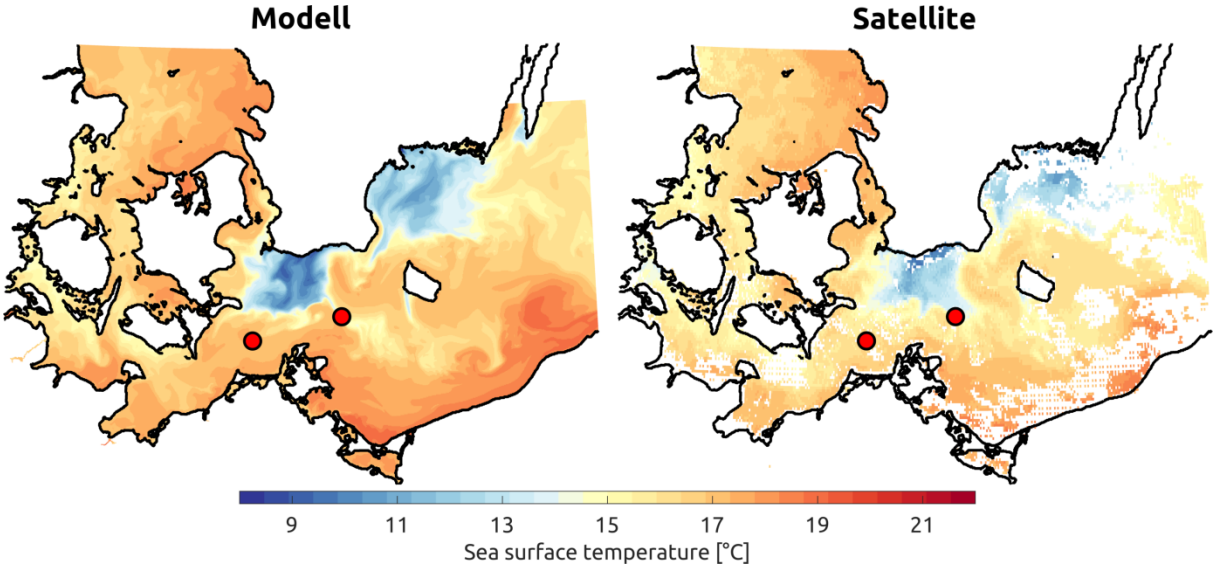

Fig. 15: Comparison of modelled (left) and measured (right) sea surface temperature at July 9 in the western Baltic Sea. The two red dots mark the location of the MARNET stations Darss Sill and Arkona Buoy.

After the warmest day, 28th August, the surface and bottom waters started to cool down. Until the start of December, the bottom waters showed a nearly linear decline, indicating that vertical diffusion was the main driver of the cooling.

At the end of **September**, some highly saline waters reached Arkona Buoy. Peak salinities of 21 g/kg were observed. Since the measurements at Darss Sill only showed peak values of 20 g/kg (Fig. 9), part of the arriving water took the path through the Öresund. Indeed, the numerical model indicates two inflows at Drogden Sill. The first happened from 3rd September to 8th September. Here, the model predicts maximum salinities of 22 g/kg. Shortly after, a second inflow occurred. Now, it lasted from 14th September to the 19th September. During this period, peak salinities only reached 19 g/kg. These inflows in September also left a footprint in the oxygen concentration. The oxygen saturation increased from 30% to nearly 90% (Fig. 14).

At the first day of **December**, the bottom temperature dropped to 8 °C. At the same time, the bottom salinity started to increase to peak values of 21 g/kg. The inflow, already described above, had reached Arkona Buoy. Again, since the measured salinities of 21 g/kg were well above the values recorded at Darss Sill (18 g/kg, Fig. 9), we had another look into the numerical model. The model predicts peak salinities of nearly 25 g/kg during the period 6th December to 9th December. From 23rd December on, the bottom salinities at Arkona Buoy started to decline, indicating that the inflow had passed the station to propagate further into the Bornholm Basin.

3.4 Observations at the MARNET monitoring buoy “Oder Bank”

The water mass distribution and circulation in the Pomeranian Bight have been investigated in the past as part of the TRUMP project (Transport und Umsatzprozesse in der Pommerschen Bucht) (v. BODUNGEN et al. 1995, TRUMP 1998), and were described in detail by SIEGEL et al. (1996),

MOHRHOLZ (1998) and LASS et al. (2001). For westerly winds, well-mixed water is observed in the Pomeranian Bight with a small amount of surface water from the Arkona Basin admixed to it. For easterly winds, water from the Oder Lagoon flows via the rivers Świna and Peenestrom into the Pomeranian Bight, where it stratifies on top of the bay water off the coast of Usedom. As shown below, these processes have an important influence on primary production and vertical oxygen structure in the Pomeranian Bight.

The Oder Bank monitoring station (OB) is located approximately 5 nm north-east of Koserow/Usedom at a water depth of 15 m, recording temperature, salinity, and oxygen at depths of 3 m and 12 m. The oxygen measurements were validated with the help of water samples taken during the regular maintenance cruises using the Winkler method. After the winter break, the monitoring station OB was brought back to service on 27 April 2019, similar to 2018. Starting from that date, the station provided continuous time series of all parameters until 21 November, when it was again demobilized to avoid damage from floating ice.

Temperatures and salinity at OB are plotted in Fig. 16; associated oxygen readings are presented in Fig. 17. Similar to the other MARNET stations, the maximum temperatures that were reached during the summer period were lower than in 2018 (maximum temperature at OB 24.8°C), but comparable with the years 2010, 2013, and 2014, when temperatures of up to 23 °C were observed at station OB. In 2019, the **maximum hourly mean temperature**, reached on 31st August 22.5 °C. As in the previous years, surface temperatures at the monitoring station OB were significantly larger compared to those at the deeper and more energetic stations in the Arkona Basin and the Darss Sill (see Fig. 10 and 13), which reflects the shallower and more protected location of this station.

On average years, there is also a dynamical reason for the stronger warming of the surface layer at station OB, related to the suppression of vertical mixing due to the transport of less saline (i.e., less dense) waters from the Oder Lagoon on top of the more salty bottom waters (e.g. LASS et al., 2001). However, during 2019 the precipitation over most of the Oder catchment was like in 2018: lower than the long-term mean. The missing rain leads to lower water levels in the Oder until late autumn. Thus, the impact of the Oder plume in the Pomeranian Bight was of less dynamical importance in 2019.

One month after the start of service at the end of **May**, a temperature and haline stratification developed. The temperature gradient between the surface and bottom layers varied around 5 K. At the end of **June** peak values of 8 K were reached.

The **massive upwelling** in the Arkona Basin in **July** (see Sec. 4.2) also had consequence for the Pomeranian Bight. The cold upwelled water along the Swedish coast did not make it to the Oder Bank. However, the colder water in the central Arkona Basin, prior to the upwelling 18 °C at Arkona Buoy, was laterally advected to the Pomeranian Bight. The simultaneously occurring downwelling along the southern coast further accelerated the process. The water temperature at the Oder Bank buoy dropped to 18°C, the values from the central Arkona Basin. The downwelling forced a near bottom flow towards the north, leading to a collapse of the thermal and haline stratification at Oder Bank buoy.

From an ecological perspective, the most important consequences of the build-up of stratification and the suppression of turbulent mixing in **June** were the decrease in near-bottom oxygen concentrations due to the de-coupling of the bottom layer from direct atmospheric ventilation. Their impact on the oxygen budget of the Pomeranian Bight becomes evident from Figure 17, showing oxygen concentrations at depths of 3 m and 12 m. For June, a distinct correlation can be identified between increasing oxygen saturation in the surface layer and a decrease in the near-bottom layer, reflecting the effects of primary production and the oxygen demand from remineralisation, respectively.

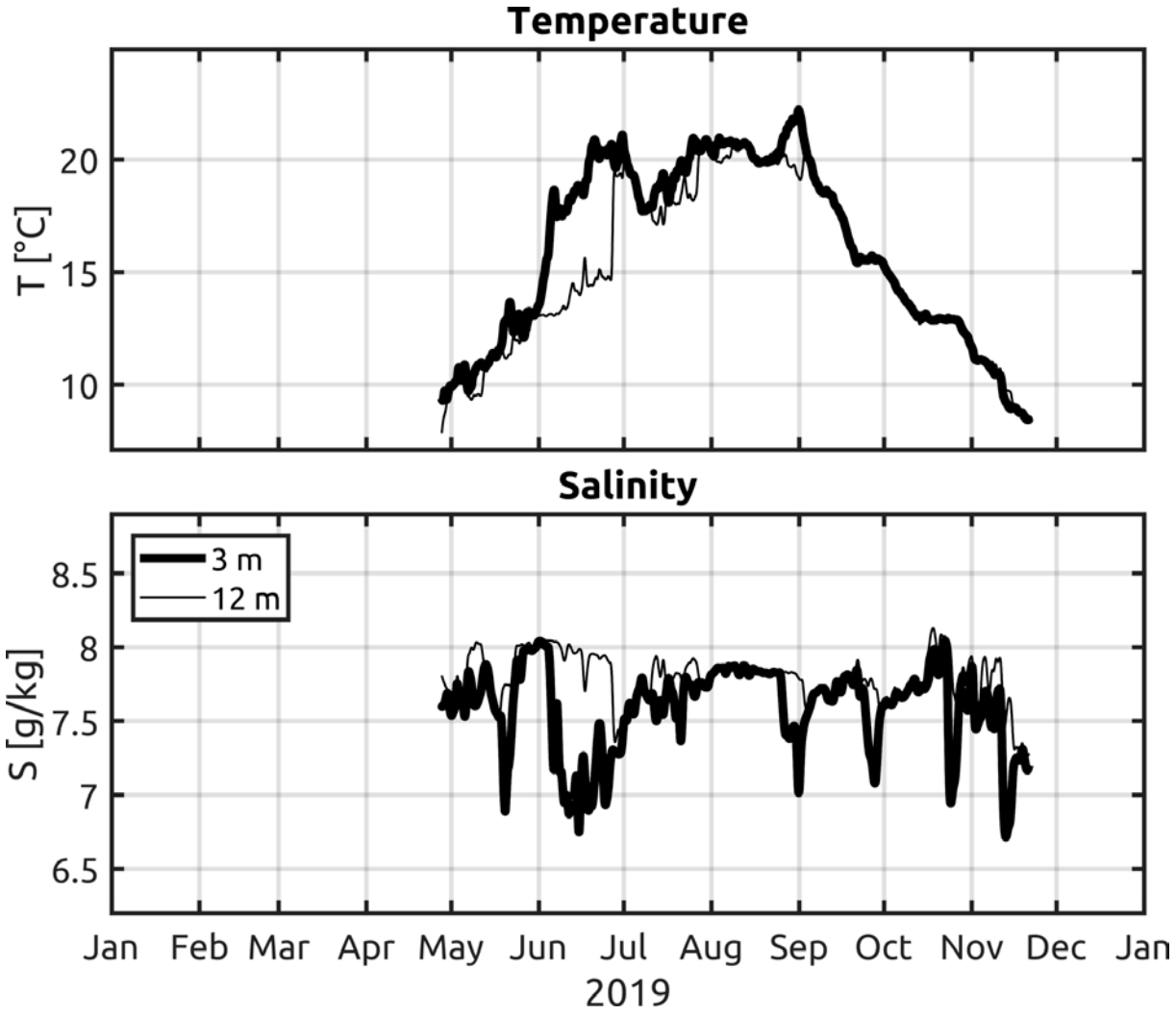

Fig. 16: Water temperature (above) and salinity (below) measured in the surface layer and near bottom layer at the station OB in the Pomeranian Bight in 2019.

Lowest near-bottom oxygen concentrations (see Fig. 17) in 2019 were observed at the end of June, with hourly saturation values as low as 50%. However, the upwelling event in the Arkona Basin helped to recover the near bottom oxygen concentration to nearly surface values of 95%. A second stratification event around the start of **September** resulted in minimum oxygen saturations of 58% (1st September). This event was caused by a calm wind period and a strong

atmospheric warming (Fig. 10), that helped to establish a thermocline in the already 20 °C warm water. The near bottom waters stayed close to the initial temperature level, while the sea surface heated up for additional 4 K. With the onset of a slow atmospheric cooling and some stronger winds, the thermal stratification vanished and near bottom oxygen levels recovered to 90% saturation.

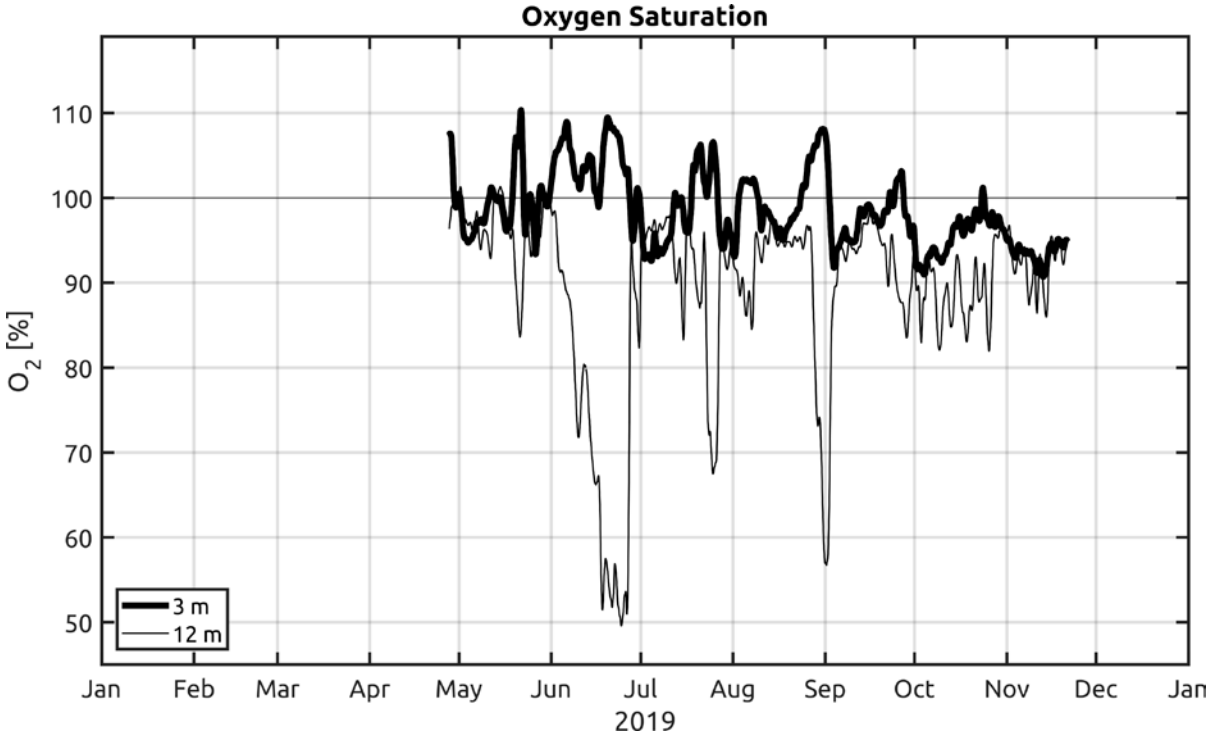

Fig. 17: Oxygen saturation measured in the surface and bottom layer at the station OB in the Pomeranian Bight in 2019.

Finally, it is worth noting that the increase in primary production of biomass in the Oder Lagoon, induced by the lateral transport of lagoon water to station OB, is likely to have resulted in the super-saturated oxygen concentrations that were observed in the surface-layer during all of the above events (Figure 17). Highest near-surface oxygen concentrations with approximately 10% above the saturation level were found in May and June. In addition, the lagoon water is known to export high nutrient concentrations towards the station. This may have resulted in locally increased production rates, which in turn may explain the increased oxygen concentrations in the surface layer. The correlation between the oxygen increase in the surface layer and the decrease in the near-bottom layer points at increased oxygen consumption rates induced by the decay of freshly deposited biomass (“fluff”).

4. Results of the routine monitoring cruises: Hydrographic and hydrochemical conditions along the thalweg

The routine monitoring cruises carried out by IOW provide the basic data for the assessments of hydrographic conditions in the western and central Baltic Sea. In 2019, monitoring cruises were performed in February, March, May, early August and October.

4.1 Water temperature

Snapshots of the temperature distribution along the Baltic thalweg transect obtained during each cruise are depicted in Figures 18 and 19. This data set is complemented by monthly observations at central stations in each of the Baltic basins carried out by Sweden's SMHI. Additionally, continuous time series data are collected in the eastern Gotland Basin. Here the IOW operates two long-term moorings that monitor the hydrographic conditions in the deep water layer. The results of these observations are given in Figures 20 and 23.

The **surface temperature (SST)** of the Baltic Sea is mainly determined by local heat flux between the sea surface and the atmosphere. In contrast, the temperature signal below the halocline is detached from the surface and the intermediate winter water layer and reflects the lateral heat flows due to salt-water inflows from the North Sea and diapycnal mixing. The temperature of the intermediate winter water layer conserves the late winter surface conditions of the Baltic till the early autumn, when the surface cooling leads to deeper mixing of the upper layer.

In the central Baltic, the development of vertical temperature distribution above the halocline follows with some delay the **annual cycle of atmospheric temperature** (cf. chapter 2). As in the previous year the winter of 2018/2019 started very mild. Only the **January** 2019, that depicted a temperature anomaly of +0.6 K, was close to the long term mean. During **February** and **March** the mean air temperature was considerably warmer (›2.6K) than the long term mean. Thus, the surface cooling of the Baltic was strongly reduced. **The sea surface temperatures remained well above the density maximum**. The higher than normal temperatures are also reflected by the low maximum ice coverage of 106,000 km², which was only half of the long-term average. The higher than normal air temperature was continued during the spring. Only the **May** depicted air temperatures close the long term mean. The air temperatures remained at a higher than normal level for the rest of the year. From June to December 2019, the monthly air temperature anomaly ranged between 0.4 and 3.2 K (cf. chapter 2).

The **deep water conditions** in the central Baltic in 2019 were mainly controlled by **subsequent minor inflow events** of 2016 to 2019 (MOHRHOLZ 2018). The most recent barotropic inflow events were observed in October and December 2018, and in December 2019.

At the beginning of **February** the winter cooling of the surface layer has reduced the surface temperatures in the Baltic to 3 to 4°C. However, as a result of the warmer than average winter (compare chapter 2), surface temperatures were well above the long term mean for February. The lowest surface temperatures of about 2.5 to 3.0°C were observed on the Belt Sea and the shallow areas of the Mecklenburg Bight. This was well above the climatological mean of 1.8°C, but below the February values of 2018. Surface temperatures in the Arkona Sea were slightly higher. At the

central station TF0113 the SST was about 3.2°C (climatological mean 1.9°C). **In the entire Baltic the surface temperatures were well above the density maximum.** Thus, further surface cooling will force temperature driven convection. However, in the central Baltic the temperature driven mixing has not homogenized the surface layer and the former winter water layer completely, as it is usually observed in February. Surface patches of cooler and less saline water, and slightly warmer and more saline water lenses right above the main halocline modified the stratification. The main thermocline at station TF271 in the eastern Gotland Sea was found at a depth of 60 m, and coincides with the permanent halocline. A secondary thermocline was observed at 35m depth. The temperature in the surface layer was 3.4°C. Below 35m the temperature increased to 4.0°C. The unusual stratification above the permanent halocline may be caused by high river discharges and patches of inflowing saline water, which were not dense enough to penetrate the main halocline of the central basins. Generally, the surface temperatures in the central Baltic between 3.2 and 4.0°C were about 1 to 1.5 K above the long term average and slightly below the extreme warm temperatures in February 2018.

The temperature distribution below the halocline reflects the impact of the inflow events of saline water from the North Sea. A series of small inflows between September 2018 and January 2018 transported about 113 km³ of warm saline water into the western Baltic. **The last of these minor inflows stopped on 18th January.** These inflows dominated the bottom temperature distribution in the Arkona and the Bornholm Basin. Waters of the January inflow covered a 15m thick bottom layer in the centre of the Arkona Basin, with a bottom temperature of 5.9°C. Baroclinic late summer inflows and the minor inflows in autumn 2018 have flushed the halocline of the Bornholm Basin with saline water of different temperatures. The deep water in the Bornholm Basin depicted in February a very patchy temperature distribution. Whereas the bottom layer is covered by the warmer and more saline waters from the autumn inflows, the cooler January inflow is spreading in the halocline of the western Bornholm basin. It has not reached the Slupsk Sill. Parts of the old halocline water were shifted eastward and overflowed the Slupsk Sill. The maximum temperature in the halocline of the Bornholm Basin was about 9.5°C. The deep layers of the Bornholm Basin were also covered by the warm and highly saline waters from recent inflow events. Here, the bottom temperature was about 9.2°C. Due to mixing with ambient water in the Slupsk Sill overflow the temperature of the inflowing water patches decreased eastward. In the Slupsk Furrow bottom water temperatures of 8 to 8.5°C were observed. Between the eastern outlet of the Slupsk Furrow and the entrance of the eastern Gotland Basin some warm water plumes were observed in the bottom layer. These plumes spread eastward and originated from pulse-like overflows of the eastern sill of Slupsk Furrow. Due to their relatively high density the warm water penetrated the permanent halocline in the Gotland Basin and interleaved at depths of 100 to 140m. The deep water in the Gotland Basin was still covered by the warmer inflow waters of the recent years. However, the bottom temperature at station TF 0271 has recently increased to 7.6°C, about 0.7K above the value observed in February 2018. The bottom water temperature in the Farö Deep of 6.8°C did not change since the last year. It was 0.1K higher than the temperature in the eastern Gotland Basin at 120m, which is the sill depth between both locations. Thus, the bottom layers of the Farö Deep were not reached by eastward spreading waters from the Gotland Basin.

The unusual warm air temperatures in February and March 2019 led to warming of the surface layer in the western and partly the central Baltic, whereas the SST further decreased in the northern parts of the Baltic Proper. In the western Baltic the surface temperatures observed during the monitoring cruise in March ranged between to 3.9 and 4.5°C, which was about 1.5 to 2.0 K above the climatological mean. As a result of the early warming, the surface temperature of the western Baltic was still well above the temperature of density maximum, and enabled the very early onset of seasonal temperature stratification. In the eastern Gotland basin the SST was about 3.2°C, only 0,2 K cooler than in February. Towards the northern Baltic the SST decreases dropped to values close to the temperature of maximum density. In the northern Gotland Basin the SST was about 2.3°C.

Below the surface layer the ongoing eastward advection of the warm water body from the recent inflows caused some changes. The warmer water layer at the bottom of the Arkona Basin vanished. The patchy temperature distribution in the Bornholm Basin was reduced by lateral mixing and advection. The bottom water temperature in the Bornholm basin of 8.5°C was slightly reduced, compared to the value of February. The warm halocline layer in the Bornholm basin was further cooled by the waters from the January inflow and partly due to entrainment of surface layer water. A significant part of the halocline water left the basin via the Slupsk Sill and formed the new cooler bottom water layer in the Slupsk Furrow. Here, the bottom water temperature decreased to 7.6°C. The former deep waters from the Slupsk Furrow have left the basin. The warm inflow water patches reached the eastern Gotland basin as a series of warm water plumes. According to its density the water has been sandwiched in the upper deep water of the eastern Gotland Basin, and could be observed throughout the basin. A particular warm water patch with a core temperature of 8.5°C was located near the sill to the Farö deep. The bottom temperatures at station TF 0271 (Gotland Deep) and in the Farö Deep did not change significantly and were still at 7.5°C and 6.8°C, respectively.

The increasing air temperatures and the above average solar radiation during April caused a strong warming of the surface water between March and May. The surface temperatures ranged between 9.3°C in the Kiel Bight, 7.4°C in the Arkona Basin and in the Bornholm Basin, and 6.6°C in the eastern Gotland Basin. The SST was only slightly about the climatological mean values for May, and 2 to 3K lower than in May 2018. In the western Baltic the SST depicted a patchy distribution, whereas it was more uniform in the Baltic Proper. The seasonal thermal stratification was well pronounced in the western Baltic, in contrast to a weaker vertical temperature gradient in the northern Gotland basin. The thermocline depth varied between 25 and 35 m along the thalweg transect, with a decreasing trend from southwest to northeast. The winter water layer was well pronounced in the central Baltic. Generally, the core temperature of winter was unusual high, since the SST did not reach the value of maximum density during the winter season. In the eastern Gotland Sea, the minimum temperature of intermediate winter water was 3.6°C, 1.3 K higher than in May 2018. The minimum temperature of 3.1°C was observed in the intermediate layer of the northern Gotland Basin. In the Bornholm Basin and the Slupsk Furrow winter water layer depicted a very patchy structure, most probably caused by lateral intrusions.

Below the intermediate layer the temperatures increase with depth. In the halocline of the Bornholm Basin the remains of the warm inflow waters were mixed up with the cold water from the intermediate layer. Here, the maximum temperature decreased from 7,6°C in March to about 5.5°C. The bottom water temperature in the Bornholm Basin cooled down to 8.5°C. In the Slupsk Furrow the conditions remained nearly unchanged, although parts of the warm deep water have further spread towards the eastern Gotland Basin. The warm water patches observed in the southern and eastern Gotland Basin in March were mostly mixed up by isopycnal mixing. The mixed water formed a warm intermediate layer between 100 and 150m depth. Its core temperature was about 7.3 to 7.5°C. This warmer layer spread over the northern sill into the Farö deep. The bottom layer temperatures in the eastern Gotland Basin did not change and remained at 7.45°C, whereas in the Farö deep an increase of the bottom temperature to 7.2°C was observed.

In the beginning of **August** the surface temperature in the Baltic has reached its annual maximum. The ongoing positive air temperature anomalies and the low cloud coverage in June lead to a higher than usual SST, and established a strong summer thermal stratification throughout the Baltic Sea. The seasonal thermocline lay at depths between 15m and 25m, and separated the warm layer of surface water from the cool winter intermediate water. The temperatures in the Arkona Basin reached 20.1°C in a surface layer of 8 to 12m thickness. Below this mixed layer the temperature decreased with depth to about 13°C at 20m depth. At station TF213 in the Bornholm Basin an SST of 18.9°C was recorded on 1st August, which was more than 4K less than in the extremely warm July 2018. At station TF271 in the eastern Gotland Basin 17.8°C was observed. There, the climatological mean value for July is 16.0°C. Generally, the SST was 1.0 to 3.0K above the long term mean, but not that extreme as during previous summer.

Below the surface layer the minimum temperatures in the intermediate water were about 4.2 °C in the eastern Gotland Basin, and 3.6°C in the northern Gotland Basin, which caused a strong vertical temperature gradient between 20 and 35m. In the Bornholm Basin the winter water was still present, but its core temperature of more than 6°C was unusual high. The reduced wind mixing prevented an efficient erosion of the winter water layer here. In June/July a minor barotropic inflow event transported 20 km³ saline water through the Öresund into the Arkona Basin. Additionally, baroclinic inflow conditions at the Darss Sill in the second half of July forced the transport of warm and high saline water through the Belt Sea. This water mass formed a thick warm bottom layer in the entire Arkona Basin, with bottom temperatures up to 14.7°C. A major part of this water body has passed the Bornholmgat, and entered the halocline of the Bornholm Basin at depth of 50 to 70m. The core temperature of this water body was about 14.0°C. The bottom layer of the Bornholm Basin was still covered with water from the autumn inflows of the previous year. At the central station TF0213 the bottom temperature was about 8.6°C. In the Slupsk Furrow similar considerably lower temperatures of 7.2°C were observed. The deep water conditions in the central Baltic remained mainly unchanged. The weak diapycnal mixing in the basin smoothed the vertical temperature gradients in the deep water layer near the warm core of inflow water. The bottom temperature in the eastern Gotland Basin was slightly reduced to 7.4°C.

In October 2019 the temperature distribution depicted the beginning autumnal cooling and the erosion of the seasonal thermocline in the surface layer. Due to the ongoing positive air temperature anomaly, the SST observed in October 2019 was still higher than normal. The surface mixed layer has deepened to 30 to 40m in the western Baltic and to 30m depth in the eastern Gotland Basin. In the Arkona Basin surface temperatures between 11°C and 13°C were observed. Also in the Bornholm Basin the SST was still high, with 12.7°C at station TF213. This is 1.5K above the climatological mean for October. In the eastern part of the Slupsk Furrow the maximum SST of 13.5°C was detected. Further to the eastern Gotland Basin and the Farö deep a slightly decreasing surface temperature was found. The stations TF271 and the Faro Deep depicted surface temperatures of 12.1°C and 10.9°C, respectively, which exceed the climatological mean also by 1.5K. The deepening of thermocline reduced the vertical extent of the intermediate winter water layer in the central Baltic to a layer of 25 m to 40 m thickness, with minimum temperatures of 4.0°C (station TF286). Only small remains of intermediate winter water were present in the Bornholm Basin and the of Slupsk Furrow.

The inflow events in the summer and autumn brought significant amounts of warm saline water into the western Baltic. This water spread along the bottom of the Arkona Basin and the halocline of the Bornholm Basin eastward. Maximum temperatures in this water body of 15.2°C and 15.0°C were observed in the Arkona Basin and Bornholm Basin, respectively. The major part of the water is still in the Arkona Basin and the western Bornholm Basin. However, also the deep layer of the Slupsk Furrow was completely flushed with warm waters. The temperature of the deep water body in the Slupsk Sill increased from 7.2°C in August to up to 10°C in October. The tip of the warm water passed the eastern sill of the Slupsk Furrow, and a small warm plume spread eastward to the Gotland Basin. The deep water temperature conditions in the Gotland Basin remained unchanged compared to August.

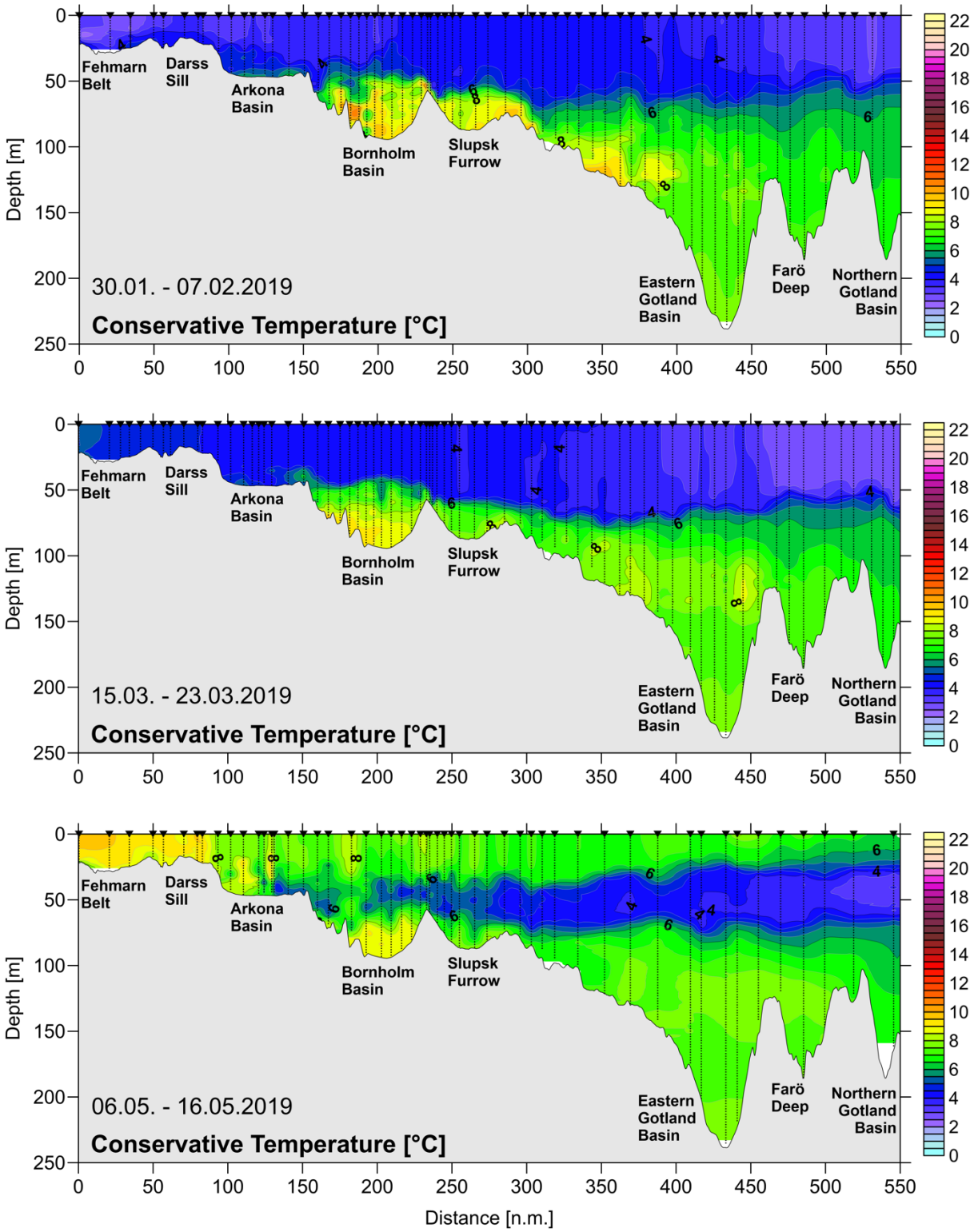

Fig. 18: Temperature distribution along the thalweg transect through the Baltic Sea between Darss Sill and northern Gotland Basin during the February, March and May cruises.

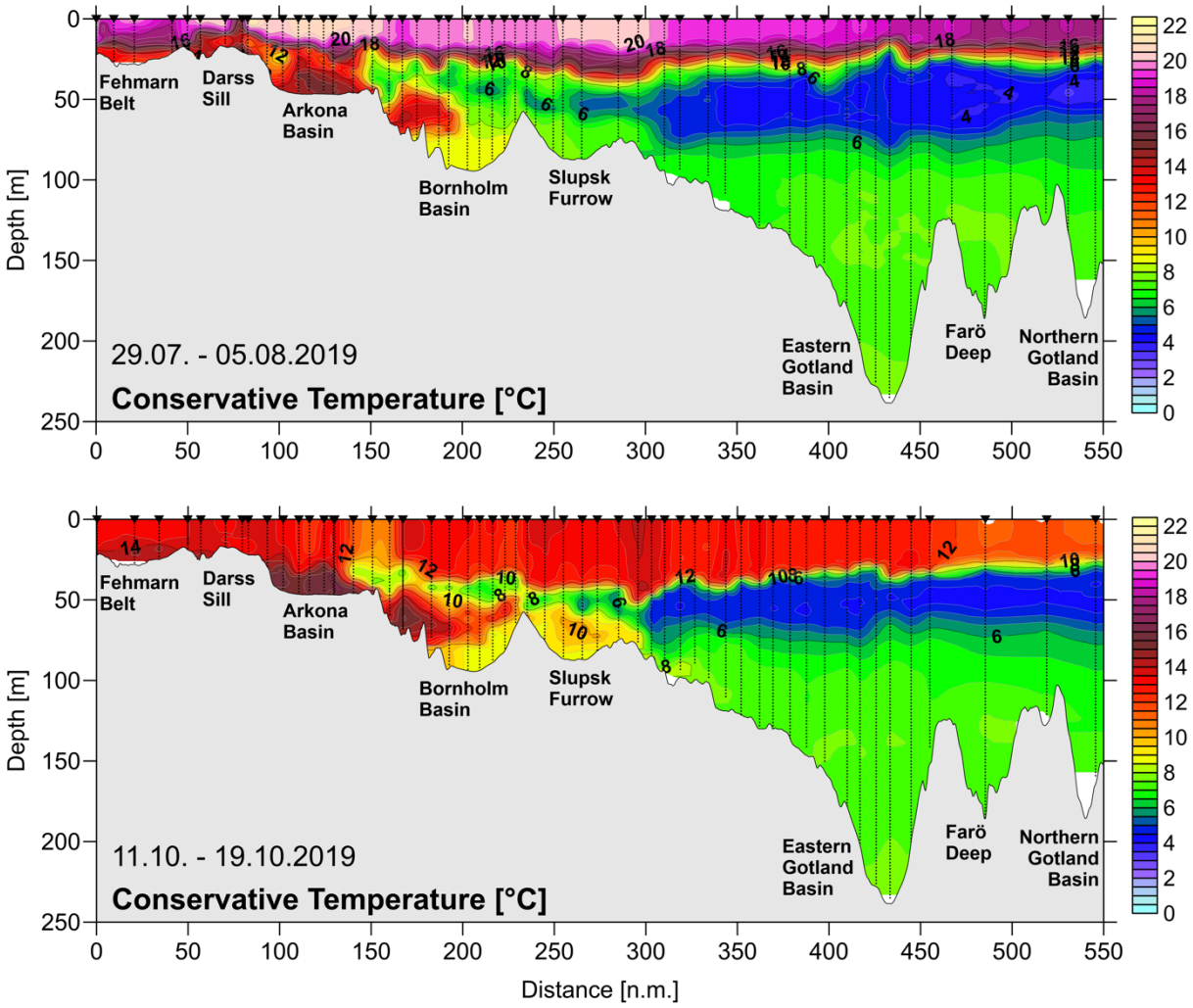

Fig. 19: Temperature distribution along the thalweg transect through the Baltic Sea between Darss Sill and northern Gotland Basin during the August and October cruises.

As part of its long-term monitoring programme, IOW operates since October 2010 **hydrographic moorings near station TF271 in the eastern Gotland Basin.** In contrast to the Gotland Northeast mooring, operational since 1998 and from where the well-known 'Hagen Curve' is derived, the mooring at TF271 also collects salinity and oxygen data. The gathered time series data allow the description of the development of hydrographic conditions in the deep water of the Gotland Basin in high temporal resolution. This time series greatly enhances the IOW's ship-based monitoring programme. Figure 20 shows the temperature time series at five depths in the deep water of the eastern Gotland Basin between July 2018 and December 2019. The temperature stratification in the deep water is characterized by a downward increasing temperature. However, the temperature gradient was rather weak before December 2018. The temperature difference between 140m depth and the bottom was about 0.2 to 0.3K. By mid of December 2018 an extreme temperature increase in the bottom layer was observed, starting in the bottom layer. Maximum temperature of 8.6°C was detected by the end of December. This is an extremely high temperature for the bottom layer in the central Baltic. It was caused by the arrival of the densest water from the warm baroclinic summer inflows. The temperature increase in the shallower layers was only moderate. It points to a low inflow volume of the warm water body. In **February** 2019 a

new pulse of warm water intrusion occurred in the upper deep water a 140m depth. Subsequent inflow pulses in this depth layer were observed also in **March and April**. In the course of the following month the strong vertical temperature gradient was smoothed. In **September** 2019 it reached values that were comparable to **November** 2018 before the warm inflow. The overall deep water temperature was increased by the warm inflows from 6.8°C to about 7.2°c.

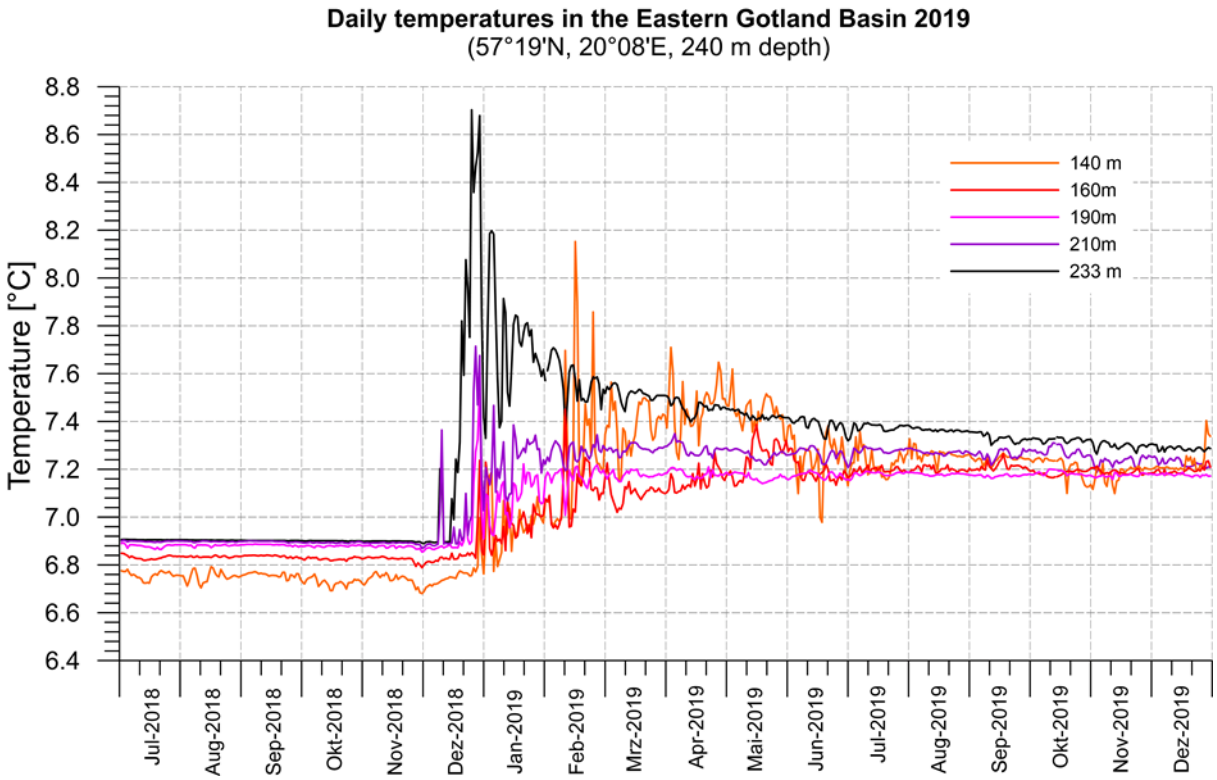

Fig. 20: Temporal development of deep water temperature in the Eastern Gotland Basin (station TF271) from July 2018 to December 2019 (daily averages of original data with 10 min sampling interval).

Table 7 summarises the annual means and standard deviations of temperature in the deep water of the central Baltic based on CTD measurements over the past five years. Compared to 2018 the deep water temperatures in the Bornholm Basin, the eastern Gotland Basin and the Farö Deep increased significantly, due to the warm baroclinic inflows in summer and autumn. This continued the increasing trend since the extreme Christmas MBI in 2014.In the western Gotland Basin only minor changes in deep water temperature were recorded. Apart from the Karlsö Deep, the bottom temperatures in the central Baltic were the highest observed in the last five years. The standard deviations of temperature fluctuations in 2019 were on a usual level.

Table 7: Annual means and standard deviations of temperature, salinity and oxygen concentration in the deep water of the central Baltic Sea: IOW- and SMHI data (n= 5-26).

Water temperature (°C; maximum in bold)

Station	Depth/m	2015	2016	2017	2018	2019
213 (Bornholm Deep)	80	7.01 ±0.08	7.06 ±0.63	7.06 ±0.28	7.81 ±1.49	**8.65 ±0.12**
271 (Gotland Deep)	200	6.79 ±0.19	7.06 ±0.12	7.05 ±0.15	6.89 ±0.01	**7.20 ±0.07**
286 (Fårö Deep)	150	6.33 ±0.25	6.56 ±0.06	6.83 ±0.15	6.70 ±0.04	**7.05 ±0.18**
284 (Landsort Deep)	400	5.46 ±0.30	5.92 ±0.10	6.14 ±0.19	6.27 ±0.03	**6.37 ±0.15**
245 (Karlsö Deep)	100	5.03 ±0.06	5.28 ±0.09	5.53 ±0.06	**5.67 ±0.12**	5.64 ±0.12

Salinity (maximum in bold)

Station	Depth/m	2015	2016	2017	2018	2019
213 (Bornholm Deep)	80	**18.86 ±0.25**	18.26 ±0.40	17.40 ±0.46	16.64 ±0.32	16.63 ±0.27
271 (Gotland Deep)	200	12.95 ±0.35	**13.35 ±0.09**	13.30 ±0.04	13.17 ±0.03	13.16 ±0.03
286 (Fårö Deep)	150	11.93 ±0.22	12.35 ±0.12	**12.58 ±0.07**	12.50 ±0.12	12.46 ±0.08
284 (Landsort Deep)	400	10.63 ±0.33	11.12 ±0.13	11.29 ±0.19	**11.41 ±0.05**	11.33 ±0.06
245 (Karlsö Deep)	100	9.64 ±0.17	10.00 ±0.16	10.28 ±0.11	**10.44 ±0.21**	10.35 ±0.24

Oxygen concentration (ml/l; hydrogen sulphide is expressed as negative oxygen equivalents; maximum in bold)

Station	Depth/m	2015	2016	2017	2018	2019
213 (Bornholm Deep)	80	**3.60 ±1.75**	1.30 ±0.93	0.90 ±0.83	0.16 ±0.37	0.97 ±1.50
271 (Gotland Deep)	200	**0.93 ±0.80**	0.55 ±0.26	0.13 ±0.11	-0.85 ±0.50	-2.48 ±1.18
286 (Fårö Deep)	150	-0.87 ±0.20	-0.05 ±0.23	**0.34 ±0.33**	-0.73 ±0.42	-1.74 ±0.41
284 (Landsort Deep)	400	-0.86 ±0.18	-0.98 ±0.23	**-0.41 ±0.31**	-0.57 ±0.40	-1.49 ±0.25
245 (Karlsö Deep)	100	-0.87 ±0.51	-0.93 ±0.47	**-0.75 ±0.66**	-1.89 ±0.72	-1.95 ±1.25

4.2 Salinity

The vertical distribution of salinity in the western and central Baltic Sea during IOW's five monitoring cruises is shown in Figures 21 and 22. Salinity distribution is markedly less variable than temperature distribution, and a west-to-east gradient in the surface and the bottom water is typical. Greater fluctuations in salinity are observed particularly in the western Baltic Sea, where the influence of salt-water inflows from the North Sea is strongest. The duration and influence of minor inflow events is usually too small to be reflected in the overall salinity distribution. Only combined they can lead to slow, long-term changes in salinity. The salinity distributions shown in Figure 21/22 are mere 'snapshots' that cannot provide a complete picture of inflow activity.

In 2019, the evolution of salinity distribution was mainly controlled by the minor barotropic inflows in autumn and winter 2018/2019 and the baroclinic inflows in late summer and autumn 2019. None of these inflows could be completely covered by the IOW monitoring cruises. Only the March cruise depicted an active inflow situation in the western Baltic. However, it is not possible to produce meaningful statistics on inflow events, by using only the monitoring cruises. The analyses of the sea level changes and the salinity observations in the western Baltic revealed three minor barotropic inflows in September 2018 (1.1 Gt salt), December 2018 (1.4 Gt salt), and January 2019 (0.8 Gt salt), which transported about 3.3 Gt salt into the western Baltic. A fourth event in December 2019 (1.0 Gt salt) occurred after the last monitoring cruise in October.

At the beginning of **February** a saline bottom water body was detected in the Fehmarn Belt, representing the last parts of the January inflow. The maximum salinity was only 20.8 g/kg. In the Arkona Basin a saline bottom layer of 15m thickness and 14 g/kg mean salinity was found, which consisted of the main part of the January inflow waters. The maximum salinity near the bottom was 18.1 g/kg. A minor part of the inflow waters has passed the Bornholmgat. The deep layers of Bornholm Basin were still filled with high saline water from the inflows in autumn 2018, illustrated by the several warm water patches. Here, the bottom salinity was about 17.3 g/kg. The halocline depth was at 50m, well above the sill depth of the Slupsk Sill. The overflow of the sill was still ongoing as visible in the shape of the isohalines over the sill. The Slupsk Furrow, too, was filled with saline water from the autumn inflows to an extent that the shallow halocline exceeded the sill depth at the eastern edge of the furrow. There, the halocline water of the Slupsk Furrow spread into the southern Gotland Basin. After the inflow series of the recent years the salinity in the deep water of the central Baltic Sea was still at a high level at the beginning of 2019. On the seabed in the Gotland Deep, a salinity of 13.37 g/kg was recorded. This was slightly higher than in February 2018, and still close to the overall maximum of 13.6 g/kg observed after the extreme inflow event in 1951. The 12 g/kg isohaline lay at a depth of around 118m, after 115m in February 2018. The 13 g/kg isohaline was found at 166m depth, 5m deeper than one year before. The bottom salinity in the Landsort deep was 11.30g/kg (11.38g/kg in February 2018). These values indicated an ongoing stagnation in the bottom waters of the central Baltic.

Until the second half of **March** the salinity distribution depicted only minor changes, due to a lack of substantial inflows. Highly saline waters were found west of the Darss Sill in the Fehmarn

Belt. However, this inflow stopped before the saline water could pass the Darss Sill. The pool of saline water at the bottom of the Arkona Basin decreased significantly, indicated by the increasing halocline depth. The bottom salinity in the Bornholm Basin decreased slightly to 17.2 g/kg in the central part of the basin. The halocline depth in the Bornholm Basin was still above the sill depth of the Slupsk Sill. Thus, the drainage of saline water into the Slupsk Furrow was still active in March 2019. In the Slupsk Furrow the bottom salinity of 14.1 g/kg was comparable to the former mean deep water salinity of the Bornholm Basin. In the eastern Gotland Basin the conditions remained nearly unchanged. At the Gotland Deep, the 12 g/kg and the 13 g/kg isohalines were found at 116m and 161m, respectively, indicating a minor increase in bottom water volume, but the bottom salinity remained 13.36 g/kg. In the Farö Deep, the 12 g/kg isohaline was observed at 120m depth. The bottom salinity was 12.58 g/kg here, 0.2 g/kg less than in March 2018.

In **May** a bottom water body of highly saline water was observed in the Fehmarn Belt. However, its maximum salinity of 25.8 g/kg was restricted to a very thin bottom layer. Water with a salinity of about 15 g/kg was found at the Darss Sill flowing into the Arkona Basin, refilling the saline water pool in that basin. The halocline was found at 35 to 40m depth in the centre of the basin. The bottom salinity was about 16.3 g/kg, significantly lower than in March. The halocline depth in the Bornholm Basin was 55m, which is the sill depth of the Slupsk Sill. The overflow of the sill has stopped. The bottom salinity in the Bornholm Basin remained unchanged at 17.2 g/kg. The saline deep water volume in the Slupsk Furrow was significantly reduced due to the eastward advection of saline water from depth above eastern sill depth of the furrow. However, the bottom salinity in the furrow increased to 14.8 g/kg. No changes of the deep water conditions were observed at station TF271 (Gotland Deep). There, the bottom salinity was unchanged with 13.3 g/kg. The 13 g/kg isohaline dropped from 161m in March to a depth of 163 m. The 12 g/kg isohaline changed their depth from 120m to 117m, due to the inflow of warm water in the upper deep water. In the Farö Deep, the position of the 12 g/kg isohaline was nearly unchanged at 118m depth. The bottom salinity was slightly increased to 12.65 g/kg.

In **August**, the observed salinity distribution in the western Baltic depicted the typical pattern of the baroclinic summer inflows, which enhanced the stratification in the Fehmarn Belt. A strong halocline at 10 to 15m depth separated the brackish surface water from the saline inflow at the bottom, where a salinity of 22 g/kg was measured. When the warm waters from the baroclinic inflows filled the pool of saline bottom water in the Arkona Basin, its maximum salinity was already reduced to about 17.7 g/kg. In the Bornholm Basin, mixing with overlaying water caused a further slight dilution of deep water leading to a bottom salinity of 16.9 g/kg. In the course of these events the saline deep water pool in the Slupsk Furrow had also been refilled. Here, only a further reduced salinity of 13.9 g/kg was detected in the inflow water near the bottom. At the eastern rim of the furrow, an active overflow into the Gotland Basin was visible. In the central Baltic basins again no significant changes were observed. The depth of the 13 g/kg isohaline in the Gotland Deep was at 166m, slightly deeper than in May. The bottom salinity in the Gotland Deep and the Farö Deep was 13.28 g/kg and 12.63 g/kg, respectively.

In **October** 2019, an inflow signature was visible in the Belt Sea. The bottom salinity in the

Fehmarn Belt increased to 24.3 g/kg. The tip of the inflowing water has reached the Darss Sill, but with strongly reduced salinity. In the Arkona Basin, warm and highly saline water from the baroclinic summer/autumn inflows covered the bottom layer. The maximum bottom salinity amounted to 18.9 g/kg. The halocline depth was at 30 to 35 m depth. The warm saline water had reached the halocline layer of the Bornholm Basin. However, the bottom salinity in the basin decreased to 16.7 g/kg. The halocline depth in the Bornholm Basin rose to 50m, which is about 5m above the sill depth of the Slupsk Sill. This forces the overflow of the sill and led to flushing the Slupsk Furrow with warm saline water. The bottom salinity in the Slupsk Furrow increased to 14.9 g/kg. The overflow of saline water at the eastern sill of the Furrow was still active during the October cruise. A small plume of saline water moved towards the eastern Gotland Basin. There, the deep water conditions had not changed since August 2019. The bottom salinity decreased very slowly in the Gotland Deep and the Farö Deep to 13.25 g/kg and 12.61 g/kg, respectively.

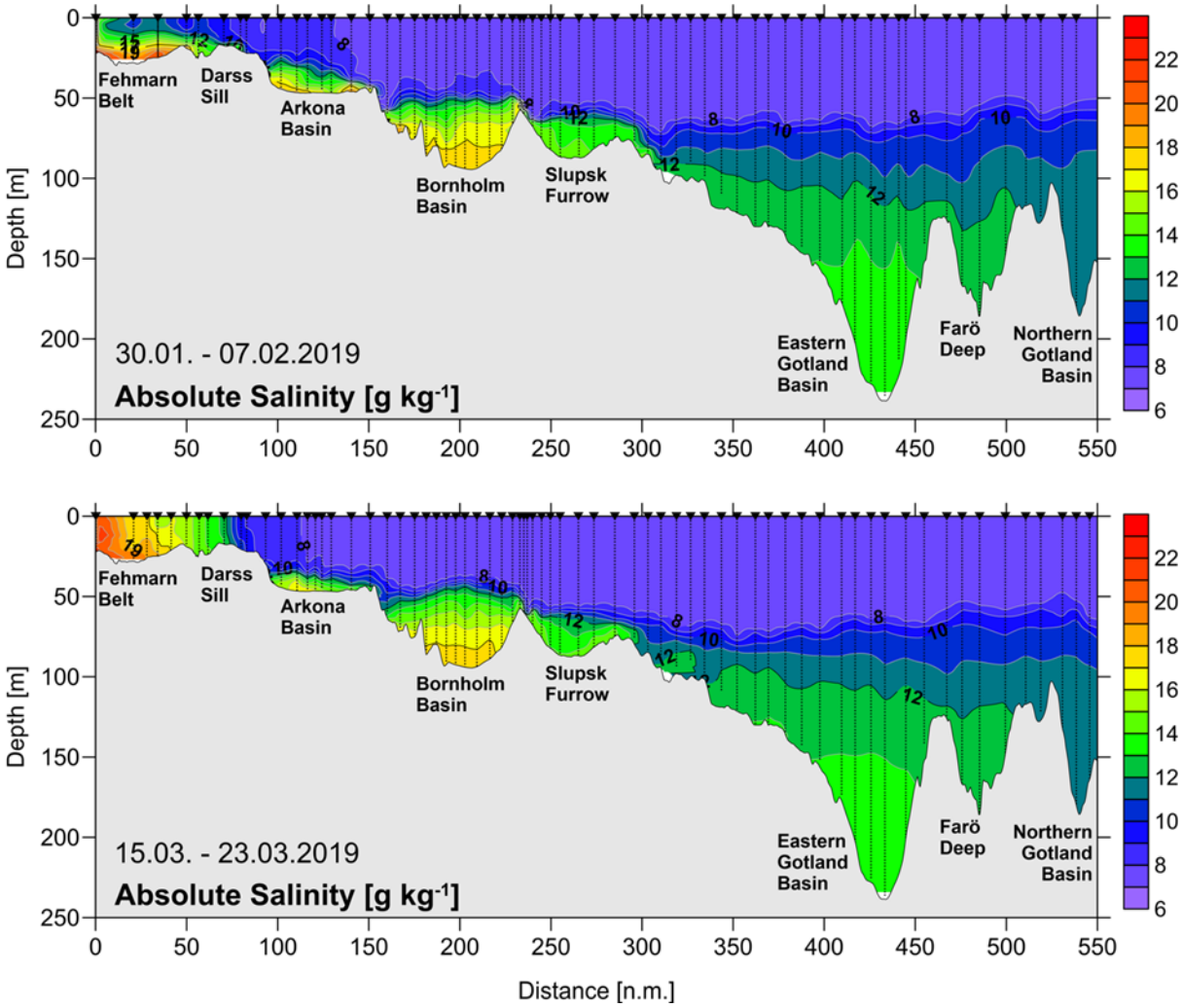

Fig. 21: Salinity distribution along the thalweg transect through the Baltic Sea between Darss Sill and northern Gotland Basin during the February and March cruises.

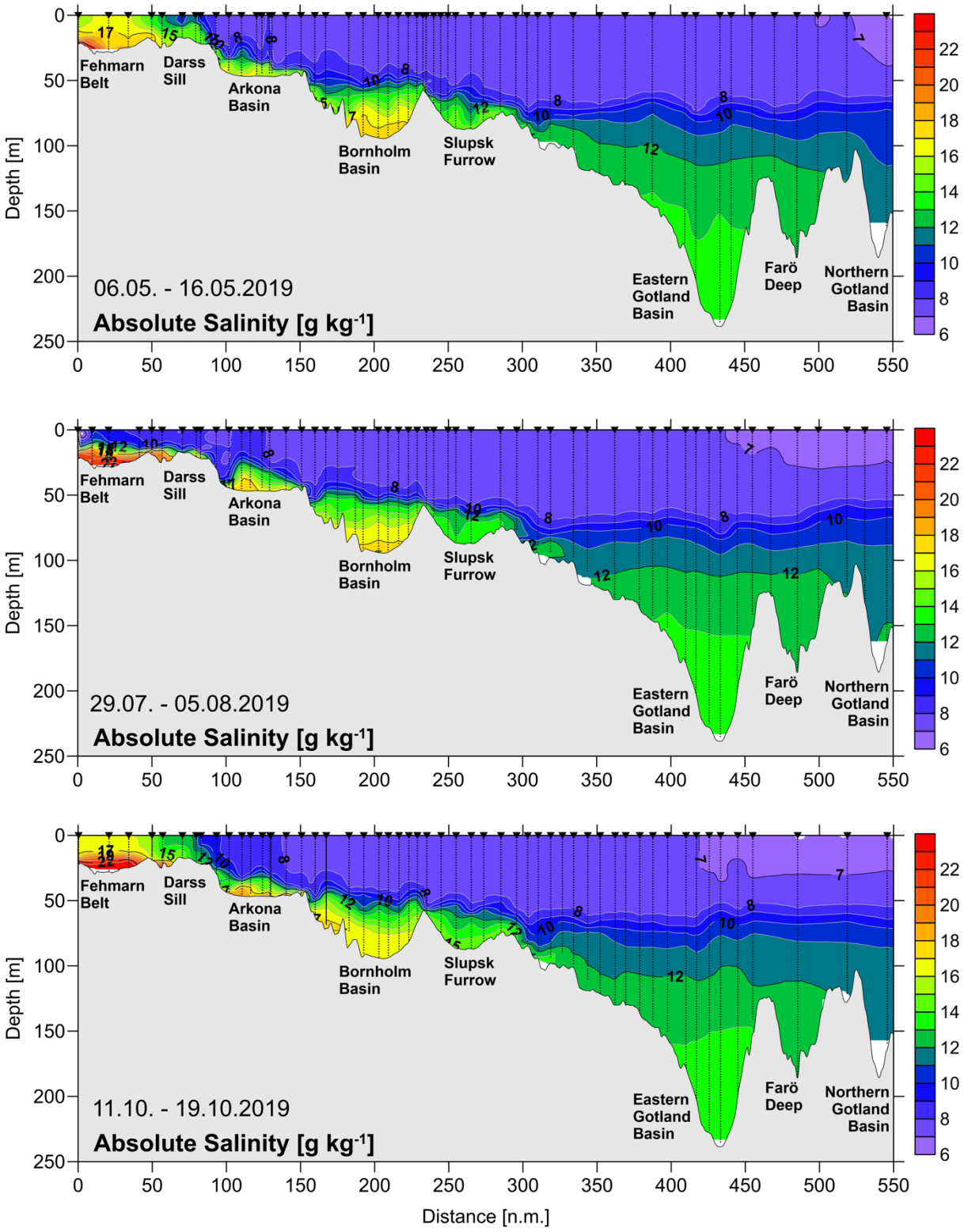

Fig. 22: Salinity distribution along the thalweg transect through the Baltic Sea between Darss Sill and northern Gotland Basin during the May, August and October cruises.

Table 7 shows the overall trend of salinity in the deep water of the Baltic in the past five years. After the series of inflow events in 2014 to 2016 the bottom salinity in the Gotland Deep and Farö Deep reached its maximum in 2016 and 2017. Although warm saline waters from summer and

autumn inflows 2018 reached the deep layer of the Gotland Basin in December 2018, no permanent change in salinity stratification was observed at the central station TF271. In 2019, the deep water salinity in both basins dropped only slightly due to mixing. In the past five years, the deep water salinity in the Karlsö Deep and Landsort Deep had reached its maximum values in 2018. In 2019, deep water salinity in both locations decreased by about 0.09 g/kg. In the Bornholm Basin, the mean deep water salinity remained constant in 2019. However, also here the salinity was still high. The high standard deviation of salinity in the Bornholm Basin and the Karlsö Deep points to rapid fluctuations, caused by particular inflow events.

As in the recent year, no clear trend emerges over the past five years for salinity in the surface layer of the Baltic. Table 8 summarises the variations in surface layer salinity. Compared to the values in 2018, surface layer salinity in the Bornholm Basin and the eastern Gotland Basin increased slightly in 2019. This may be caused by the slow upward mixing of saline water from the deep water body, which has a very high salinity compared to the long term mean. The surface salinity decreased in the Farö Deep, and in the western Gotland Basin. Except in the Bornholm Basin, the standard deviations of surface salinity were close to the level of those of the long term average. Generally, large inflow events effect the surface salinity with a delay of about ten years. Thus, a significant increase in surface salinity after the strong inflow in 2014 was not yet expected in 2019.

Table 8: Annual means of 2015 to 2019 and standard deviations of surface water salinity in the central Baltic Sea (minimum values in bold, n= 5-26). The long-term averages of the years 1952-2005 are taken from the BALTIC climate atlas (FEISTEL et al. 2008)

Station	1952-2005	2015	2016	2017	2018	2019
213 (Bornholm Deep)	7.60±0.29	7.76±0.20	7.75±0.26	**7.46±0.20**	7.53±0.08	7.63±0.11
271 (Gotland Deep)	7.26±0.32	7.06±0.15	**6.89±0.34**	7.33±0.22	7.09±0.27	7.19±0.25
286 (Fårö Deep)	6.92±0.34	6.74±0.25	**6.63±0.33**	7.13±0.43	6.92±0.34	6.78±0.33
284 (Landsort Deep)	6.75±0.35	**6.29±0.44**	6.57±0.16	6.54±0.34	6.59±0.32	6.52±0.26
245 (Karlsö Deep)	6.99±0.32	6.91±0.25	6.98±0.17	6.93±0.18	7.06±0.18	**6.89±0.24**

Figure 23 shows the temporal development of salinity in the deep water of the eastern Gotland Basin between July 2018 and December 2019, based on data from the hydrographic moorings described above. As seen in the temperature data, there were no significant changes of the saline stratification until mid-December 2018. The arrival of warm waters from the summer and autumn inflows 2018 caused a temporary increase in bottom salinity of the eastern Gotland basin. However, it caused no permanent change of salinity stratification. In February 2019, the stratification was relaxed to the conditions established before December 2018. No further impact on the salinity structure in the deep water of the eastern Gotland Basin was observed until December 2019.

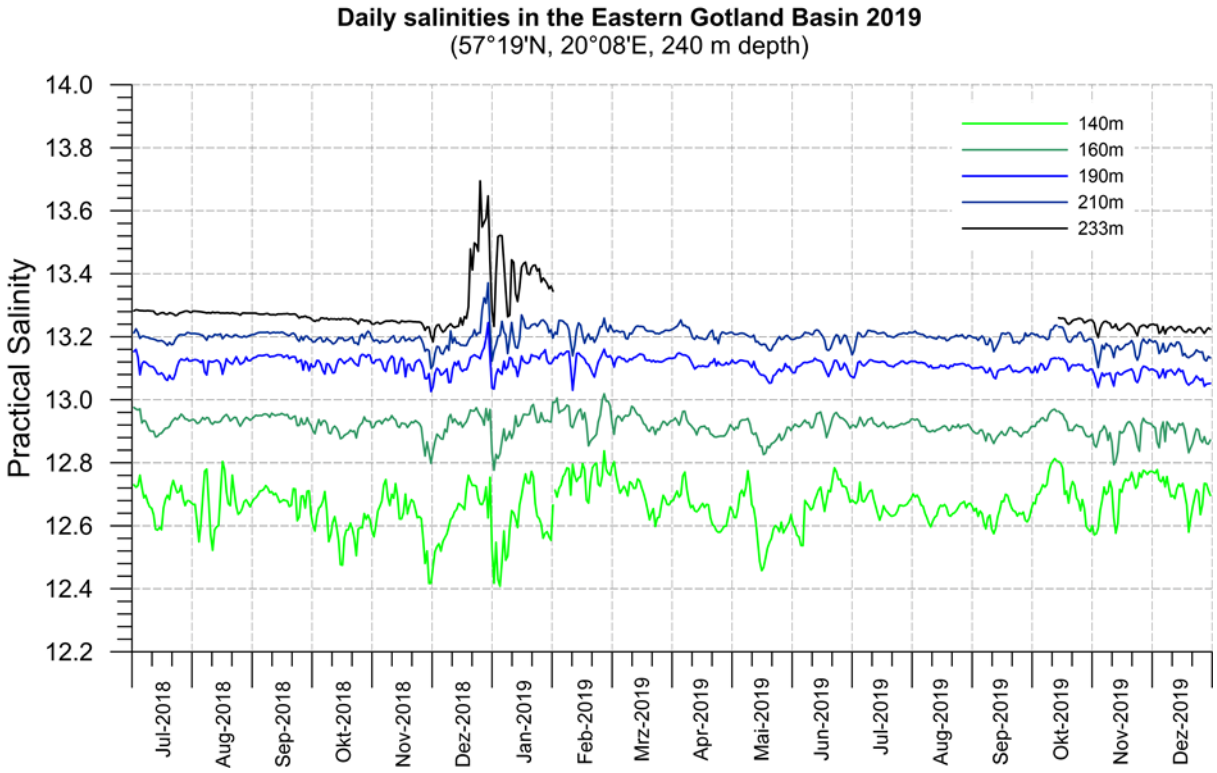

Fig. 23: Temporal development of deep water salinity in the Eastern Gotland Basin (station TF271) from July 2018 to December 2019 (Daily averages of original data with 10 min sampling interval).

4.3 Oxygen distribution

A prerequisite for the survival of higher marine organisms is the presence of sufficient oxygen. For the Baltic Sea, it is known that oxygen reaches low levels in deep waters and after a few years of stagnation, the water below the permanent halocline turns into anoxic and then to euxinic conditions, hostile to life. This reflects the consumption of oxygen during the mineralization of organic matter, and subsequently of other oxidants, especially of sulphate as a major constituent of Baltic Sea seawater. Thereby, sulphate is converted to poisonous hydrogen sulphide and turns bottom areas into dead zones (DIAZ & ROSENBERG 2008). The lack of oxygen is evaluated by HELCOM by using the oxygen debt indicator for the deep basins below the halocline to figure out a potential deviation from a "good environmental status" (HELCOM 2013).

However, it raised emerging concern that also shallow Baltic Sea areas are more often subjected to temporally low oxygen values. "Shallow areas" in this context are regions, in which the water column is too shallow for the establishment of a permanent halocline, thus, usually shallower than 60 m. Hypertrophication of the Baltic Sea primarily causes intensified phytoplankton blooms. Subsequently, the episodic remineralization activity of accumulated organic matter on the sea floor is intensified. To observe and finally to recommend measures, the bottom water oxygen concentration in shallow areas is aimed to be characterized by an indicator that appropriately describes the oxygen condition also for these areas apart from the central deep basins. In surface waters as well as in shallow areas, the gas exchange with the atmosphere maintains an elevated oxygen content of seawater. Thus, oxygen is usually close to saturation

that is mainly controlled by temperature (Fig. 24, upper panel). The situation changes, when a stable thermocline develops separating oxygenated surface waters from the waters below. Then, assimilation and dissimilation processes that change the oxygen content in seawater are mainly separated and in deeper waters, without contact to the atmosphere, oxygen concentration clearly declines by respiration (Fig. 24, lower panel). Strong temperature and/or salinity changes hinders mixing between the bottom and upper waters. Lasting oxygen consumption during organic matter degradation can lead to total depletion of oxygen (lower panel). Denitrification and subsequent reduction of sulphate result in the building of toxic hydrogen sulfide (shown as negative oxygen), which is worsening the conditions.
We generally use ml/l as the standard unit for oxygen concentration, however also mg/l was used in Fig. 25. In this case a conversion formula to ml/l is provided in the figure caption. In the hydrographic analysis of oxygen displayed in Figures 26/27 we use the chemical oceanographic unit µmol/kg, in comparison to Figures 18/19 of temperature and 21/22 of salinity.

The oxygen concentration in deep waters of the selected Baltic Sea deeps (Table 7) at respective reference depth levels showed a general decrease after the MBI of December 2014. At Gotland Deep station this decline of oxygen started already in 2015, while further north and west this was not observed before 2017. Compared to the depth range of the pycnocline and the bottom layer, where oxygen is quickly taken up by surrounding euxinic waters and thus, the variability is considerable, the selected reference depths are basically unbiased from episodic smaller inflows. The strongest impact of the 2014/2015 MBI was in the Bornholm Deep and the Gotland Deep in 2015 and at Fårö, Landsort, and Karlsö Deeps in 2017, revealing the best oxygen situation in recent years. In subsequent years, oxygen decline turned into an ongoing accumulation of hydrogen sulphide in 2019 (given as negative oxygen). The annual average in the Gotland Deep decreased to -2.48 ml/l at 200 m, in the Fårö Deep at 150 m to -1.74 ml/l, at the Landsort Deep to -1.49 ml/l, and at Karlsö Deep to -1.95 ml/l (Table 7). An exception reflected the Bornholm Deep that recovered by smaller inflow events in winter 2018/2019. There, an annual average oxygen concentration of 0.97 ml/l, similar to the 2015 was determined for 80 m depth, however with strong changes during 2019. The oxygen maxima of the Bornholm Sea and the eastern Gotland Sea and the Karlsö Deep were still the values from 2015 and for the northern and western deeps, Fårö Deep, Landsort Deep and Karlsö Deep, the values of 2017, which were as well the consequences of the MBI 2014/2015 (Table 7).

The seasonal cycle of the surface water temperature controlled the oxygen concentration in the **surface water** due to the temperature dependence of the oxygen solubility (upper panel of Fig. 24). The highest value was 9 ml/l oxygen in the northern Gotland Sea in **March**. Lowest values of below 6 ml/l were observed in surface waters in summer at dominating highest temperatures. During autumn cooling in **October,** the oxygen values slightly increased again in surface waters. The **bottom water** of the shallow western Baltic Sea showed a similar seasonal pattern governed by temperature. The Belt Sea and the Mecklenburg Bight showed a decreasing oxygen concentration during the development of the thermocline from **March to May** and further to August 2019 and slightly recovered in autumn. But for the Arkona Sea, no recovery of the bottom

water oxygen is observed in October. Moreover, it further decreased from 4 ml/l in August to 3 ml/l in October 2019. In the Bornholm Sea the bottom water conditions first clearly improved from oxygen values of 0.9 ml/l in February to 2.8 ml/l in March by an inflow of an oxygenated water mass. Thereafter, the oxygen concentration declined until October to -0.3 ml/l indicating a change to sulphidic conditions. The southern Gotland Sea received the oxygenated water from the Bornholm Sea in summer with a peak of 0.7 ml/l in August. The eastern Gotland Sea bottom water accumulated hydrogen sulphide with oxygen equivalents of -4.8 ml/l in February to -6.5 ml/l in October with a slight improvement in March of -3.6 ml/l oxygen. In comparison, the situation in the northern and western Gotland Sea bottom waters appeared relatively stable with values of about 2 ml/l.

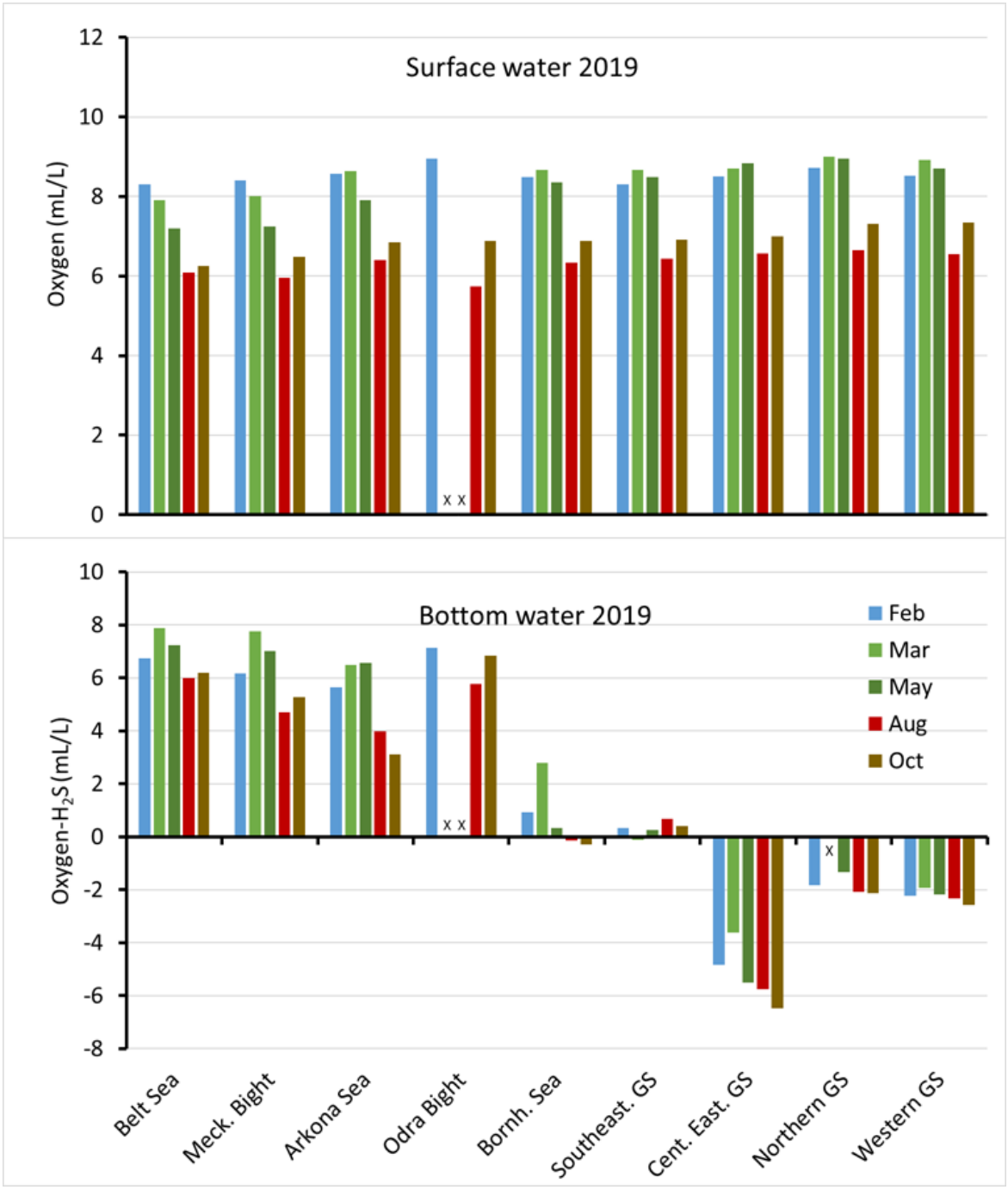

Fig. 24: Comparison of average oxygen concentrations in surface waters (upper panel, including O_2-sensor data) and average oxygen/hydrogen sulfide concentrations in bottom waters (lower panel, without sensor data) of the studied Baltic Sea areas of February to October 2019: Belt Sea, Mecklenburg Bight, Arkona Sea, Odra Bight, Bornholm Sea, southern Gotland Sea, central Eastern Gotland Sea, Northern Gotland Sea, and Western Gotland Sea.

A period most critical for oxygen concentration in bottom waters of the shallow Baltic Sea areas is the time at the end of summer/early autumn, when usually the strongest oxygen depletion is observed. Since IOW does not perform a monitoring campaign that covers that time period, we turn to the findings of the State Agency for Agriculture, Environment and Rural Areas Schleswig-Holstein (LLUR), which routinely measures near-bottom oxygen concentrations at that time of the year (LLUR 2019). Investigations in 2019 were conducted from September 2rd to 11th. Near-bottom oxygen concentrations were measured on 41 stations. Thereof, 29 stations showed a water depth deeper than 15 m and 12 station were between 7 and 13 m deep (Figure 25).

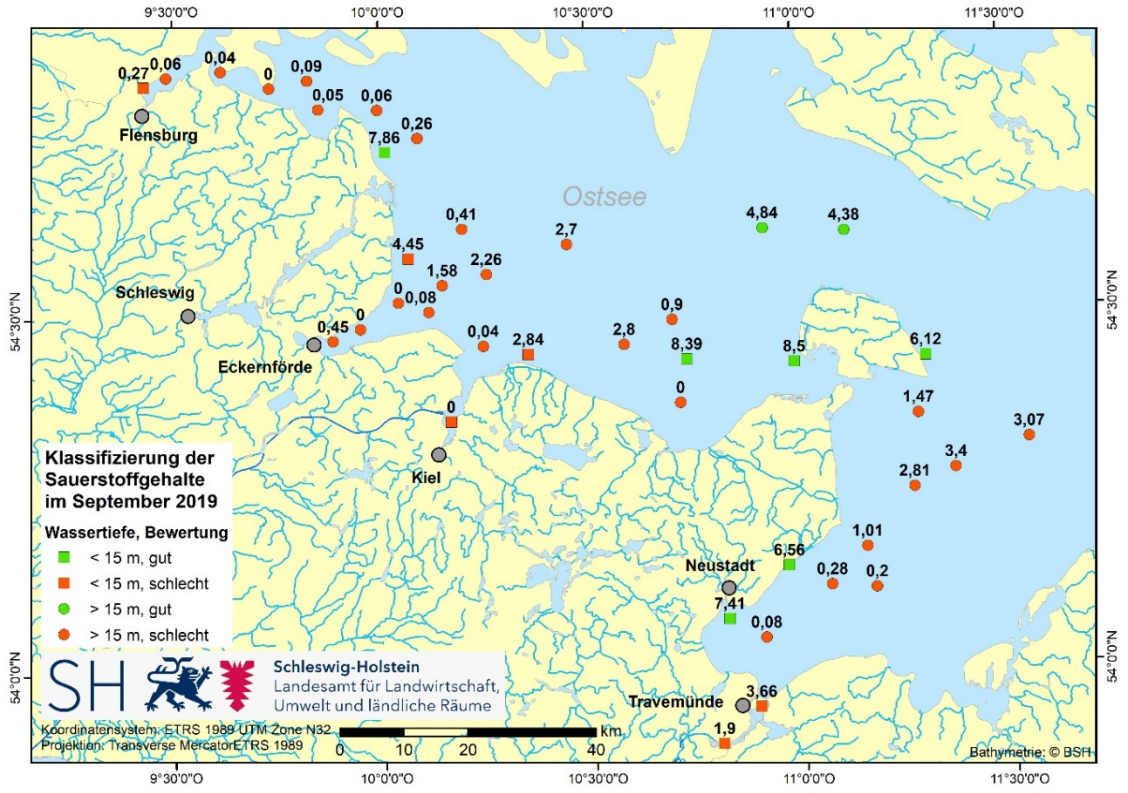

Fig. 25: Classified oxygen concentrations in the Belt Sea in September 2019 (LLUR 2019) – O2 [mg/l] x 0.7 = O2 [ml/l].

Measured bottom water oxygen concentrations (Figure 25) are given at the respective sampling sites. In September 2019, 27 of the 29 stations in deeper water (›15m) showed values below the threshold value of 4 mg/l (93%). Thus, the oxygen status in September 2019 is worse than in September 2018 with only 80% of the deeper stations below the threshold (LLUR 2018). Moreover, at 6 of the 12 stations in shallower water (‹15m) the oxygen concentration was below the threshold value of 6 mg/l (50 %), which in 2018 was the case at 25% of the shallower stations only. For a more detailed analysis of the seasonal development of oxygen saturation, see the measurements from Darss Sill (chapter 3.2), the Arkona Basin (chapter 3.3), and Oder Bank (chapter 3.4).

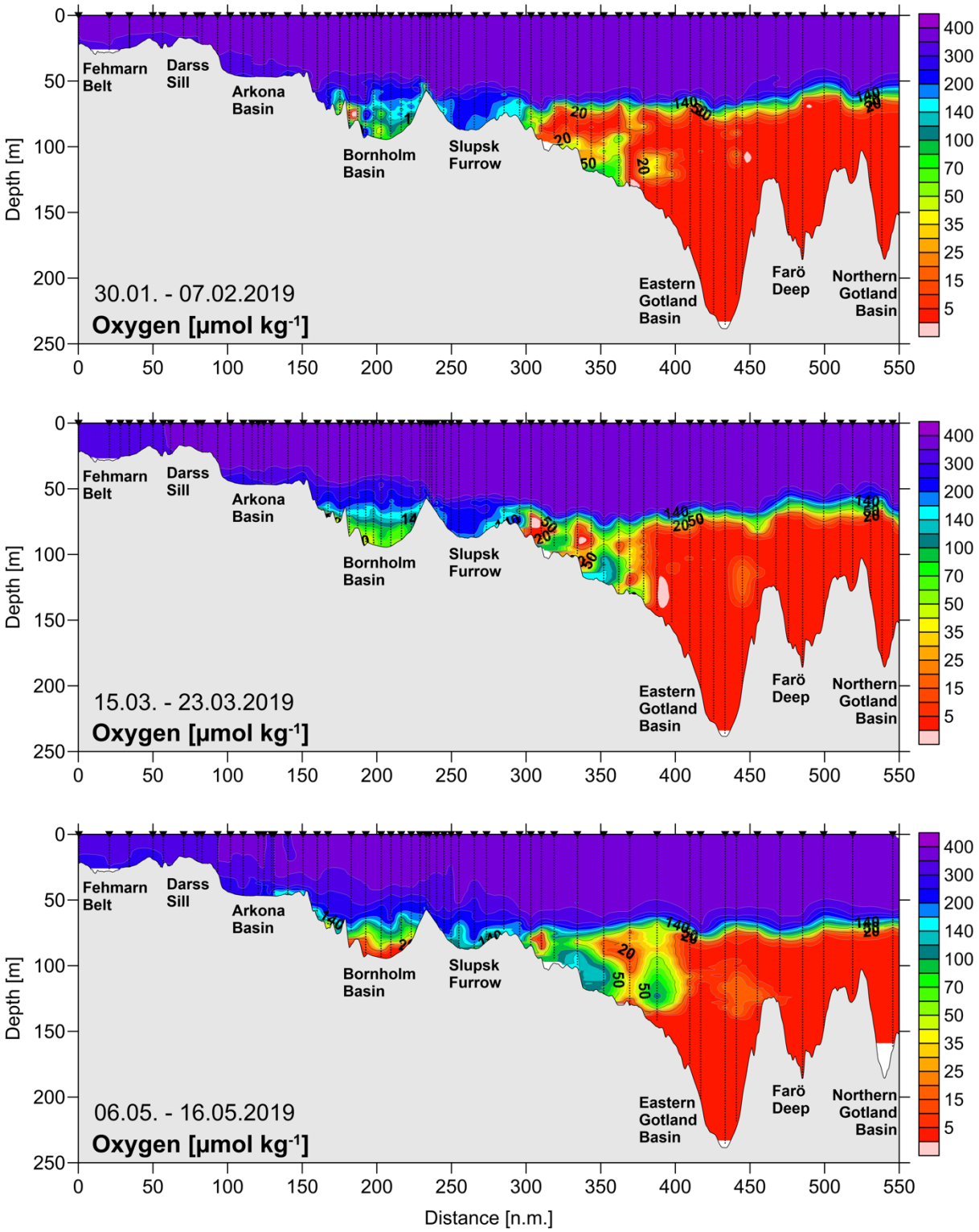

Fig. 26: Vertical distribution of oxygen (without H2S) during the February, March and May cruises in 2019 between the Darss Sill and the northern Gotland Basin. Values below 1 µmol/kg could not be distinguished from 0 µmol/kg.

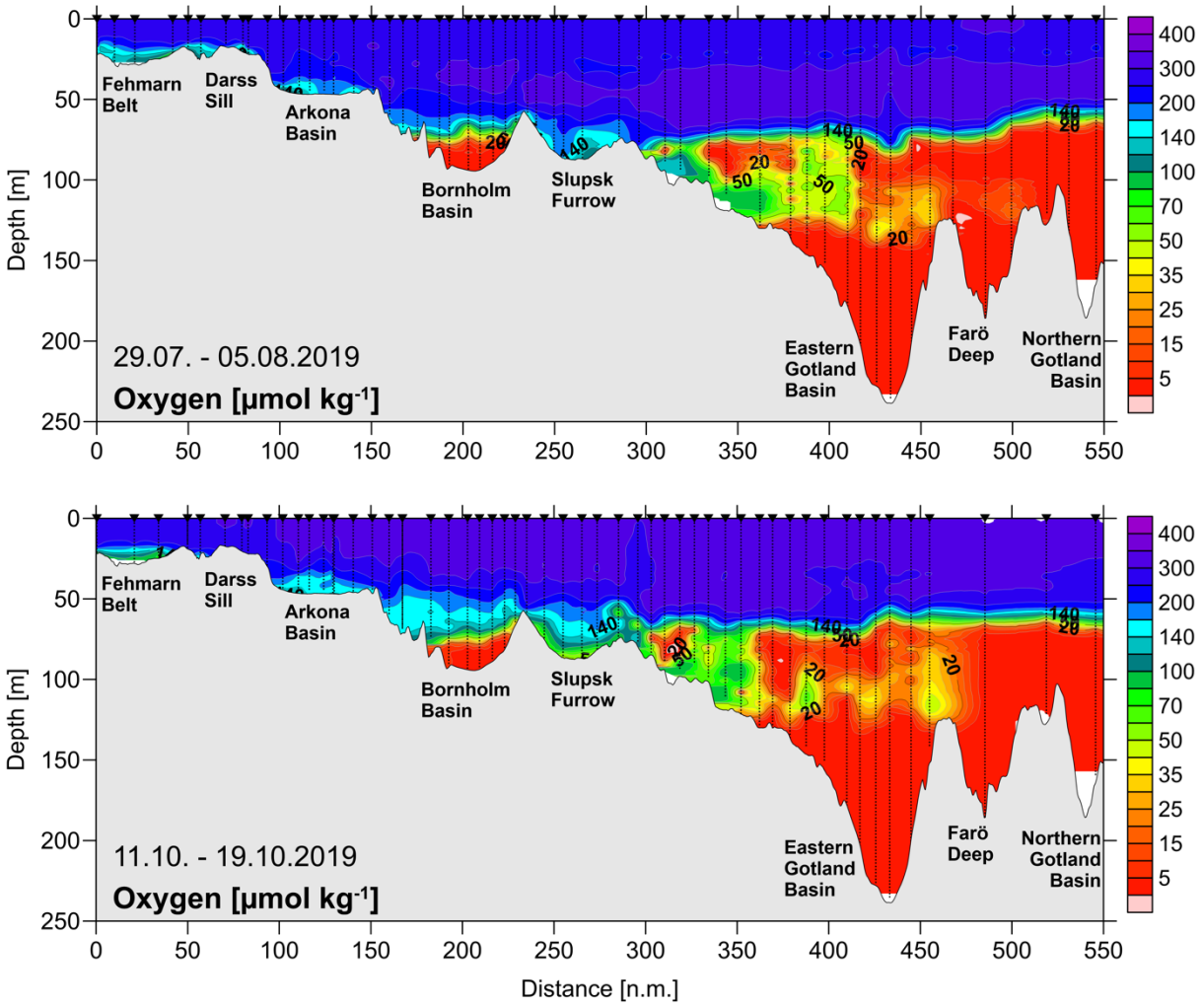

Fig. 27: Vertical distribution of oxygen (without H2S) during the August and October cruises in 2019 between the Darss Sill and the northern Gotland Basin. Values below 1 µmol/kg could not be distinguished from 0 µmol/kg.

In the deep basins of the central Baltic Sea, deep-water conditions are primarily influenced by the occurrence or absence of moderate and strong barotropic and/or baroclinic inflows. In 2019 a sequence of pulses of oxygenated water apparently propagated from the Bornholm Sea deep waters, where it originated from a depth range of 60-70 m, further east (Fig. 26). The water mass contained about 200 µmol/kg oxygen, entrained into the southern Gotland Sea below the pycnocline via the Słupsk channel in March and May with still 140 µmol/kg and contained about 80 µmol/kg oxygen in July and October. The water spread in the eastern Gotland Basin roughly between 80-120 m with a lateral extension of up to 50 km versus the central basin (Kuss 2019). In August, it showed a concentration of about 30-50 µmol/kg oxygen in the central eastern Gotland Basin and already has reached the Fårö Deep. In October the remains of oxygenated waters in the Fårö Deep apparently were already consumed, but a major pulse of the oxygenated water mass has reached the northern sill of the eastern Gotland basin (Fig. 27).

4.4 Nutrients: Inorganic nutrients

According to the second "State of the Baltic Sea" report, 97% of the Baltic Sea area is affected by eutrophication and 12% is assessed as being in the worst status category (HELCOM 2018a). Thus, the eutrophication of the Baltic Sea remains a major concern despite many reduction measures that have been implemented in the last decades. A drastic description of the consequences of eutrophication is given by DUARTE et al. (2009) "The effects of eutrophication include the development of noxious blooms of opportunistic algae and toxic algae, the development of hypoxia, loss of valuable seagrasses, and in general a deterioration of the ecosystem quality and the services they provide".

Comparing the Pollution Load Compilation for the year 2010 (PLC-5.5) (HELCOM 2015) with that for 2014 (PLC-6) (HELCOM 2018b), **total waterborne and airborne inputs of nitrogen to the Baltic Sea** decreased from 977,000 megagrams (Mg) to 826,000 Mg annually. For **phosphorus** the decline was given for 2006 to 2014 from annual 35,500 Mg to 31,000 Mg without accounting for the less important atmospheric deposition of about 2,100 Mg determined for 2010.

The 826,000 Mg total nitrogen that was delivered to the Baltic Sea shared between 27.1 % from the atmosphere, 3.5 % from direct sources and 69.4 % from rivers, correspondingly, of the 31,000 Mg of total phosphorous, 5.2 % were from direct sources and 94.8 % by riverine supply (HELCOM 2018b). In turn, 61 % of the atmospheric deposition of total nitrogen to the Baltic Sea of overall 228,000 Mg originated from surrounding HELCOM countries, 8 % from Baltic Sea shipping (+ 5 % from North Sea shipping), 21 % from EU countries which are not HELCOM Contracting Parties, and the remaining 5 % from other countries and distant sources outside the Baltic Sea region in 2017 (GAUSS et al. 2020). Thereby, a major contribution of almost 35,000 Mg originates from agriculture in Germany, which is 25 % of the HELCOM countries atmospheric total nitrogen supply to the Baltic Sea of 140 000 Mg. The aim of the European Union's ambitious Marine Strategy Framework Directive is to protect more effectively the marine environment across Europe. The Marine Directive aims to achieve Good Environmental Status (GES) of the EU's marine waters by 2020 and to protect the resource base upon which marine-related economic and social activities depend (http://ec.europa.eu/environment/marine/eu-coast-and-marine-policy/marine-strategy-framework-directive/index_en.htm).

In Germany, riverine inputs of total phosphorus declined between 2006 and 2014 by 14%. In the same time-period, total nitrogen input decreased by 31% (HELCOM, 2018b). Despite this positive development, German territorial waters and bordering sea areas of the Baltic Sea remained hypertrophied by up to 50% in the western and up to 100% in the eastern part (HELCOM 2018a). To determine the effects of changes in nutrient inputs and to evaluate the results of reduction measures undertaken, the frequent monitoring of the nutrient situation is mandatory. Nutrients are core parameters since HELCOM established a standardized monitoring programme at the end of the 1970ies.

4.4.1 Surface water processes

Nitrate and phosphate concentrations in the surface waters of temperate latitudes exhibit a typical annual cycle with high concentrations in winter, depletion during spring and summer, and recovery in autumn (NAUSCH & NEHRING 1996, NEHRING & MATTHÄUS 1991). However, in recent years it appears more and more clear that nitrate is completely taken up by the spring bloom and replenished during late autumn and winter, whereas phosphate is significantly declining in April/May, but persists at low concentration almost throughout the summer. Thus, blooms of diazotrophic cyanobacteria, which use dinitrogen gas in addition to phosphate for growth, are always enabled.

Figure 28 illustrates the annual cycle of nitrate and phosphate concentrations in surface waters at the stations Gotland Deep and Bornholm Deep in 2019. For this purpose, the data of five monitoring cruises of the IOW were combined with data of the Swedish Meteorological and Hydrological Institute (SMHI) to get a better resolution of the seasonal patterns. In the central Baltic Sea, a typical phase of elevated nutrient concentrations developed during winter, which lasted two to three months (NAUSCH et al. 2008). In 2019, maximum nutrient concentrations were measured in early February of 4.0 µmol/l nitrate and 0.68 µmol/l phosphate in the central eastern Gotland basin and 2.7 µmol/l nitrate and 0.61 µmol/l phosphate in the central Bornholm Sea, respectively. The decline of nitrate started at the Gotland Deep station in mid-March and reached the detection limit in early May at a surface water temperature of 6.5 °C. At Bornholm Deep station nitrate appeared to have declined in mid-February and reached the detection limit already on 23rd March at only 4.4 °C. The phosphate reserves lasted at both stations well into the summer and were only shortly close to the detection limit at the Bornholm Deep station on August 1st and at Gotland Deep station on October 17th. Thus, spring bloom in 2019 likely ended in the Bornholm Sea by mid-March and relatively late by the beginning of May in the eastern Gotland Sea. A significant increase of these basic major nutrients in the surface waters at both stations did not take place before early November. At that time, cooling to below 10°C enabled wind induced mixing and a supply of nutrients from deeper layers. Mineralization processes at depth had caused an increase of nutrient concentrations that subsequently replenished the surface water until the end of the year.

The incomplete uptake of phosphate is likely caused by the low dissolved inorganic nitrogen/phosphorus ratio (DIN/DIP) present in the winter surface water of the Baltic Sea that in turn leads to nitrate exhaustion before phosphate is completely consumed. The favorable uptake ratio of about 16 was already shown by an early study of Redfield (Redfield et al., 1963) and was proven to be a valuable approximation many times thereafter. The DIN/DIP ratio (mol/mol) was determined from the sum of ammonium, nitrate, and nitrite concentrations versus the phosphate concentration. In the investigated areas the values scatter around 8 mol/mol in the western part with a decreasing tendency since 2017, and around 5 mol/mol in the eastern part in recent years (Fig. 29). This already indicated that nitrogen was a limiting factor especially in 2019 giving diazotrophic cyanobacteria an advantage compared to primary producer that depend on nitrate. Beside the Gotland Sea, Bornholm Sea that showed really low dissolved inorganic N/P ratio for several years, also the Arkona Sea, Mecklenburg Bight and even the Belt Sea are affected by an unfavorable nutrient ratio. The DIN/DIP ratio of the central Eastern Gotland Basin was almost stable in recent years, whereas the ratio dropped in the western Gotland Sea to about 3 mol/mol

in 2019. The exceptional high DIN/DIP ratio of about 20 mol/mol in the Odra Bank area, which was even above the "Redfield ratio" since 2017, was measured again in 2019.

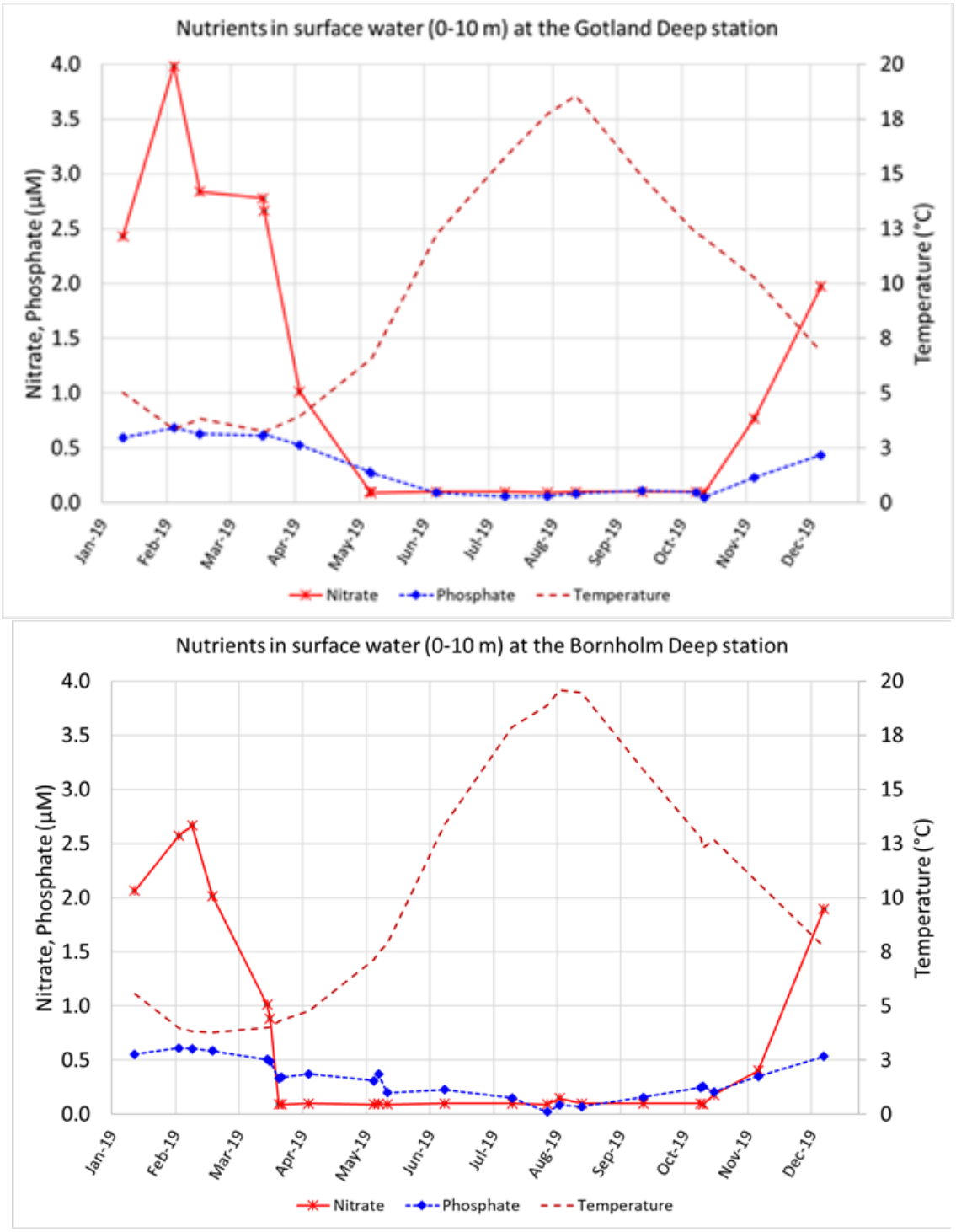

Fig. 28: Seasonal cycle of the average phosphate and nitrate concentrations in 2019 compared to temperature of the surface layer (0-10 m) at the Gotland Deep station (TF271 – upper panel) and at the Bornholm Deep station (TF213 – lower panel), respectively, by using IOW and SMHI data.

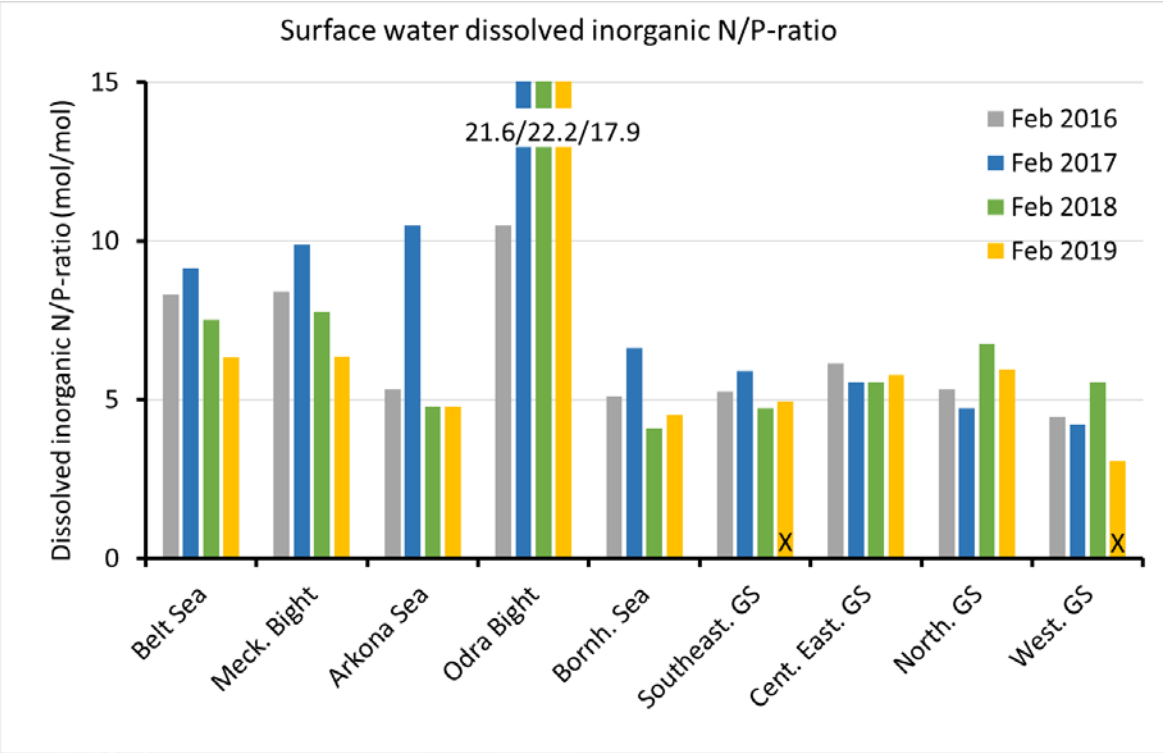

Fig. 29: Average dissolved inorganic nitrogen versus phosphate ratio in surface waters of selected Baltic Sea areas in February of 2016 to 2019; for the cross-marked bars the ammonium concentration (a minor contribution to DIN) was estimated. Three very high ratios from the Odra Bight are indicated as numbers to avoid prolonging the y-axis.

Table 10 shows winter phosphate and nitrate concentrations in surface waters for the February months of recent years. In general, the values obtained for February 2019 were well in the range of previous years. Slightly lower values were determined for phosphate at the Fehmarn Belt Station and in the western Gotland Sea at Karlsö Deep station, reflecting values of 0.42 and 0.65 µmol/l in surface waters, respectively. Similarly for nitrate, clearly lower values were determined at Fehmarn Belt, Mecklenburg Bight, Arkona Sea and Karlsö stations of 1.7, 2.8, 2.6, and 1.2 µmol/l, respectively. Only a minor variability was observed at Gotland Deep, Fårö Deep, and Landsort Deep. The changes during the last five years indicate an interannual variability, but the reductions in nutrient concentrations that have already been observed in coastal waters are up to now not reflected in the nutrients concentrations of the central Baltic Sea basins (NAUSCH et al. 2011b, NAUSCH et al. 2014). By comparison with nutrient target values elaborated in the TARGEV project (HELCOM 2013), a clear discrepancy is observed between the phosphate and dissolved inorganic nitrogen (DIN), basically nitrate in surface waters, in terms of reaching the targets. The target values of phosphate and DIN are for the Belt Sea (Danish straits) 0.58, 5.11 µmol/l, for the Arkona Basin 0.38, 2.62 µmol/l, for the Bornholm Sea 0.31, 2.70 µmol/l, and for the Baltic Proper 0.29, 2.62 µmol/l, respectively. This indicates that for nitrate (ammonium and nitrite reflect minor contributions) the target values are likely reached within the next years, but for phosphate it may need some more decades to reach the Good Environmental Status at business as usual. However, it has to be noted that the lower winter nitrate concentration could be significantly caused by increased anoxia in deep waters that likely constitute a considerable nitrate sink by denitrification. Thus, it may be - at least partly - not a good sign.

Table 10: Mean nutrient concentrations in the surface layer (0-10 m) in winter in the western and central Baltic Sea (IOW data).

Surface water phosphate concentrations (µmol/l) in February (Minima in bold)

Station	2015	2016	2017	2018	2019
360 (Fehmarn Belt)	0.64 ± 0.01	0.66 ± 0.04	0.54 ± 0.01	0.66 ± 0.02	**0.42 ± 0.00**
022 (Lübeck Bight)	0.63 ± 0.02	0.79 ± 0.15	**0.53 ± 0.09**	0.69 ± 0.00	-
012 (Meckl. Bight)	0.60 ± 0.01	0.68 ± 0.01	**0.56 ± 0.00**	0.70 ± 0.00	0.58 ± 0.00
113 (Arkona Sea)	0.56 ± 0.00	0.64 ± 0.01	**0.53 ± 0.00**	0.67 ± 0.01	0.59 ± 0.00
213 (Bornholm Deep)	**0.60 ± 0.00**	0.67 ± 0.06	0.61 ± 0.06	0.65 ± 0.01	0.61 ± 0.02
271 (Gotland Deep)	**0.50 ± 0.02**	0.67 ± 0.04	0.70 ± 0.08	0.67 ± 0.01	0.68 ± 0.02
286 (Fårö Deep)	**0.60 ± 0.00**	0.65 ± 0.08	0.69 ± 0.01	0.64 ± 0.01	0.71 ± 0.01
284 (Landsort Deep)	-	0.75 ± 0.01	0.79 ± 0.03	**0.59 ± 0.01**	0.70 ± 0.01
245 (Karls Deep)	0.80 ± 0.00	0.87 ± 0.09	0.91 ± 0.07	0.70 ± 0.01	**0.65 ± 0.01**

Surface water nitrate concentrations (µmol/l) in February (Minima in bold)

Station	2015	2016	2017	2018	2019
360 (Fehmarn Belt)	7.5 ± 0.1	4.5 ± 0.5	3.2 ± 0.1	3.7 ± 0.0	**1.7 ± 0.1**
022 (Lübeck Bight)	9.3 ± 0.2	6.3 ± 0.1	**4.5 ± 0.7**	6.1 ± 0.0	-
012 (Meckl. Bight)	5.5 ±0.0	4.8 ± 0.1	4.4 ± 0.0	4.7 ± 0.3	**2.8 ± 0.1**
113 (Arkona Sea)	3.7 ± 0.0	3.2 ±0.2	5.2 ± 0.0	2.8 ± 0.0	**2.6 ± 0.0**
213 (Bornholm Deep)	3.3 ± 0.2	2.8 ± 0.2	3.8 ± 0.1	**2.5 ± 0.0**	2.6 ± 0.1
271 (Gotland Deep)	**3.1 ± 0.0**	3.4 ± 0.4	3.9 ± 0.3	3.4 ± 0.0	4.0 ± 0.0
286 (Fårö Deep)	3.4 ± 0.0	**3.3 ± 0.5**	3.9 ± 0.1	3.9 ± 0.0	4.0 ± 0.0
284 (Landsort Deep)		3.9 ± 0.0	**3.4 ± 0.2**	3.9 ± 0.0	4.0 ± 0.0
245 (Karls Deep)	3.2 ± 0.0	3.3 ± 0.3	3.3 ± 0.1	3.6 ± 0.0	**1.2 ± 0.1**

4.4.2 Deep water processes in 2019

In central Baltic Sea deep waters, the nutrient distribution is primarily influenced by the occurrence or absence of strong barotropic and/or baroclinic inflows and, thus, by its oxygen/hydrogen sulphide concentrations in deep waters. The annual average phosphate concentration maxima of 2014 in the Gotland Sea is almost reached in 2019. Thus, the influence of the MBI that flushed the Gotland Deep in 2015 with oxygenated water vanishes year by year. Before the inflow, the annual average phosphate concentration was 4.50 µmol/l, dropped to 2.16 µmol/l in 2015 and steadily increased thereafter to 4.38 µmol/l in 2019 at the deep waters reference depth of 200 m (Table 11). During oxic conditions phosphate was bound to iron as well as to manganese and was transported to the sediment by particles. The particles are dissolved during anoxia and then release the phosphate back to the water column. Interestingly, the influence of the MBI showed a clear shift along the thalweg. The Fårö Deep as well as Landsort Deep reached the lowest phosphate concentration in 2017.

The fading of the MBI impact is also reflected in the depletion of nitrate in deep waters. Only the Bornholm Deep recovered in 2019 in terms of oxygen, and consequently showed elevated annual average nitrate concentration of 6.8 µmol/l. All other investigated stations at the selected reference depths show average annual nitrate concentrations below the detection limit (Table 11). It should be noted that anoxic conditions prevent mineralization of organic matter to nitrate. Instead, ammonium is formed and represents the end product of the degradation of biogenic material. Therefore, accumulation of ammonium in deep waters was recorded in Baltic Sea deep waters. In the Gotland Deep ammonium increased from 6.0 to 12.2 µmol/l, in the Fårö Deep from 3.6 to 9.1, and in the Landsort Deep from 5.0 to 8.0 µmol/l from 2018 to 2019. In the Bornholm Deep and the Karlsö Deep no significant changes were observed with regard to ammonium (Table 10). Figure 30 illustrates the nutrient distributions in the water column on the transect between the Darss Sill and the Northern Gotland Sea for the year 2019.

The stagnation period that has started in the Eastern Gotland Sea already in 2015, thus, shortly after the MBI of December 2014 (NAUMANN et al. 2018), was basically ongoing in 2019. Oxygen is decreasing and after depletion, hydrogen sulphide is accumulating in deep waters (Table 9). This is accompanied by phosphate and ammonium increase and a depletion of nitrate (Table 11). In 2019 the Bornholm Sea and the southern Gotland Sea received pulses of oxygenated waters in the bottom range. Afterwards, plumes of water bearing oxygen residues were entrained all over the eastern Gotland Basin in the 80 to 120 m depth range and could in August 2019 be detected as far as the Fårö Deep.

Table 11: Annual means and standard deviations for phosphate (Tab. 11.1), nitrate (Tab. 11.2) and ammonium (Tab. 11.3) in the deep water of the central Baltic Sea (IOW data).

11.1 Annual mean deep water phosphate concentration (µmol/l; Maxima in bold)

Station	depth/m	2015	2016	2017	2018	2019
213 (Bornholm Deep)	80	1.57 ± 0.44	2.23 ± 0.29	2.51 ± 1.15	**4.73 ± 1.56**	3.78 ± 1.40
271 (Gotland Deep)	200	2.16 ± 0.29	2.56 ± 0.14	2.91 ± 0.92	4.08 ± 0.13	**4.38 ± 0.25**
286 (Fårö Deep)	150	3.26 ± 0.23	2.93 ± 0.22	2.49 ± 0.12	3.55 ± 0.68	**4.02 ± 0.45**
284 (Landsort Deep)	400	3.57 ± 0.26	3.25 ± 0.31	3.08 ± 0.22	3.12 ± 0.22	**3.64 ± 0.57**
245 (Karls Deep)	100	3.92 ± 0.19	**4.25 ± 0.34**	3.77 ± 0.24	3.63 ± 0.34	3.51 ± 0.29

11.2 Annual mean deep water nitrate concentration (µmol/l; Minima in bold)

Station	depth/m	2015	2016	2017	2018	2019
213 (Bornholm Deep)	80	11.1 ± 2.5	10.4 ± 1.9	7.5 ± 2.3	**1.6 ± 1.5**	6.8 ± 2.9
271 (Gotland Deep)	200	7.5 ± 3.3	9.3 ± 0.7	1.8 ± 2.2	**0.0 ± 0.0**	**0.0 ± 0.0**
286 (Fårö Deep)	150	**0.0 ± 00**	1.4 ± 1.7	5.5 ± 3.5	**0.0 ± 0.0**	**0.0 ± 0.0**
284 (Landsort Deep)	400	**0.0 ± 00**	**0.0 ± 0.0**	**0.0 ± 0.1**	**0.0 ± 0.0**	**0.0 ± 0.0**
245 (Karls Deep)	100	**0.0 ± 00**	0.1 ± 00	0.1 ± 0.0	**0.0 ± 0.0**	**0.0 ± 0.0**

11.3 Annual mean deep water ammonium concentration (µmol/l; Maxima in bold)

Station	depth/m	2015	2016	2017	2018	2019
213 (Bornholm Deep)	80	0.2 ± 0.1	0.2 ± 0.1	0.2 ± 0.3	**1.9 ± 2.4**	1.5 ± 3.1
271 (Gotland Deep)	200	1.6 ± 3.7	0.2 ± 0.0	0.8 ± 0.9	6.0 ± 2.3	**12.2 ± 3.8**
286 (Fårö Deep)	150	7.2 ± 2.1	2.0 ± 2.0	0.1 ± 0.0	3.6 ± 1.7	**9.1 ± 1.2**
284 (Landsort Deep)	400	6.5 ± 1.1	7.8 ± 3.3	3.8 ± 1.9	5.0 ± 2.2	**8.0 ± 1.**0
245 (Karls Deep)	100	7.7 ± 1.2	9.7 ± 1.7	8.4 ± 1.5	**10.4 ± 2.9**	9.4 ± 5.1

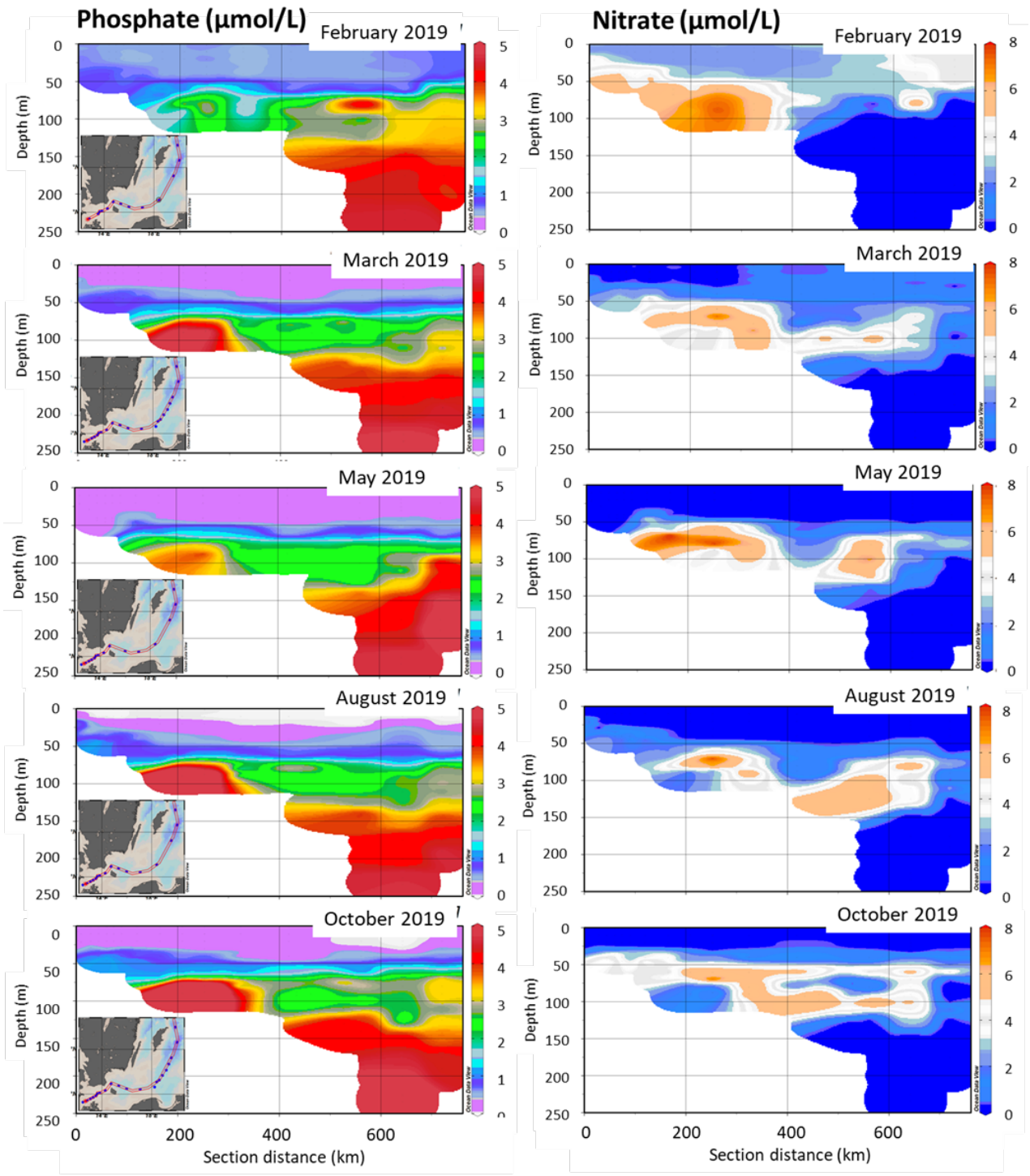

Fig. 30: Vertical distribution of phosphate (left column) and nitrate (right column) in 2019 between the Darss Sill and the northern Gotland Basin measured on the monitoring cruises in February, March, May, August and October (figure panels were prepared by using ODV 5, (SCHLITZER 2018)).

In **surface water** a south-north gradient was documented in February from 2 to 4 µmol/l for nitrate and a patchy distribution of the phosphate concentration usually between 0.5 and 1 µmol/l with higher values in the North. In March nitrate was already depleted in surface water in the western half of the transect and was completely depleted in May 2019 in surface waters. Phosphate show residues below about 0.5 µmol/l from March to October indicating the lowest concentration in August in the upper 15 m of the water column (Figure 30).

The nitrate and phosphate concentration in **deep waters** of the eastern Gotland basin are 0 ml/l and 4.5 - 5 µmol/l, respectively. In the range between 60 and 150 m depth also the inflow of warm/haline waters impacted nitrate and phosphate concentrations in these intermediate and deep waters similarly as for oxygen. Plumes of water with elevated nitrate concentrations of 5 to 8 µmol/l from the Bornholm Basin entered the eastern Gotland Basin during 2019 between 80 and 120 m depth. In October, the inflow water leveled in between 80 and 120m depth, still showing a nitrate concentration of 4 – 6 µmol/l and a phosphate concentration of 2.5 to 3 µmol/l (Figure 30).

4.5 Nutrients: Particulate organic carbon and nitrogen (POC, PON)

The organic matter (OM) consisting of thousands of compounds is important to understand the carbon cycle in the ocean (HANSELL 2002, KULINSKI & PEMPKOWIAK 2011). For practical reasons OM is divided in dissolved organic matter (DOM) and particulate organic matter (POM) defined by filtration of seawater. Both POM and DOM originate from internal and external sources (river runoff, atmosphere, sediments, water exchange and biological production). For carbon the dominating species is dissolved inorganic carbon (DIC), representing more than 90% of the total carbon in the oceans. In the Baltic Sea contribution of organic bound carbon and nitrogen is different. DIC is about 85% (1,850 mmol/kg C), the dissolved organic carbon (DOC) is about 15% (320 mmol/kg) and POC accounts for less than 1% (7 mmol/kg) on average (NAUSCH et al. 2008). A review of POC and DOC measurements in the Baltic Sea can be found in MACIEJEWSKA & PEMPKOWIAK (2014). The nitrogen fractions are more variable, the total DIN is only 5-10% (5 µmol/kg), DON about 66% (15 µmol/kg) and PON about 15% (3 µmol/kg).

The concentrations of organic matter in the Baltic Sea are higher than those found in open ocean water and even higher concentrations are found close to the rivers running into the Baltic Sea (terrestrial sources indicated).

In the surface layer POC and PON concentrations are mainly controlled by the presence, growth and degradation of biological produced material. POC and PON values show a clear seasonal signal with higher values in spring and summer (Fig. 31-34). At deeper stations with a seasonal thermocline or permanent halocline, the accumulation of sinking particle at the bottom or bottom layer resulted in higher POC/PON concentrations after the bloom periods (Figure 35). This signal is not always visible (depending on the sampling time and resolution) as degradation of the organic matter is fast.

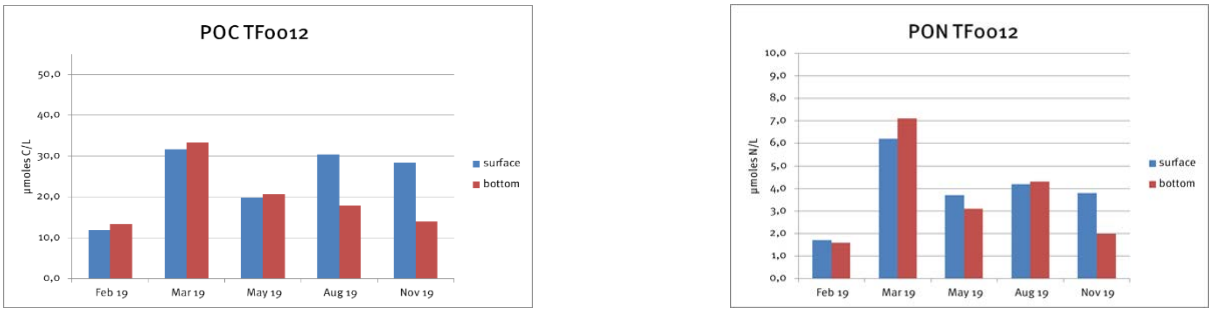

*Fig. 31: Changes of particulate organic carbon and particulate organic nitrogen at key station **Mecklenburg Bight** (TF0012) during the year 2019 - surface (2m) and bottom (24 m) in (µmol/l)*

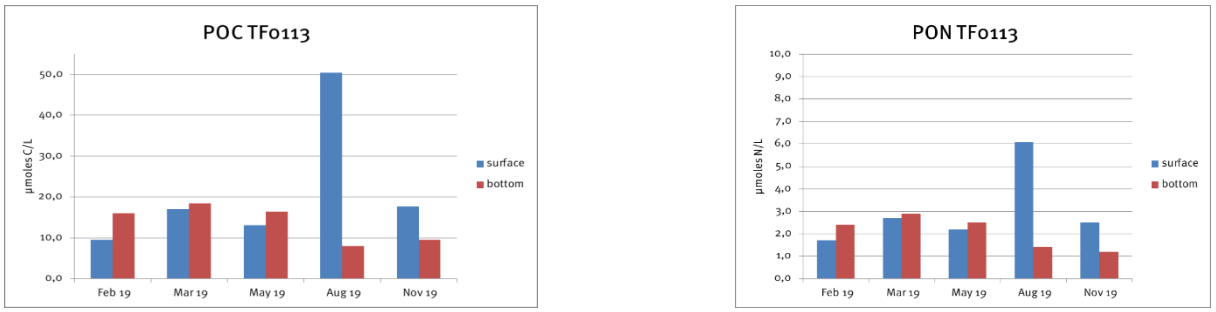

*Fig. 32: Changes of particulate organic carbon and particulate organic nitrogen at key station **Arkona Basin** (TF0113) during the year 2019 - surface (2m) and bottom (46 m) in (µmol/l).*

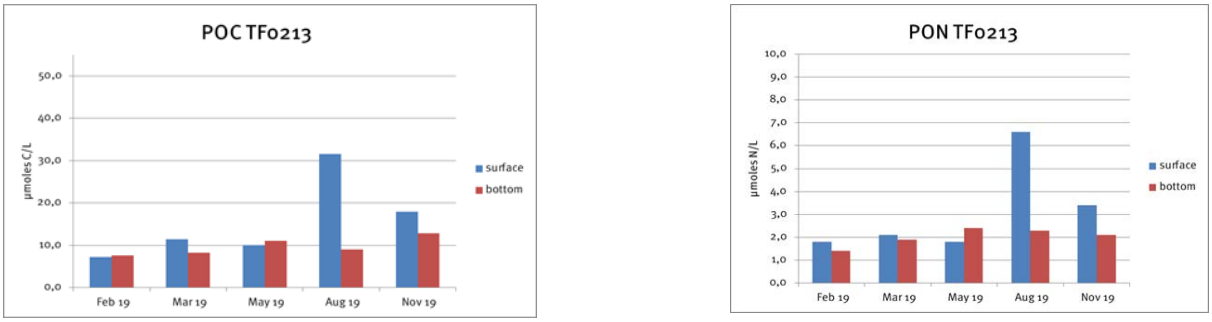

*Fig. 33: Changes of particulate organic carbon and particulate organic nitrogen at key station **Bornholm Basin** (TF0213) during the year 2019 - surface (2m) and bottom (88 m) in (µmol/l).*

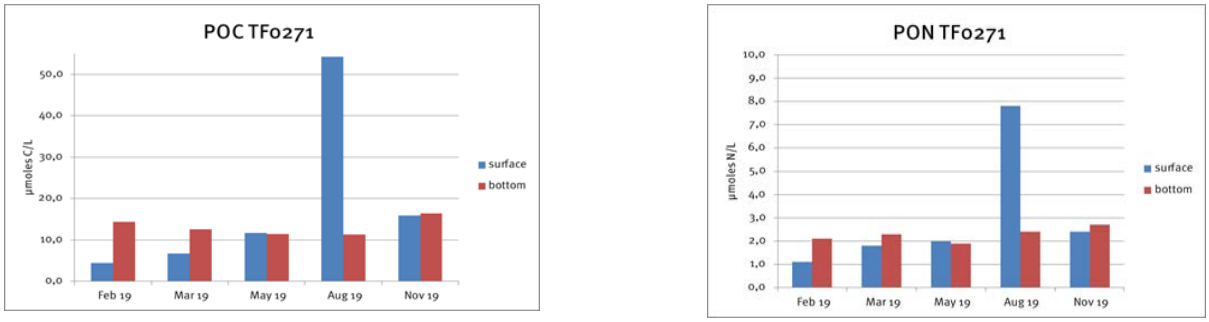

*Fig. 34: Changes of particulate organic carbon and particulate organic nitrogen at key station **Gotland Deep /Eastern Gotland Basin** (TF0271) during the year 2019 - surface (2m) and bottom (236 m) in (µmol/l).*

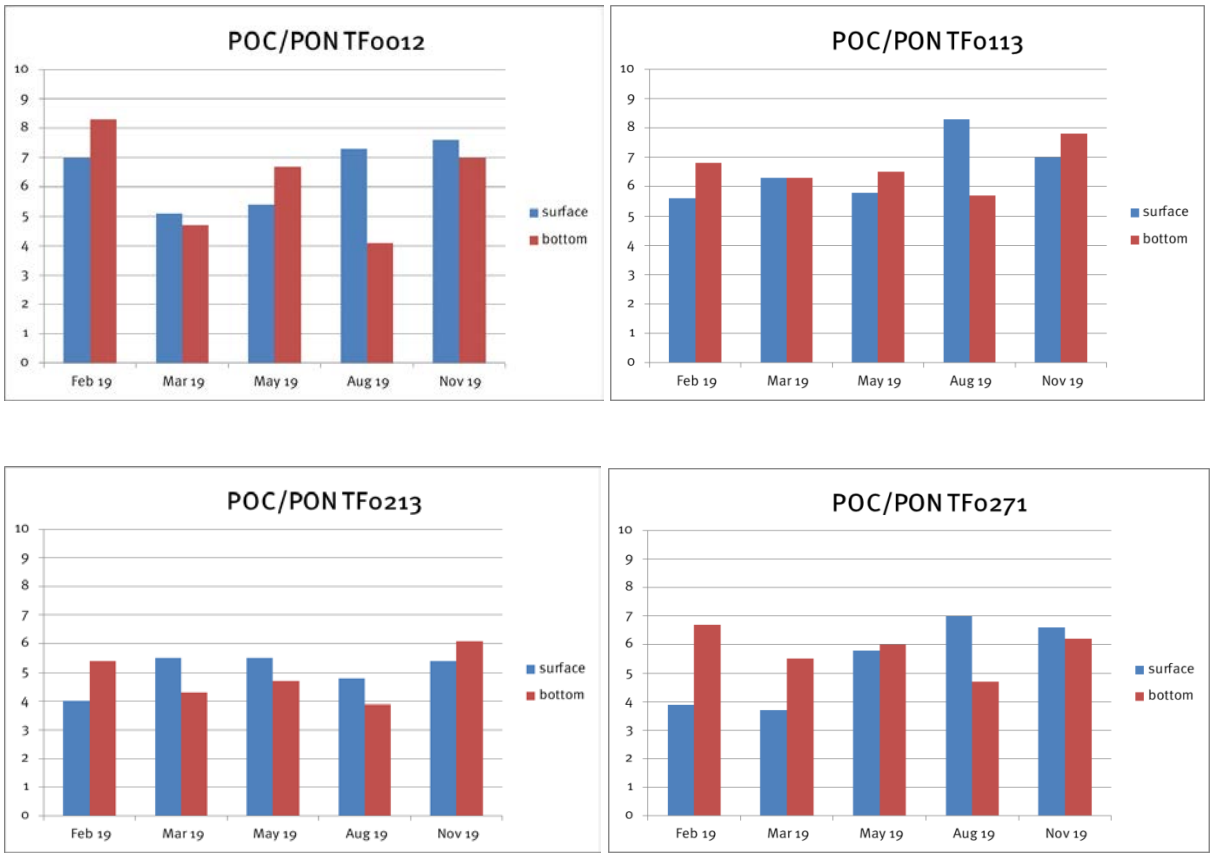

Fig. 35: Comparison of POC/PON ratios in surface and bottom samples at the key stations Mecklenburg Bight (TF0012), Arkona Basin (TF0113), Bornholm Basin (TF0213), Gotland Deep /Eastern Gotland Basin (TF0271).

Besides the production of organic matter during photosynthesis and following biological processes, the terrestrial input by rivers is another source of organic compounds. For DOC a clear relation between DOC concentration and salinity is found (NAGEL 2005), showing the dominance of terrestrial DOM. The input of POM from land is less important (Fig. 36).

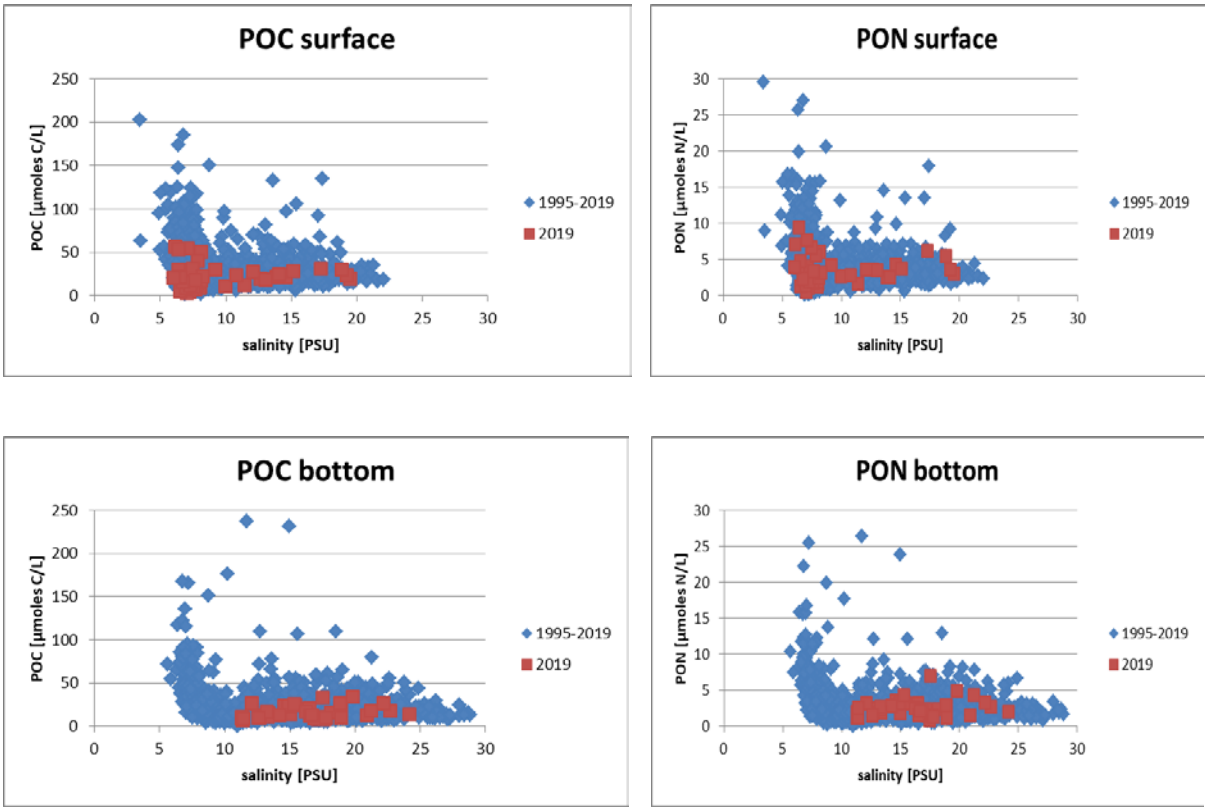

Fig. 36: Particulate organic carbon in the surface and bottom water from 1995-2019.

The results from the year 2019 are in any parameter within the expected range.

4.6 Organic hazardous substances in Baltic Sea surface water in winter 2019

The Baltic Sea is largely affected through contamination since the onset of the industrialization in the late 19th century. The partially uncontrolled release of industrial and agricultural chemicals in its catchment area led to a subsequent contamination of coastal and marine environments giving rise to consequences to marine organisms' health. Measures were taken to regulate production and use of some of the organic pollutants on national level as well as through international regulations such as the Stockholm Convention or the International Maritime Organization (HELCOM 2010b, 2010a, 2018a).

In this report obtained data for chlorinated (CHC) and polycyclic aromatic hydrocarbons (PAH) in Baltic Sea surface water from the January/February 2019 observation are summarized (for an overview see Figure 37), time series data are pursued and results are assessed based on criteria of the Marine Strategy Framework Directive and HELCOM.

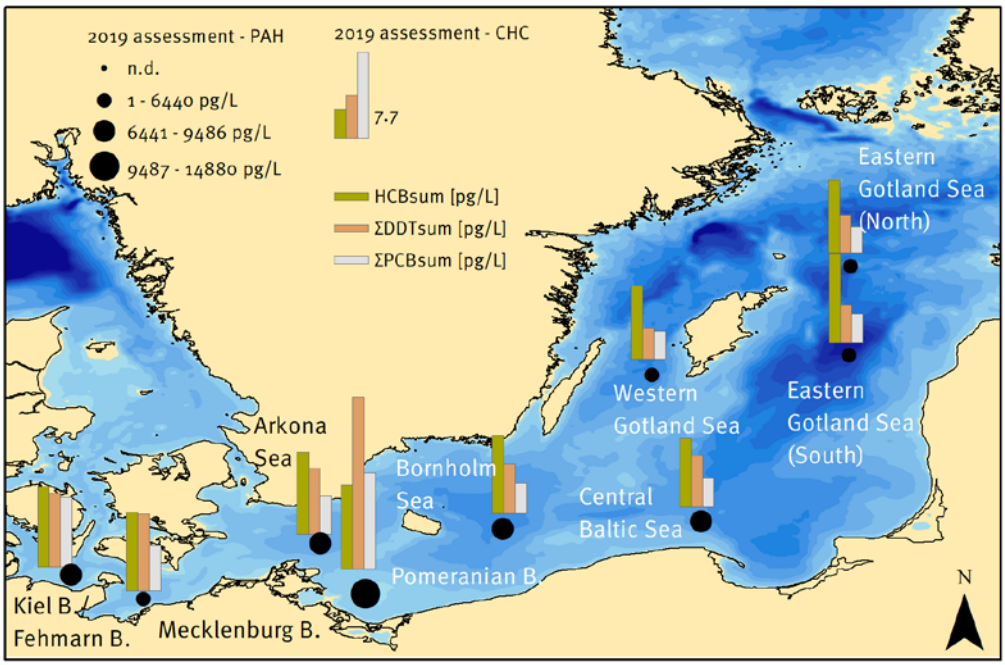

Fig. 37: Summary of obtained data for polycyclic aromatic hydrocarbons (U.S. EPA PAH exc. Naph) and chlorinated hydrocarbons (CHC) in Baltic Sea surface water in winter 2019 (ΣPAH_{sum}: summarized 15 U.S. EPA PAH indicator compounds (exc. Naph) in dissolved and particulate water fraction, HCB_{SUM}: summarized HCB concentration for dissolved and particulate fraction, ΣDDT_{sum}: summarized concentrations of DDT and metabolites in dissolved and particulate fraction, ΣPCB_{sum}: summarized concentrations of seven PCB_{ICES} of dissolved and particulate fraction).

Surface water samples were taken in winter season, at which the Baltic Sea water is most unaffected by biological conditions such as through algal blooms. Thus, samples were acquired during the expedition EMB206 with RV *Elisabeth Mann Borgese* in January/February 2019 at sites in the Kiel Bight (T1), Mecklenburg Bight (T2), Arkona Sea (T3), Pomeranian Bight (T4), Bornholm Sea (T5), Central Baltic Sea (T6) as well as in the Eastern Gotland Sea (South and North, T7 and T8), and the Western Gotland Sea (T9).

The water samples were obtained by transect sampling in the respective Baltic Sea area (Figure 38). During the transect route a pump/filtration system was used to continuously pump surface water from 5 m below surface through a GF/F filter and subsequently through an XAD-2 resin packed column with a flow rate of about 1.1 l/min for 4 to 6 hours. Extraction of filters and columns was conducted at IOW. Chemical analysis of the CHC and PAH in the dissolved and particulate water fractions was conducted as described before (Schulz-Bull et al. 2011) and followed accredited procedures. In Table 12 the analysed substances are summarized.

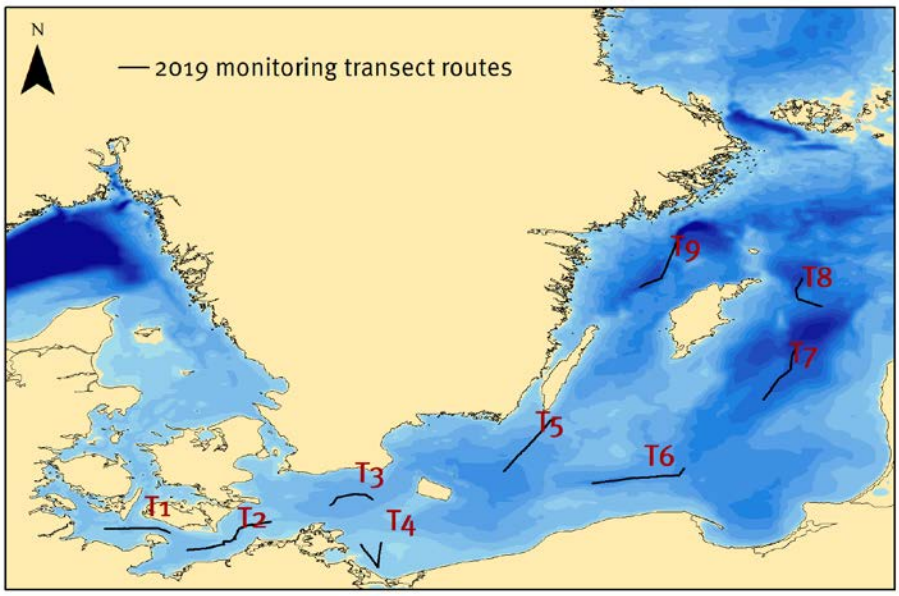

Fig. 38: Transect routes of the research vessel during winter monitoring 2019. T1: Kiel Bight/Fehmarn Belt, T2: Mecklenburg Bight, T3: Arkona Sea, T4: Pomeranian Bight, T5: Bornholm Sea, T6: Central Baltic Sea, T7 Eastern Gotland Sea (South), T8: Eastern Gotland Sea (North), T9: Western Gotland Sea.

Table 12: Analyzed compounds in Baltic Sea surface water during the winter 2019 observation.

Chlorinated hydrocarbons	7 ICES-polychlorinated biphenyls (PCB_{ICES})	PCB28/31, PCB52, PCB101, PCB118, PCB153, PCB138, PCB180
	Dichlorodiphenyl-trichloroethane (DDT) and metabolites	*p,p'*-DDT, *o,p'*-DDT dichlorodiphenyldichloroethylene (DDE): *p,p'*-DDE dichlorodiphenyldichloroethane (DDD): *p,p'*-DDD
		Hexachlorobenzene (HCB)
Polycyclic aromatic hydrocarbons	U.S. EPA PAH indicator compounds except naphthalene	acenaphthylene (ACNLE), acenaphthene (ACNE), fluorine (FlE), phenanthrene (PA), anthracene (ANT), fluoranthene (FLU), pyrene (PYR), benzo(*a*)anthracene (BAA), chrysene (CHR), benzo(*b*)fluoranthene (BBF), benzo(*k*)fluoranthene (BKF), benzo(*a*)pyrene (BAP), indeno(1,2,3-*cd*)pyrene (ICDP), dibenzo(*a,h*)anthracene (DBAH), benzo(*g,h,i*)perylene (BGHIP)

4.6.1 Chlorinated Hydrocarbons (CHC): DDT and metabolites

The insecticide DDT has been used as a contact and feeding poison in agriculture and forestry since the 1940s. DDT technical formulations were mixtures of *o,p'* and *p,p'* congeners with *p,p'*-DDT as the predominant one (Figure 39). In the environment DDT degrades to the stable metabolites DDE and DDD. Due to their chemical stability and lipophilic properties, these contaminants accumulate in the tissues of animals and humans via the food chain. Endocrine activity was shown for the *p,p'*-DDT and *p,p'*-DDE, and they were classified as "probably carcinogenic in humans" by the WHO in 2015.

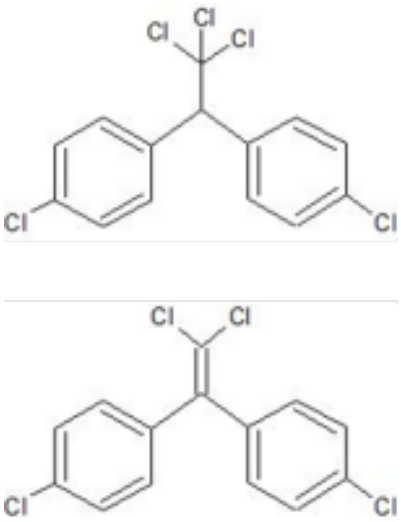

Fig. 39: Chemical structures of p,p'-DDT and its metabolite p,p'-DDE.

Since the 1970s DDT has been banned in most of the western industrialized countries. Production and use of DDT is internationally restricted with the initial Stockholm Convention of 2004. However, in some countries DDT is still used today, particularly for the control of disease-transmitting insects such as *Anopheles*.

In January/February 2019 concentrations of DDT and metabolites in Baltic Sea surface water ranged from about 3 pg/L ΣDDT_{sum} [2] in the Western Gotland Sea (T9) to about 16 pg/L ΣDDT_{sum} in the Pomeranian Bight (T4) (Appendix Table 1, Figure 40). Basically, concentrations of ΣDDT_{part} [3] correlate with concentrations of suspended matter (SPM) (Figure 39, upper panel). Thus, highest observed SPM concentrations at the Pomeranian Bight (about 1.4 mg/L) and Fehmarn Belt/Kiel Bight (about 0.8 mg/L) are accompanied with highest particulate ΣDDT_{part} concentrations of about 9 pg/L and 2 pg/L. Thus, the particulate fraction of the water largely contributes to the DDT contaminant load of the Baltic Sea surface water. Despite this, also ΣDDT_{diss} [4] was highest at the Pomeranian Bight (T4) indicating highest pressure for DDT and metabolites in this area brought by river Odra. Overall, with exception of the Pomeranian Bight, concentrations of DDT and its metabolites decrease from the Western Baltic Sea with about 7 pg/L ΣDDT_{sum} to the western Gotland Sea with about 3 pg/L ΣDDT_{sum}.

As observed in previous years, too, higher concentrations of the long-lived degradation product *p,p'*-DDE compared to *p,p'*-DDT were recorded in the entire study area. This implies no recent input of DDT, which is also reflected by the *p,p'*-DDT/*p,p'*-DDE ratios mostly below 0.5 (Table 13)

[2] ΣDDT_{sum}: summarized concentration of DDT congeners and their metabolites in particulate and dissolved fraction
[3] ΣDDT_{part}: summarized concentration of DDT congeners and their metabolites in particulate fraction
[4] ΣDDT_{diss}: summarized concentration of DDT congeners and their metabolites in dissolved fraction

(STRANDBERG et al. 1998). Interestingly, the ratio was particularly low at the Pomeranian Bight (4), where highest ΣDDT_{sum} concentrations were found. Thus, mostly degradation products of DDT were transported by the river Odra into the Baltic Sea.

Table 13: Ratios of p,p'-DDT/p,p'-DDE for the determined concentrations of DDT and metabolites in Baltic Sea surface water of winter 2019.

	T1	T2	T3	T4	T5	T6	T7	T8	T9
p,p'-DDT/*p,p'*-DDE [5]	0.40	0.49	0.49	0.22	0.46	0.49	0.48	0.51	0.45

[5] Ratios were determined from summarized particulate and dissolved concentrations

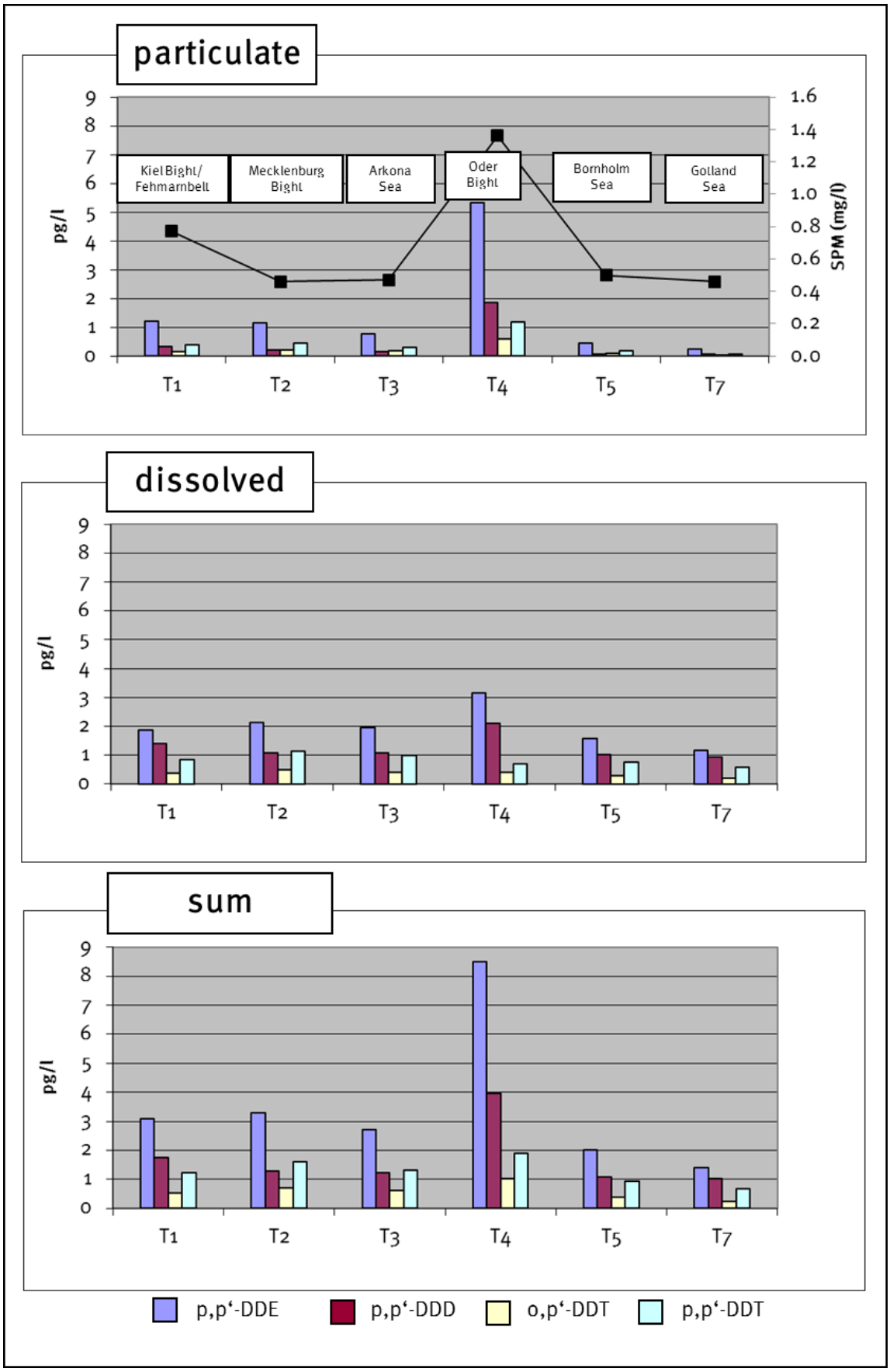

Fig. 40: Concentrations of DDT and metabolites in the dissolved and particulate fractions of Baltic Sea surface water samples of the winter 2019 surveillance (see Figure 38 for sampling areas).

Concentrations of dissolved *p,p'*-DDE and *p,p'*-DDT from winter observations since 2002 are shown in Figure 41 for the sites Mecklenburg Bight and Arkona Sea. Overall, decreasing concentrations of both compounds can be observed for both sites. Obviously, dissolved *p,p'*-DDT is subjected to higher annual variations than *p,p'*-DDE.

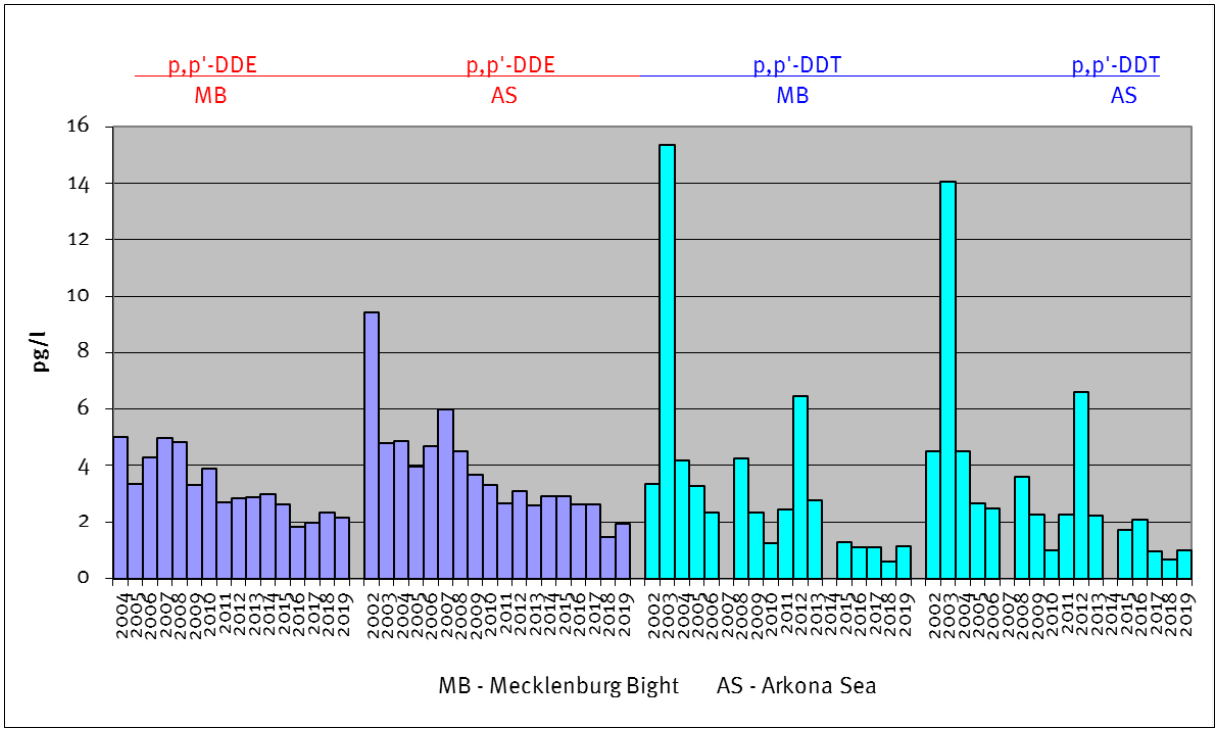

Fig. 41: Time series of p,p'-DDT and p,p'-DDE concentrations for the dissolved fraction of sampled surface water of the Mecklenburg Bight and Arkona Sea since 2002.

4.6.2 Chlorinated Hydrocarbons (CHC): Hexachlorobenzene (HCB)

HCB is a fungicide (Figure 42), which was mainly used for seed treatment and as wood preservative, but also as plasticizer and flame retardant in plastic materials. HCB is a persistent contaminant and has bioaccumulative properties. It is toxic to aquatic organism. Use and production of HCB is internationally banned through the Stockholm Convention of 2004.

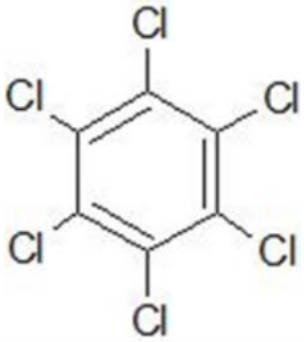

Fig. 42: Chemical structure of HCB.

Observed concentrations for HCB_{sum}[6] in Baltic Sea surface water were very similar at the study sites and ranged from about 6 to 8 pg/L HCB_{sum} (Appendix Table 2). HCB was mainly found in the dissolved fractions. HCB_{diss}[7] is uniformly distributed in the Baltic Sea, which implies that there

[6] HCB_{SUM}: summarized HCB concentrations of particulate and dissolved fraction
[7] HCB_{diss}: HCB concentrations in the dissolved fraction

are no local inputs such as from riverine sources. Highest HCB_{part}[8] concentrations were found for the Pomeranian Bight and the Fehmarn Belt/Kiel Bight, which is attributed to the high SPM concentrations at these sites.

The long-term development of dissolved HCB concentrations since 2001 for the areas Mecklenburg Bight and Arkona Sea are shown in Figure 43. Courses of HCB_{diss} concentrations in both areas are similar. The pattern depicts regularly increasing HCB_{diss} concentrations from certain years such as from 2002, 2008 and 2016, which declined thereafter. This implies that HCB is periodically introduced into the Baltic Sea, presumably by riverine inflow. Overall, since 2001 dissolved HCB concentrations have decreased only slightly, which reflects the persistence of HCB in the marine environment.

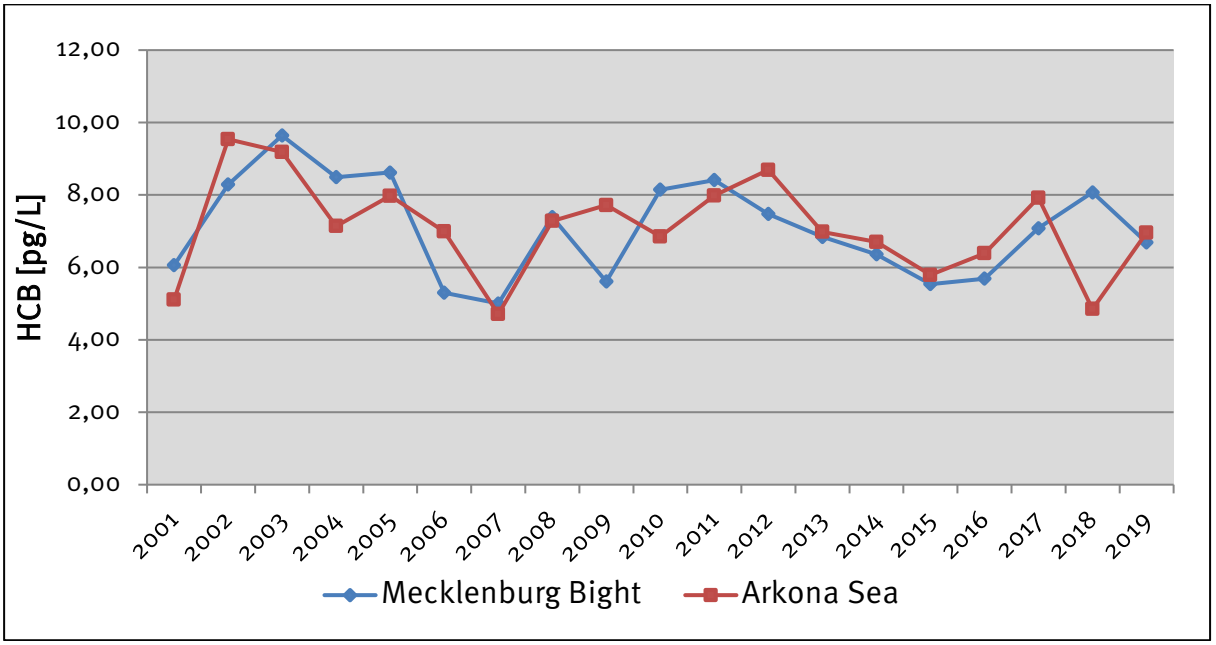

Fig. 43: Concentrations of dissolved HCB in Baltic Sea surface water of the Mecklenburg Bight and Arkona Sea since 2001.

4.6.3 Chlorinated Hydrocarbons (CHC): Polychlorinated Biphenyls (PCB)

Since the 1930s PCBs (Figure 44) had been used as fluids in hydraulic systems, as lubricants and insulating and cooling fluids in transformers and electrical capacitors. Furthermore, PCBs were utilized as plasticizers in paints, sealants and plastic materials. With their classification as one of the Persistent Organic Pollutants, their production and use was internationally banned by the

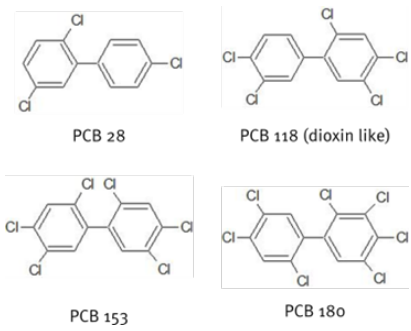

Fig. 44: Chemical structures of some PCB congeners.

[8] HCB_{part}: HCB concentrations in the particulate fractions

initial Stockholm Convention of 2004.

Commercial PCB formulations usually consisted of a wide range of PCB congeners which differ in the number and position of substituted chlorine on the biphenyl rings. Seven of these PCB congeners were suggested as indicators of environmental monitoring by the International Council of the Exploration of the Sea (ICES, PCB_{ICES}), due to their high concentrations in technical formulations and wide chlorination range (WEBSTER et al. 2013). PCB118 is representative for the most toxic dioxin-like PCBs.

Observed PCB_{ICES} concentrations ranged from about 2.3 pg/L in the Eastern Gotland Sea (South, T7) to about 9 pg/L ΣPCB_{sum} [9] in the Pomeranian Bight (T4) (Appendix Table 2, Figure 45). The low chlorinated PCB congeners such as PCB28/31 were mainly found in the dissolved water fraction whereas higher chlorinated congeners, particularly PCB153 and PCB138, are associated to the particulate fraction.

Highest concentrations for ΣPCB_{part} [10] were found at those sites with highest SPM concentrations, thus, at the Kiel Bight/Fehmarn Belt (T1) with about 3 pg/L and the Pomeranian Bight (T4) with about 6 pg/L. This might derive from contaminant resuspension from the surface sediments due to strong winds at the shallow sites of the Fehmarn Belt/Kiel Bight. At the Pomeranian Bight the high load of SPM presumably derives from the riverine inflow of the river Odra.

Concentrations of ΣPCB_{diss} [11] decrease from the western Baltic Sea to the area of the Gotland Sea (Appendix Table 2, Figure 45). Particularly the higher chlorinated PCB congeners such as PCB153 and PCB180 and the dioxin-like PCB118 are highest in the area of the Kiel Bight/Fehmarn Belt which shows that at this site contaminant pressure from PCB contamination is highest among the investigated sites.

Concentrations for ΣPCB_{diss} in the study areas Mecklenburg Bight and Arkona Sea since 2001 are shown in Figure 46. At both sites concentrations decreased continuously from about 15 pg/L in 2002 to currently about 4 pg/L.

[9] ΣPCB_{SUM}: summarized concentrations of PCB_{ICES} congeners of the dissolved and particulate fraction
[10] ΣPCB_{part}: summarized concentrations of PCB_{ICES} congeners in the particulate fraction
[11] ΣPCB_{diss} : summarized concentrations of PCB_{ICES} congeners in the dissolved fraction

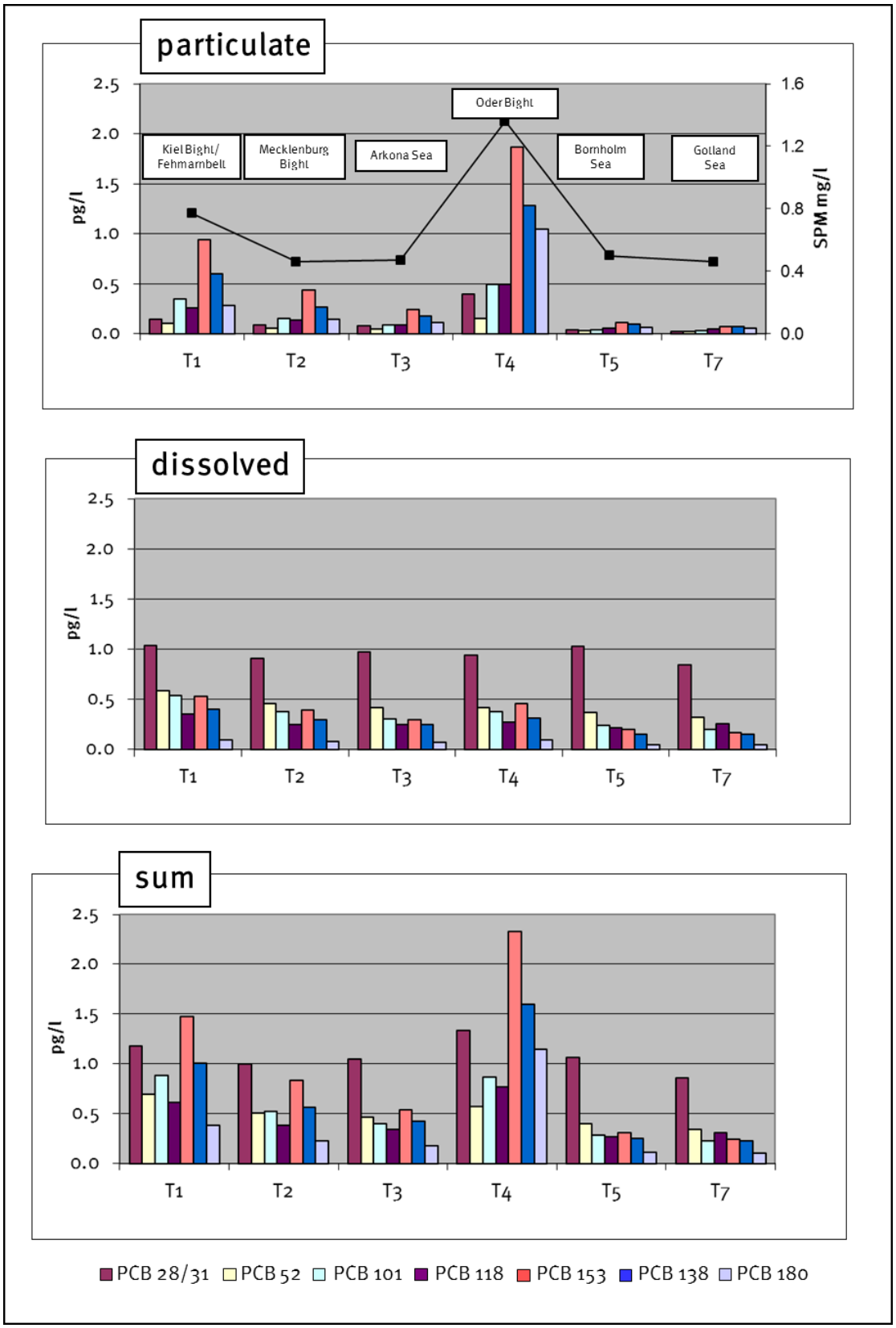

Fig. 45: Concentrations of PCB$_{ICES}$ in the particulate and dissolved fractions of Baltic Sea surface waters in winter 2019 (see Figure 38 for sampling areas).

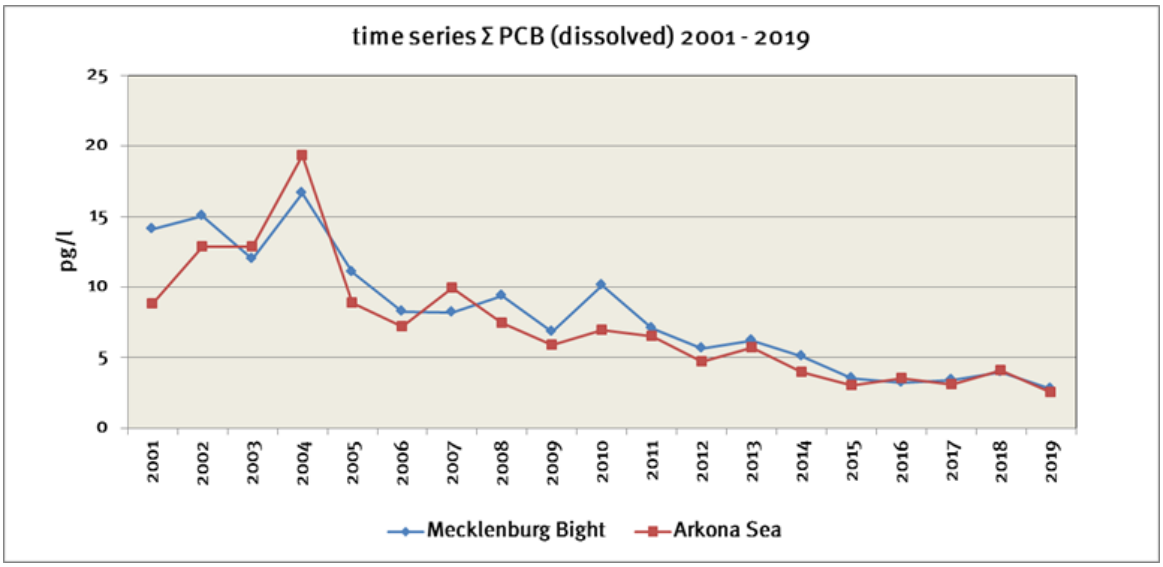

Fig. 46: Time series of ΣPCB_{diss} concentrations of the dissolved fraction of Baltic Sea surface water at the Mecklenburg Bight and Arkona Sea since 2001.

4.6.4 Polycyclic Aromatic Hydrocarbons (PAH)

Polycyclic aromatic hydrocarbons (PAH) are a group of organic substances with at least two connected aromatic rings (Figure 47). PAHs result from incomplete combustion of organic material. Therefore, they largely derive from industrial combustion processes such as from fossil fuel or wood combustion. Thus, the presence of these pollutants in the environment is strongly associated to anthropogenic activities. However, they also derive from natural sources such as during maturation of coal and oil as well as from forest fires and volcanic eruptions. PAHs enter the marine ecosystem particularly through oil spills from shipping, river discharges and the atmosphere.

The properties of the individual PAHs are mainly characterized by the number of condensed aromatic rings. The 2 to 3 ring low molecular weight PAHs are water soluble and are mainly found in the dissolved water fraction, while high molecular weight PAHs are mostly associated to the particulate water fraction and sediments. With increasing number of aromatic rings lipophilicity of the PAHs increases and they accumulate in the fatty tissue of organisms. PAHs are persistent in the environment and have toxic, carcinogenic as well as reprotoxic properties.

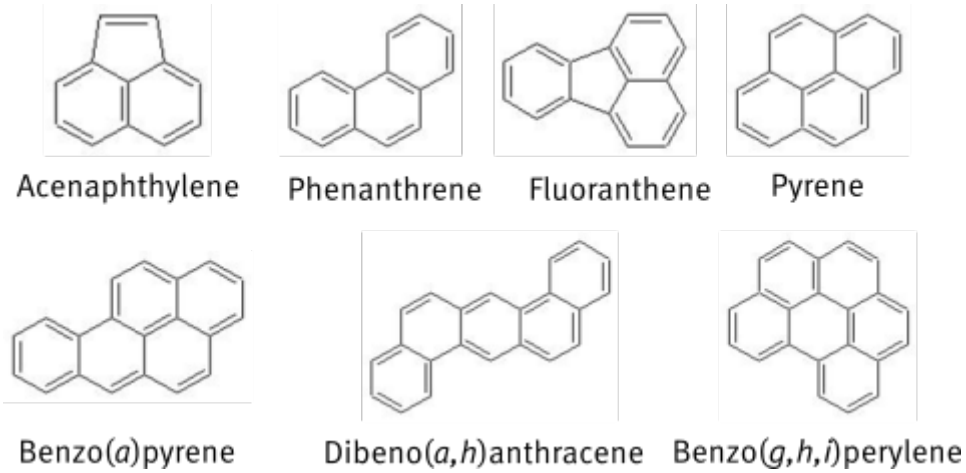

Fig. 47: Chemical structures of some PAH compounds.

PAHs belong to the main environmental pollutants; a number of 16 compounds – the U.S. EPA PAH indicator compounds – serve as representatives for PAH contamination in the environment (KEITH 2015) and, thus, are an inherent part in environmental surveillance.

With an increasing number of aromatic rings the octanol/water partition coefficients ($logK_{ow}$) of the PAH increase, and thus, their water solubility decrease. Therefore, in the surface waters of the Baltic Sea low molecular weight PAH were predominantly found in the dissolved water fraction, particularly fluorine, phenanthrene and fluoranthene, whereas high molecular weight PAH such as indeno(1,2,3-*cd*)pyrene and benzo(*g,h,i*)perylene were mostly found in the particulate fraction (Figure 48). Interestingly, highest concentrations of high molecular weight PAH in the dissolved and particulate water fractions were found in the Pomeranian Bight, Bornholm Sea, Central Baltic Sea and the Eastern Gotland Sea (South) (Appendix Table 3, Figure 48).

Obtained concentrations for ΣPAH_{sum}[12] in the Baltic Sea surface water ranged from about 4,400 pg/L in the western Gotland Sea to about 15,000 pg/L at the Pomeranian Bight (Figure 48). Highest concentrations for ΣPAH_{sum} were found in the Kiel Bight/Fehmarn Belt (T1, about 8,000 pg/L) and the Pomeranian Bight (T4, about 15,000 pg/L). In contrast to the chlorinated hydrocarbons, this is not solely attributable to higher SPM concentrations at those sites, because also highest concentrations for ΣPAH_{diss}[13] were determined at T1 and T4. Thus, the areas Kiel Bight/Fehmarn Belt and Pomeranian Bight are mostly contaminated with PAH among the investigated sites.

Diagnostic ratios can be utilized to identify the sources of PAH contamination. The ratio BAA/(BAA+CHR) is often applied to distinguish petrogenic (‹ 0.2) and combustion (› 0.35) as sources and was shown to be most stable over long distances during the environmental fate of PAH (Katsoyiannis & Breivik, 2014). Application to the obtained PAH data revealed ratios ranging from 0.2-0.35 indicating mixed PAH sources for all investigated sites (Table 14). The diagnostic ratio benzo(*a*)pyrene/benzo(*g,h,i*)perylene (BAP/BGHIP) can be utilized to identify PAH contamination from traffic derived sources, which is usually indicated with a ratio above 0.6 (e.g., YUNKER et al., 2002). For the investigated sites BAP/BGHIP › 0.6 were found for the sites Pomeranian Bight (T4), Central Baltic Sea (T6) and the Eastern Gotland Sea (North) (T8), which implies that marine traffic contributes to the PAH pressure at those sites (Table 14).

Table 14: Diagnostic ratios BAP/BGHIP and BAA/(BAA+CHR) for the identification of PAH sources in Baltic Sea surface water in winter 2019.

	T1	T2	T3	T4	T5	T6	T7	T8	T9
BAP/BGHIP	0.52	0.45	0.49	0.79	0.47	0.61	0.55	0.66	0.53
BAA/(BAA+CHR)	0.27	0.23	0.23	0.35	0.28	0.27	0.28	0.25	0.25

Concentrations for dissolved ΣPAH_{diss} since 2001 for the areas Mecklenburg Bight and Arkona Sea are shown in Figure 49. The pattern depicts no decreasing trend for both sites and high

[12] ΣPAH_{sum}: summarized U.S. EPA PAH indicator compounds (exc. Naph) for dissolved and particulate fraction
[13] ΣPAH_{diss}: summarized U.S. EPA PAH indicator compounds (exc. Naph) for dissolved fraction

variations of the concentrations. Concentrations varied particularly at the Mecklenburg Bight, which indicates temporally intense PAH sources.

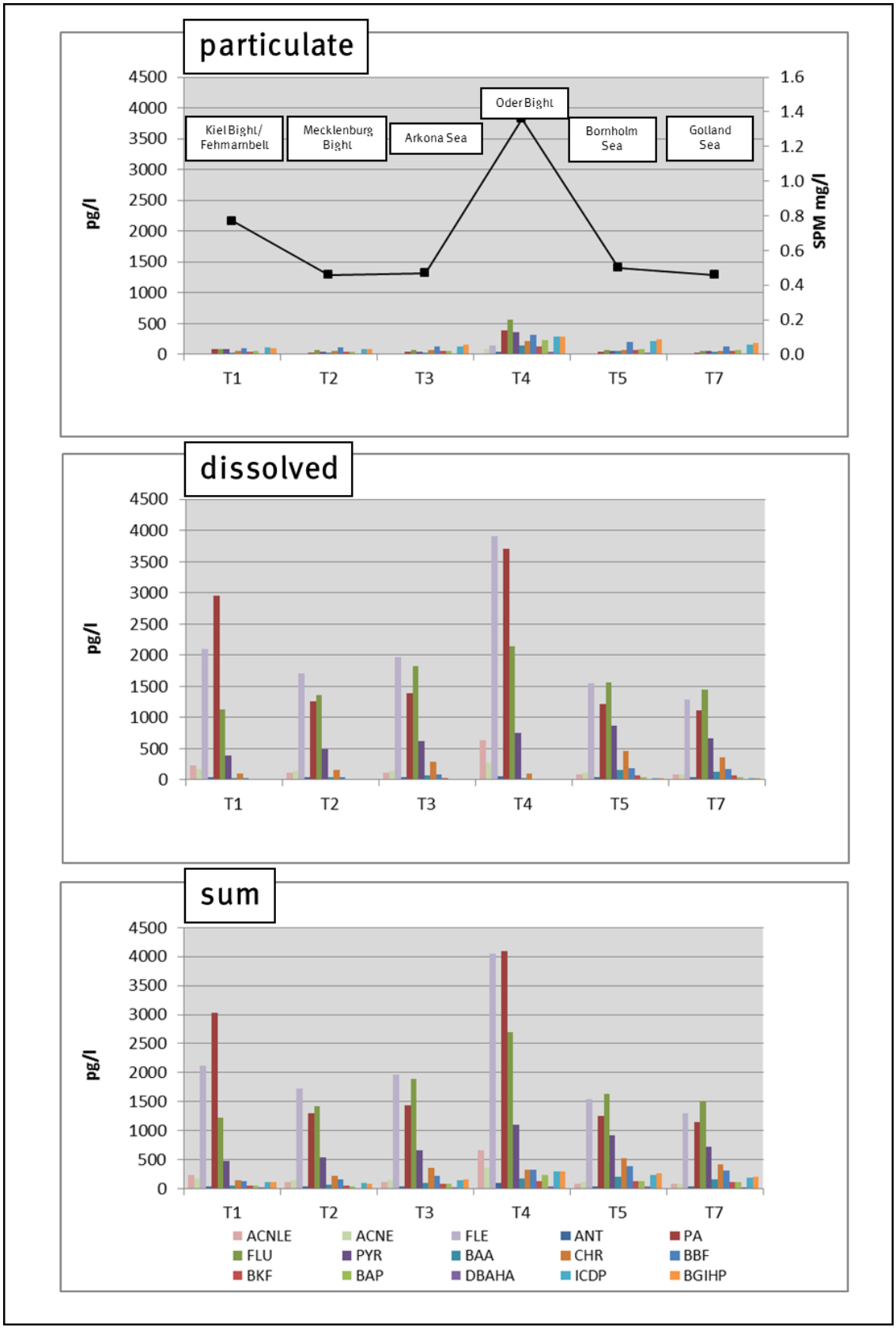

Fig. 48: Concentrations of PAHs in surface waters of the Baltic Sea in winter 2019 (see Figure 38 for sampling areas).

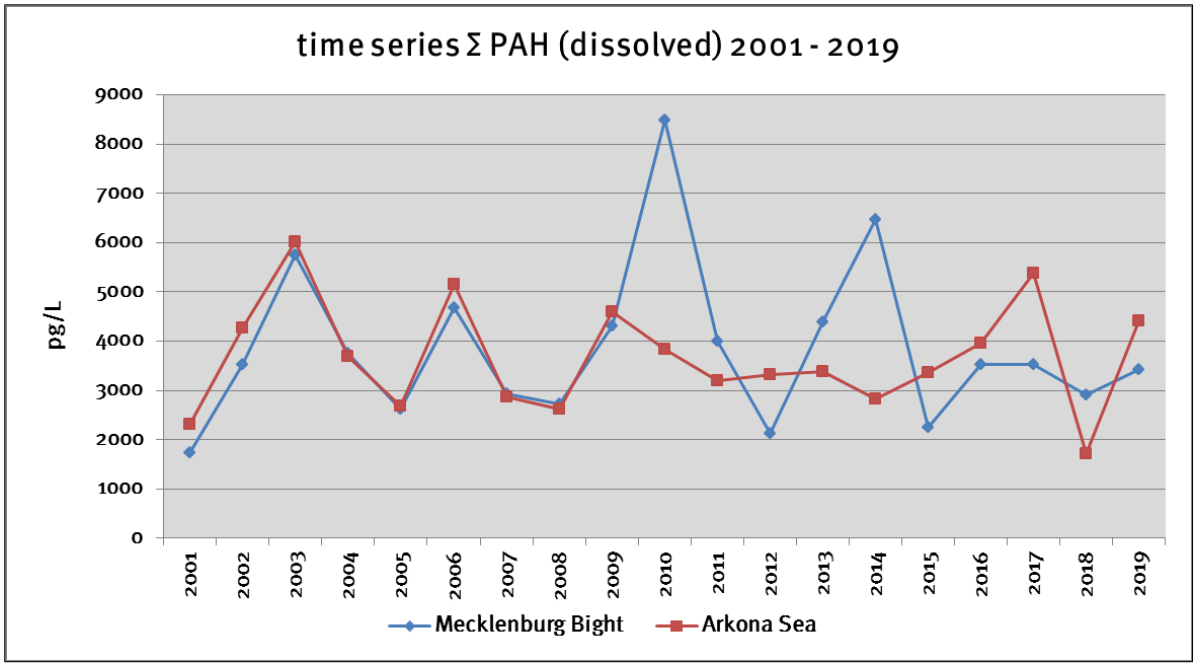

Fig. 49: Concentrations of dissolved PAH in surface waters of the Mecklenburg Bight and Arkona Sea since 2001.

4.6.5 Assessment of results

Quantitative limits for contaminants in the Baltic Sea have been defined within the framework of European water policy and the HELCOM commitment within the scope of the Baltic Sea Action Plan. Under European legislation monitoring of hazardous substances in the Baltic Sea is directed through the Marine Strategy Framework Directive (MSFD) (2008/56/EC, MSFD) (EC 2008a) and the Water Framework Directive (2000/60/EG, 2008/105/EG, 2013/39/EU, WFD) (EC 2000, 2008b, 2013). The priority substances of the WFD and defined Environmental Quality Standards (EQS) for surface waters serve as the basis to evaluate the data for Baltic Sea surface water in the winter 2019 (Table 15).

None of the obtained contaminant results exceeds defined maximum allowable concentration EQS (MAC-EQS). Determined concentrations for DDT/metabolites and HCB do not exceed annual average EQS (AA-EQS) values as well. However, for a number of high molecular weight PAH compounds, in particular for benzo(*j*)fluoranthene, benzo(*g,h,i*)perylene and the indeno(1,2,3-*cd*)pyrene at the sites Pomeranian Bight, Bornholm Sea, Central Baltic Sea, Eastern Gotland Sea (North, South) and the Western Gotland Sea concentrations were found, which exceeded the AA-EQS. For the most carcinogenic PAH compound benzp(*a*)pyrene the AA-EQS was exceeded at the Pomeranian Bight station. Thus, at those sites negative effects to aquatic organisms might derive from PAH contamination.

Nonetheless, even if EQS values are *per se* not exceeded, concentrations of indeno(1,2,3-*cd*)pyrene and benzo(*g,h,i*)perylene in the Arkona Sea are close to the AA-EQS. In view of the fact that this area is located in the open Baltic Sea, where regular dilution is expected, those concentrations yet might be considered as of concern for marine organisms, too.

Table 15: Determined concentrations of selected contaminants in surface water of the Baltic Sea in winter 2019 in relation to the EQS of the Water Framework Directive. red values: exceeded EQS.

Substance	Other Surface waters AA-EQS	Other Surface waters MAC-EQS	Kiel Bight/ Fehmarn-Belt (T1)	Mecklenburg Bight (T2)	Arkona Sea (T3)	Pomeranian Bight (T4)	Bornholm Sea (T5)	Central Baltic Sea (T6)	Eastern Gotland Sea (South) (T7)	Eastern Gotland Sea (North) (T8)	Western Gotland Sea (T9)
	µg/L[1]		µg/L[1]								
ΣDDT$_{sum}$	0.025	-	0.000007	0.000007	0.000006	0.000016	0.000005	0.000005	0.000003	0.000003	0.000003
p,p'-DDT$_{sum}$	0.01	-	0.000001	0.000002	0.000001	0.000002	0.000001	0.000001	0.000001	0.000001	0.000001
HCB$_{sum}$	-	0.05	0.000007	0.000007	0.000007	0.000008	0.000007	0.000006	0.000006	0.000008	0.000007
ANT$_{sum}$	0.1	0.1	0.00004	0.00004	0.00005	0.00010	0.00004	0.00004	0.00004	0.00003	0.00003
FLU$_{sum}$	0.0063	0.12	0.0012	0.0014	0.0019	0.0027	0.0016	0.0022	0.0015	0.0016	0.0010
BBF$_{sum}$	0.00017	0.017	0.00014	0.00015	0.00023	0.00033	0.00039	0.00036	0.00031	0.00029	0.00020
BKF$_{sum}$	0.00017	0.017	0.00005	0.00006	0.00009	0.00013	0.00014	0.00014	0.00012	0.00010	0.00008
BAP$_{sum}$	0.00017	0.027	0.00006	0.00004	0.00008	0.00023	0.00013	0.00014	0.00012	0.00009	0.00006
BGHIP$_{sum}$	0.00017	0.0082	0.00011	0.00009	0.00017	0.00029	0.00027	0.00022	0.00021	0.00013	0.00011
ICDP$_{sum}$	0.00017	-	0.00012	0.00010	0.00015	0.00030	0.00024	0.00024	0.00020	0.00013	0.00010

AA-EQS: annual average value, MAC-EQS: maximum allowable concentration, [1]Total concentration in water sample

Summary

For the southern Baltic Sea area, the Warnemünde station recorded in the winter 2018/2019 a With a “cold sum” of the air temperature of 18.3 Kd at the Warnemünde station, the winter 2018/2019 was a mild one. The summer “heat sum” of 283.1 Kd reflects a summer colder than the last year’s record of 394.5 Kd, but warmer than the long-term average 158.6 +/- 68.9 Kd.

The situation in the deep basins of the Baltic Sea was mainly characterized by stagnation and widespread hypoxic to euxinic areas. The baroclinic inflows of the record summer 2018 reached the deep-water of the central Baltic Sea and caused record high 8.6 °C at the bottom of the Gotland Deep. Additional inflow pulses of warm water arrived in March and April 2019. Three smaller barotropic inflows occurred from autumn 2018 to December /January 2019 and imported 3 Gt of salt into the western Baltic Sea. Four more barotropic inflows of weak intensity occurred in April, June, September and December. The last one imported 1 Gt of salt. These events propagated from the Arkona Basin up to southern parts of the eastern Gotland Basin. The bottom salinity values still were on the high level caused by the several Major Baltic Inflows in the time span 2014-2016, so that the 2019 events of weak intensity could not ventilate the bottom near water body in the central basins.

The positive influence of the Major Baltic Inflow of December 2014 on the oxygen situation in the deep basins of the eastern Gotland and less pronounced to the western Gotland Sea basins faded away. Anoxic and euxinic conditions in the deep waters intensified in 2019. This determined also the nutrient situation in the deep water of the northern and western Gotland Basin. In the eastern Gotland Sea, phosphate and ammonium concentrations were increasing since 2017. In 2019, oxygen was zero in all deep water reference depths. An exception reflected the intermittently re-oxygenated Bornholm Sea deep water with about 3 ml/l oxygen in March, leading to an annual average of about 1.0 ml/l oxygen, thus, showing a clearly increased nitrate concentration to 6.8 µmol/l in 2019, a relatively low ammonium concentration of 1.5 µmol/l, and an annual average phosphate concentration of about 3.8 µmol/l. The thalweg transects revealed a weak change at the depth range of the pycnocline: waters were entrained with some oxygen, considerable nitrate concentration and moderate phosphate values that were preformed in the Bornholm Sea and subsequently spread between 80 and 120 m through the eastern Gotland Sea.

Referring to the contaminants, the determined concentrations for CHC and U.S. EPA PAH depict high contaminant pressure for the areas Kiel Bight/Fehmarn Belt and the Pomeranian Bight, which indicates higher contaminant sources at these sites.

None of the 2019 results exceeded defined maximum allowable concentration EQS (MAC-EQS). However, a number of high molecular weight PAH compounds, exceeded the annual average EQS (AA-EQS) values at the sites Pomeranian Bight, Bornholm Sea, Central Baltic Sea, Eastern Gotland Sea (North, South) and the western Gotland Sea; for the most carcinogenic PAH compound benzp(*a*)pyrene the AA-EQS was exceeded at the Pomeranian Bight. At these sites negative effects to aquatic organisms might derive from PAH contamination.

Acknowledgements

The authors would like to thank the staff from the Leibniz Institute for Baltic Sea Research Warnemünde, who carried out measurements as part of the HELCOM's Baltic Sea monitoring programme and the IOW's long-term measuring programme, and the captain and crew of the research vessel *Elisabeth Mann Borgese* for their effort and support during monitoring cruises in 2019. The authors are also grateful to a number of other people and organisations for help: Sandra Schwegmann and Jürgen Holfort of the Sea Ice Service at the Federal Maritime and Hydrographic Agency, Hamburg and Rostock for advice in the description of the ice winter, and especially for supplying the ice cover chart; the Deutscher Wetterdienst for supplying wind data from Arkona from its online data portal; Hannah Lutterbeck from LLUR for providing the local assessment of oxygen deficiency at the coast of Schleswig-Holstein during late summer, the Swedish Meteorological and Hydrological Institute, Norrköpping, for providing gauge data from its online data portal; Lotta Fyrberg from SMHI's Oceanographic Laboratory in Gothenburg for providing us with hydrographic and hydrochemical observations from Sweden's Ocean Archive (SHARK) relating to selected stations within the Swedish national monitoring programme; the Maritime Office of the Polish Institute of Meteorology and Water Management (IMGW) in Gdynia provided observational data from the Danzig Deep; Barbara Bogdańska, IMGW in Warsaw, provided data on solar radiation at Gdynia.

References

ARNEBORG, L., FIEKAS, V., UMLAUF, L., BURCHARD, H., 2007: Gravity current dynamics and entrainment. A process study based on observations in the Arkona Basin. J. Phys. Oceangr. 37, 2094-2113.

BSH, 2009: Flächenbezogene Eisvolumensumme. http://www.bsh.de/de/Meeresdaten/Beobachtungen/Eis/Kuesten.jsp

BSH, 2019: Wasserstandsvorhersage Ostsee. https://www.bsh.de/DE/DATEN/Wasserstand_Ostsee/wasserstand_ostsee_node.html

BURCHARD, H., JANSSEN, F., BOLDING, K., UMLAUF, L, RENNAU, H., 2009: Model simulations of dense bottom currents in the Western Baltic Sea. Cont. Shelf Res. 29, 205-220.

DIAZ, R.J., ROSENBERG, R., 2008: Spreading dead zones and consequences for marine ecosystems. Science 321 (5891), 926-929.

DUARTE, C.M., CONLEY, D.J., CARSTENSEN, J., SÁNCHEZ-CAMACHO, M., 2009: Return to Neverland: Shifting baselines affect eutrophication restoration targets. Estuaries and Coasts 32 (1), 29-36.

DWD, 2019: Monatlicher Klimastatus, Nr. 1 – 12. Deutscher Wetterdienst. https://www.dwd.de/DE/derdwd/bibliothek/fachpublikationen/selbstverlag/selbstverlag_node.html

DWD, 2020a: Windmessungen der Station Arkona in Stundenmittelwerten des Jahres 2019. ftp://ftp-cdc.dwd.de/pub/CDC/observations_germany/climate/

DWD, 2020b: Langzeitdaten von Windmessungen der Station Arkona in Tagesmittelwerten. ftp://ftp-cdc.dwd.de/pub/CDC/observations_germany/climate/daily/kl/historical/

EC, 2000: Directive 2000/60/EC of the European Parliament and of the Council of 23 October 2000 establishing a framework for Community action in the field of water policy.

EC, 2008a: Directive 2008/56/EC of the European Parliament and of the Council of 17 June 2008 establishing a framework for Community action in the field of marine environmental policy (Marine Strategy Framework Directive).

EC, 2008b: Directive 2008/105/EC of the European Parliament and the Council of 16 December 2008 on environmental quality standards in the field of water policy.

EC, 2013: Directive 2013/39/EU of the European Parliament and of the Council of 12 August 2013 amending Directives 2000/60/EC and 2008/105/EC as regards priority substances in the field of water policy.

FEISTEL, R. SEIFERT, T., FEISTEL, S., NAUSCH, G., BOGDANSKA, B., BROMAN, B., HANSEN, L., HOLFORT, J., MOHRHOLZ, V., SCHMAGER, G., HAGEN, E., PERLET, I., WASMUND, N., 2008: Digital supplement. In: FEISTEL, R., NAUSCH, G. WASMUND, N. (eds.): State and evolution of the Baltic Sea 1952-2005. John Wiley & Sons, Inc., Hoboken, New Jersey, pp. 625-667.

FU-BERLIN, 2020: Weather maps. Werden auch Sie Wetterpate! http://www.met.fu-berlin.de/wetterpate/

GAUSS, M., NYIRI, A., KLEIN, H., JALKANEN, J.P., 2020: Estimation of country-wise reductions of atmospheric nitrogen deposition, achievable by 2030 through implementation of the Gothenburg Protocol / EU-NEC Directive. Technical Report EMEP MSC-W, Report for HELCOM ENIRED II, Oslo, 35pp.

GRASSHOFF, K., ERHARDT, M., KREMLING, K., 1983: Methods of seawater analysis. 2nd ed., Verlag Chemie, Weinheim.

GRÄWE, U., NAUMANN, M., MOHRHOLZ, V., BURCHARD, H., 2015: Anatomizing one of the largest saltwater inflows in the Baltic Sea in December 2014. J. Geophys. Res. 120, 7676-7697.

HAGEN, E., FEISTEL, R., 2008: Baltic climate change. In: FEISTEL, R., NAUSCH, G., WASMUND, N. (eds.), State and evolution of the Baltic Sea 1952 – 2005. John Wiley & Sons, Inc., Hoboken, New Jersey, pp. 93-120.

HELCOM, 2000: Manual of marine monitoring in the COMBINE programme of HELCOM. Baltic Marine Environment Protection Commission, Helsinki, Updated 2002: www.helcom.fi/Monas/CombineManual2/CombineHome.htm

HELCOM, 2010a: Ecosystem health of the Baltic Sea 2003–2007. Balt. Sea Environ. Proc. 122, pp. 13–14.

HELCOM, 2010b: Hazardous substances in the Baltic Sea - An integrated thematic assessment of hazardous substances in the Baltic Sea. Balt. Sea Environ. Proc. 120B.

HELCOM, 2013: Approaches and methods for eutrophication target setting in the Baltic Sea region. Helsinki Commission, Helsinki, Finland.

HELCOM, 2015: Updated Baltic Sea pollution load compilation (PLC 5.5). Balt. Sea Environ. Proc. 145, pp. 1-143. www.helcom.fi/Lists/Publications/BSEP145_lowres.pdf

HELCOM, 2018a: State of the Baltic Sea - Second HELCOM holistic assessment 2011-2016. Balt. Sea Environ. Proc. 155. Helsinki, Finland. http://stateofthebalticsea.helcom.fi

HELCOM, 2018b: Sources and pathways of nutrients to the Baltic Sea - HELCOM PLC-6. Helsinki, Finland. www.helcom.fi/Lists/Publications/BSEP143.pdf

IMGW, 2020: Solar radiation in J/m² at the station Gdynia 2019 – unpublished data

JACOBSEN, T.S., 1980. Sea water exchange of the Baltic. Measurements and methods. The Belt Project. The National Agency for Environmental Protection, Denmark: p107

KATSOYIANNIS, A., BREIVIK, K., 2014: Model-based evaluation of the use of polycyclic aromatic hydrocarbons molecular diagnostic ratios as a source identification tool. Environmental Pollution, 184, pp. 488-494. doi: 10.1016/j.envpol.2013.09.028.

KEITH, L.H., 2015: The source of U.S. EPA's sixteen PAH priority pollutants, polycyclic aromatic compounds. Taylor & Francis, 35 (2–4), pp. 147–160. doi: 10.1080/10406638.2014.892886.

KOSLOWSKI, G., 1989: Die flächenbezogene Eisvolumensumme, eine neue Maßzahl für die Bewertung des Eiswinters an der Ostseeküste Schleswig-Holsteins und ihr

Zusammenhang mit dem Charakter des meteorologischen Winters. Dt. Hydrogr. Z. 42, 61-80.

KRÜGER, S., 2000: Basic shipboard instrumentation and fixed autonomic stations for monitoring in the Baltic Sea. In: EL-HAWARY, F. (ed.): The ocean engineering handbook. CRC Press, Boca Raton, USA, pp. 52-61.

KRÜGER, S., ROEDER, W., WLOST, K.-P., KOCH, M., KÄMMERER, H., KNUTZ, T., 1998: Autonomous instrumentation carrier (APIC) with acoustic transmission for shallow water profiling. Oceanology International 98: The Global Ocean Conf. Proc. 2, 149-158.

KUSS, J., 2019: Cruise report – EMB 218: Baltic Sea long-term observation programme, Leibniz Institute for Baltic Sea Research, Warnemünde, Germany.

LASS, H.U., MATTHÄUS, W. 2008: General oceanography of the Baltic Sea. In: FEISTEL, R., NAUSCH, G., WASMUND, N. (eds.): State and evolution of the Baltic Sea 1952 – 2005. John Wiley & Sons, Inc., Hoboken, New Jersey, pp. 5-43.

LASS, H.U., MOHRHOLZ, V., SEIFERT, T., 2001: On the dynamics of the Pomeranian Bight. Cont. Shelf. Res. 21, 1237-1261.

LISITZIN, E., 1974: Sea-level changes. Elsevier Oceanography Series, Vol. 8, Amsterdam: p286

LLUR, 2018: Sauerstoffmangel im bodennahen Wasser der westlichen Ostsee 2018. https://www.schleswig-holstein.de/DE/Fachinhalte/M/meeresschutz/chemMonitoring.html

LLUR, 2019: Sauerstoffmangel im bodennahen Wasser der westlichen Ostsee. https://www.schleswig-holstein.de/DE/Fachinhalte/M/meeresschutz/chemMonitoring.html: 7.

MATTHÄUS, W., 2006: The history of investigation of salt water inflows into the Baltic Sea - from the early beginning to recent results. Marine Science Reports, 65, 73 p.

MATTHÄUS W., FRANCK, H., 1992: Characteristics of major Baltic inflows - a statistical analysis. Cont. Shelf Res., 12, 1375-1400.

MOHRHOLZ, V., 1998: Transport- und Vermischungsprozesse in der Pommerschen Bucht. Meereswiss. Ber. Warnemünde 33, 1-106.

MOHRHOLZ, V., 2018: Major Baltic inflow statistics – reviewed. Front. Mar. Sci. 5, 384. doi: 10.3389/fmars.2018.00384

MOHRHOLZ, V., NAUMANN, M., NAUSCH, G., KRÜGER, S., GRÄWE, U., 2015: Fresh oxygen for the Baltic Sea – an exceptional saline inflow after a decade of stagnation. Journal Mar. Syst. 148, 152-166.

NAUMANN, M., UMLAUF, L., MOHRHOLZ, V., KUSS, J., SIEGEL, H., WANIEK, J.J., SCHULZ-BULL, D.E., 2018: Hydrographic-hydrochemical assessment of the Baltic Sea 2017, Meereswiss. Ber. Warnemünde 107, 97 pp. doi:10.12754/msr-2018-0107

NAUMANN, M.; GRÄWE, U.; MOHRHOLZ, V.; KUSS, J.; SIEGEL, H.; WANIEK, J.J., SCHULZ-BULL, D.E., 2019: Hydrographic-hydrochemical assessment of the Baltic Sea 2018. Meereswiss. Ber. Warnemünde 110, 90 pp. doi:10.12754/msr-2019-0110

NAUSCH, G., BACHOR, A., PETENATI, T., VOSS, J., V. WEBER, M., 2011b: Nährstoffe in den deutschen Küstengewässern der Ostsee und angrenzenden Seegebieten. Meeresumwelt Aktuell Nord- und Ostsee 2011/1.

NAUSCH, G., FEISTEL, R., LASS, H.-U., NAGEL, K., SIEGEL, H., 2002: Hydrographisch-chemische Zustandseinschätzung der Ostsee 2001. Meereswiss. Ber. Warnemünde 49, 3-77.

NAUSCH, G., FEISTEL, R., UMLAUF, L., MOHRHOLZ, V., SIEGEL, H., 2011a: Hydrographisch-chemische Zustandseinschätzung der Ostsee 2010. Meereswiss. Ber. Warnemünde 84, 1-99.

NAUSCH, G., NAUMANN, M., UMLAUF, L., MOHRHOLZ, V., SIEGEL,H., 2014: Hydrographisch-hydrochemische Zustandseinschätzung der Ostsee 2013. Meereswiss. Ber. Warnemünde 93, 1-104.

NAUSCH, G., NEHRING, D., 1996: Baltic proper, hydrochemistry. In: HELCOM (ed.): Third periodic assessment of the state of the marine environment of the Baltic Sea. Balt. Sea Environ. Proc. 64B, 80-85.

NAUSCH, G., NEHRING, D., NAGEL, K., 2008: Nutrient concentrations, trends and their relation to eutrophication. In: FEISTEL, R., NAUSCH, G., WASMUND, N. (eds.): State and evolution of the Baltic Sea, 1952-2005. John Wiley & Sons, Inc. Hoboken, New Jersey, 337-366.

NEHRING, D., MATTHÄUS, W., 1991: Current trends in hydrographic and chemical parameters and eutrophication in the Baltic Sea. Int. Revue ges. Hydrobiol. 76, 297-316.

NEHRING, D., MATTHÄUS, W., LASS, H.U., 1993: Die hydrographisch-chemischen Bedingungen in der westlichen und zentralen Ostsee im Jahre 1992. Dt. Hydrogr. Z. 45, 281-331.

NEHRING, D., MATTHÄUS, W., LASS, H.U., NAUSCH, G., NAGEL, K., 1995: Hydrographisch-chemische Zustandseinschätzung der Ostsee 1994. Meereswiss. Ber. Warnemünde 9, 1-71.

REDFIELD, A.C., KETCHUM, B.H., RICHARDS, F.A., 1963: The influence of organisms on the composition of sea water. In: HILL, M.N. (ed.): The sea. J. Wiley & Sons, pp. 26-77.

REYNOLDS, R. W., SMITH, T.M., LIU, C., CHELTON, D.B., CASEY, K.S., SCHLAX, M.G., 2007: Daily high-resolution-blended analyses for sea surface temperature. J. Clim. 20, 5473–5496.

SCHLITZER, R., 2018: OCEAN DATA VIEW 5, ODV5 RELEASE 5.1.7 (WINDOWS 64BIT) OCT. 2018. AWI-BREMERHAVEN, 2018.

SCHULZ-BULL, D., HAND, I., LERZ, A., SCHNEIDER, R., TROST, E., WODARG, D., 2011: Regionale Verteilung chlorierter Kohlenwasserstoffe (CKW) und polycyclischer aromatischer Kohlenwasserstoffe (PAK) im Pelagial und Oberflächensediment in der deutschen ausschließlichen Wirtschaftszone (AWZ) im Jahr 2010. Leibniz-Institut für Ostseeforschung an der Universität Rostock im Auftrag des Bundesamtes für Seeschifffahrt und Hydrographie Hamburg, Rostock Warnemünde.

SCHWEGMANN, S., HOLFORT, J., 2016: Der Eiswinter 2015/16 an den deutschen Nord- und Ostseeküsten mit einem Überblick über die Eisverhältnisse im gesamten Ostseeraum.

Eisdienst, Bundesamt für Seeschifffahrt und Hydrographie Rostock, 17 S. http://www.bsh.de/de/Meeresdaten/Beobachtungen/Eis/Eiswinter2015-2016.pdf

SCHWEGMANN, S., HOLFORT, J., 2017: Der Eiswinter 2016/17 an den deutschen Nord- und Ostseeküsten mit einem Überblick über die Eisverhältnisse im gesamten Ostseeraum. Eisdienst, Bundesamt für Seeschifffahrt und Hydrographie Rostock, 17 S. http://www.bsh.de/de/Meeresdaten/Beobachtungen/Eis/Eiswinter2016-2017.pdf

SCHWEGMANN, S., HOLFORT, J., 2018: Der Eiswinter 2017/18 an den deutschen Nord- und Ostseeküsten mit einem Überblick über die Eisverhältnisse im gesamten Ostseeraum. Eisdienst, Bundesamt für Seeschifffahrt und Hydrographie Rostock, 18 S.

SCHWEGMANN, S., HOLFORT, J., 2019: Der Eiswinter 2018/19 an den deutschen Nord- und Ostseeküsten mit einem Überblick über die Eisverhältnisse im gesamten Ostseeraum. Eisdienst, Bundesamt für Seeschifffahrt und Hydrographie Rostock, 18 S.

SELLSCHOPP, J., ARNEBORG, L., KNOLL, M., FIEKAS, V., GERDES, F., BURCHARD, H., LASS, H. U., MOHRHOLZ, V., UMLAUF, L., 2006: Direct observations of a medium-intensity inflow into the Baltic. Sea. Cont. Shelf Res. 26, 2393-2414.

SIEGEL, H., GERTH, M., SCHMIDT, T., 1996: Water exchange in the Pomeranian Bight – investigated by satellite data and shipborne measurements. Cont. Shelf Res 16, 1793-1817.

SMHI, 2020a: Tide gauge data at station Landort Norra in hourly means of the year 2019; geodesic reference level RH2000. http://opendata-download-ocobs.smhi.se/explore/

SMHI, 2020b: Accumulated inflow through the Öresund 2014-2019. http://www.smhi.se/hfa_coord/BOOS/Oresund.html

STRANDBERG, B., VAN BAVEL, B., BERGQVIST, P.-A., BROMAN, D., ISHAQ, R., NÄF, C., PETTERSEN, H., RAPPE, C., 1998: Occurrence, sedimentation, and spatial variations of organochlorine contaminants in settling particulate matter and sediments in the northern part of the Baltic Sea. Environmental Science & Technology. American Chemical Society 32 (12), pp. 1754–1759. doi: 10.1021/es970789m.

TRUMP, 1998: Transport- und Umsatzprozesse in der Pommerschen Bucht (TRUMP) 1994-1996. Abschlussbericht, Warnemünde, 1-32 (unveröffentlicht).

UMLAUF, L., ARNEBORG, L., 2009a: Dynamics of rotating shallow gravity currents passing through a channel. Part I: Observation of transverse structure. J. Phys. Oceanogr. 39, 2385-2401.

UMLAUF, L., ARNEBORG, L., 2009b: Dynamics of rotating shallow gravity currents passing through a channel. Part II: Analysis. J. Phys. Oceanogr. 39, 2402-2416.

UMLAUF, L., ARNEBORG, L., BURCHARD, H., FIEKAS, V., LASS, H.-U., MOHRHOLZ, V., PRANDKE, H., 2007: The transverse structure of turbulence in a rotating gravity current. Geophys. Res. Lett. 34, L08601, doi:10.1029/2007GL029521.

UMLAUF, L., ARNEBORG, L., HOFMEISTER, R., BURCHARD, H., 2010: Entrainment in shallow rotating gravity currents: A modeling study. J. Phys. Oceanogr. 40, 1819-1834.

V.BODUNGEN, B., GRAEVE, M., KUBE, J., LASS, H.U., MEYER-HARMS, B., MUMM, N., NAGEL, K., POLLEHNE, F., POWILLEIT, M., RECKERMANN, M., SATTLER, C., SIEGEL, H., WODARG, D., 1995: Stoff-Flüsse am

Grenzfluss – Transport- und Umsatzprozesse im Übergangsgebiet zwischen Oderästuar und Pommerscher Bucht (TRUMP). Geowiss. 13, 479-485.

WEBSTER, L., ROOSE, P., BERSUDER, P., KOTTERMAN, M., HAARICH, M., VORKAMP, K., 2013: Determination of polychlorinated biphenyls (PCBs) in sediment and biota. ICES Techniques in Marine Environmental Sciences 53, 18 pp.

YUNKER, M. B., MACDONALD, R.W., VINGARZAN, R., MITCHELL, R., GOYETTE, D., SYLVESTRE, S., 2002: PAHs in the Fraser River basin: A critical appraisal of PAH ratios as indicators of PAH source and composition. Organic Geochemistry 33 (4), 489–515. doi: 10.1016/S0146-6380(02)00002-5.

Appendix
Organic hazardous substances

App. Table 1: Concentrations of DDT and metabolites in the Baltic surface water in winter 2019.

Dissolved	Transect	DDE-*p,p'*	DDD-*p,p'*	DDT-*o,p'*	DDT-*p,p'*	Σ DDT_{diss}
		pg/L				
Kiel Bight/ Fehmarnbelt	T1	1.88	1.40	0.37	0.84	4.49
Mecklenburg Bight	T2	2.14	1.07	0.50	1.15	4.85
Arkona Sea	T3	1.94	1.07	0.41	1.00	4.43
Pomeranian Bight	T4	3.16	2.11	0.41	0.69	6.38
Bornholm Sea	T5	1.58	1.00	0.29	0.75	3.62
Central Baltic Sea	T6	1.63	1.17	0.30	0.83	3.92
Eastern Gotland Sea (South)	T7	1.17	0.94	0.19	0.59	2.89
Eastern Gotland Sea (North)	T8	1.14	1.18	0.26	0.62	3.19
Western Gotland Sea	T9	0.97	0.93	0.20	0.47	2.56

Particulate	Transect	DDE-*p,p'*	DDD-*p,p'*	DDT-*o,p'*	DDT-*p,p'*	Σ DDT_{part}
		pg/L				
Kiel Bight/ Fehmarnbelt	T1	1.22	0.34	0.16	0.38	2.11
Mecklenburg Bight	T2	1.14	0.21	0.21	0.46	2.01
Arkona Sea	T3	0.77	0.15	0.19	0.32	1.43
Pomeranian Bight	T4	5.33	1.85	0.60	1.19	8.97
Bornholm Sea	T5	0.45	0.07	0.08	0.18	0.78
Central Baltic Sea	T6	0.35	0.09	0.08	0.15	0.68
Eastern Gotland Sea (South)	T7	0.24	0.07	0.04	0.08	0.43
Eastern Gotland Sea (North)	T8	0.14	0.02	0.03	0.04	0.22
Western Gotland Sea	T9	0.16	0.02	0.03	0.04	0.25

Sum (dissolved + particulate)	Transect	DDE-*p,p'*	DDD-*p,p'*	DDT-*o,p'*	DDT-*p,p'*	Σ DDT_{sum}
		pg/L				
Kiel Bight/ Fehmarnbelt	T1	3.09	1.75	0.53	1.22	6.60
Mecklenburg Bight	T2	3.29	1.27	0.71	1.60	6.87
Arkona Sea	T3	2.71	1.22	0.60	1.32	5.85
Pomeranian Bight	T4	8.49	3.96	1.01	1.88	15.35
Bornholm Sea	T5	2.02	1.07	0.37	0.93	4.40
Central Baltic Sea	T6	1.99	1.26	0.38	0.98	4.61
Eastern Gotland Sea (South)	T7	1.40	1.02	0.24	0.67	3.33
Eastern Gotland Sea (North)	T8	1.28	1.19	0.29	0.66	3.41
Western Gotland Sea	T9	1.13	0.95	0.23	0.50	2.81

App. Table 2: Concentrations of HCB and PCBICES in surface waters of the Baltic Sea in winter 2019.

Dissolved	Transect	HCB	PCB 28/31	PCB 52	PCB 101	PCB 118	PCB 153	PCB 138	PCB 180	ΣPCB_{diss}
						pg/L				
Kiel Bight/ Fehmarnbelt	T1	6.71	1.04	0.59	0.54	0.35	0.53	0.40	0.10	3.56
Mecklenburg Bight	T2	6.69	0.91	0.46	0.38	0.25	0.39	0.30	0.08	2.76
Arkona Sea	T3	6.96	0.97	0.42	0.31	0.25	0.30	0.25	0.07	2.56
Pomeranian Bight	T4	5.88	0.94	0.42	0.38	0.27	0.46	0.31	0.10	2.89
Bornholm Sea	T5	6.77	1.03	0.37	0.24	0.22	0.20	0.15	0.05	2.26
Central Baltic Sea	T6	5.96	0.98	0.35	0.23	0.25	0.20	0.18	0.06	2.24
Eastern Gotland Sea (South)	T7	6.30	0.84	0.32	0.20	0.26	0.17	0.15	0.05	2.00
Eastern Gotland Sea (North)	T8	7.89	0.99	0.38	0.25	0.26	0.21	0.18	0.06	2.32
Western Gotland Sea	T9	6.47	1.01	0.34	0.22	0.22	0.18	0.15	0.05	2.18

Particulate	Transect	HCB	PCB 28/31	PCB 52	PCB 101	PCB 118	PCB 153	PCB 138	PCB 180	ΣPCB_{part}
						pg/L				
Kiel Bight/ Fehmarnbelt	T1	0.46	0.14	0.10	0.34	0.26	0.94	0.60	0.28	2.67
Mecklenburg Bight	T2	0.33	0.09	0.05	0.15	0.14	0.44	0.27	0.15	1.28
Arkona Sea	T3	0.34	0.08	0.05	0.09	0.09	0.24	0.18	0.11	0.83
Pomeranian Bight	T4	1.64	0.39	0.15	0.49	0.49	1.86	1.28	1.05	5.72
Bornholm Sea	T5	0.21	0.04	0.03	0.04	0.06	0.11	0.09	0.06	0.43
Central Baltic Sea	T6	0.17	0.03	0.02	0.03	0.06	0.09	0.09	0.06	0.37
Eastern Gotland Sea (South)	T7	0.15	0.02	0.02	0.03	0.04	0.07	0.07	0.06	0.32
Eastern Gotland Sea (North)	T8	0.10	0.01	0.02	0.02	0.04	0.06	0.06	0.05	0.27
Western Gotland Sea	T9	0.12	0.02	0.02	0.03	0.04	0.08	0.06	0.05	0.30

App. Table 2 *continued*

Sum (dissolved+ particulate)	Transect	HCB	PCB 28/31	PCB 52	PCB 101	PCB 118	PCB 153	PCB 138	PCB 180	ΣPCB_{sum}
						pg/L				
Kiel Bight/ Fehmarnbelt	T1	7.17	1.18	0.69	0.88	0.61	1.47	1.00	0.38	6.22
Mecklenburg Bight	T2	7.02	1.00	0.51	0.52	0.39	0.83	0.57	0.23	4.04
Arkona Sea	T3	7.30	1.04	0.47	0.40	0.34	0.54	0.43	0.18	3.40
Pomeranian Bight	T4	7.52	1.34	0.57	0.87	0.77	2.33	1.59	1.15	8.61
Bornholm Sea	T5	6.97	1.07	0.40	0.29	0.27	0.31	0.25	0.11	2.69
Central Baltic Sea	T6	6.13	1.00	0.38	0.27	0.30	0.29	0.26	0.12	2.62
Eastern Gotland Sea (South)	T7	6.45	0.86	0.34	0.23	0.31	0.25	0.23	0.10	2.31
Eastern Gotland Sea (North)	T8	7.99	1.00	0.40	0.27	0.30	0.27	0.24	0.11	2.60
Western Gotland Sea	T9	6.59	1.03	0.36	0.25	0.26	0.26	0.22	0.10	2.48

App. Table 3: Concentrations of dissolved and particulate PAH in Baltic Sea surface water in winter 2019.

Dissolved	Transect	ACNLE	ACNE	FLE	ANT	PA	FLU	PYR	BAA	CHR	BBF	BKF	BAP	DBAHA	ICDP	BGHIP	ΣPAH$_{diss}$
										pg/L							
Kiel Bight/ Fehmarnbelt	T1	224	175	2099	37	2953	1134	395	22	97	29	15	3.7	1.4	5.3	4.8	7197
Mecklenburg Bight	T2	114	142	1710	39	1264	1354	495	40	163	43	18	6.2	1.5	6.1	5.6	5400
Arkona Sea	T3	113	146	1965	43	1396	1821	621	71	290	91	32	16	2.6	12	10	6628
Pomeranian Bight	T4	640	278	3906	56	3702	2137	746	21	101	14	8	3.1	0.7	3.3	3.3	11620
Bornholm Sea	T5	80	108	1542	40	1218	1566	864	157	459	191	70	37	6.7	23	22	6384
Central Baltic Sea	T6	167	132	2136	42	1989	2142	865	150	444	199	68	39	7.4	23	23	8424
Eastern Gotland Sea (South)	T7	84	90	1289	40	1114	1452	669	126	366	173	67	40	7.4	26	26	5569
Eastern Gotland Sea (North)	T8	65	107	1209	26	1209	1274	621	102	333	206	59	37	6.5	26	25	5303
Western Gotland Sea	T9	43	79	919	25	857	947	473	83	272	117	50	22	4.2	15	14	3920

App. Table 3 *continued*

Particulate	Transect	ACNLE	ACNE	FLE	ANT	PA	FLU	PYR	BAA	CHR	BBF	BKF	BAP	DBAHA	ICDP	BGHIP	ΣPAH_{part}
										pg/L							
Kiel Bight/ Fehmarnbelt	T1	5.5	4.2	16	5.0	79	89	92	34	50	106	40	53	16	114	105	809
Mecklenburg Bight	T2	2.6	3.2	8.7	2.9	31	69	45	26	54	111	40	35	13	93	86	622
Arkona Sea	T3	4.8	1.1	8.1	2.9	37	67	48	35	67	135	55	64	19	134	151	828
Pomeranian Bight	T4	19	80	143	45	388	557	356	150	220	320	125	227	46	294	289	3260
Bornholm Sea	T5	7.4	0.6	6.6	4.4	39	71	64	50	71	203	68	89	29	215	248	1166
Central Baltic Sea	T6	6.1	1.0	7.4	4.2	40	74	59	40	65	161	69	96	27	212	199	1061
Eastern Gotland Sea (South)	T7	6.0	1.0	6.8	3.6	34	55	51	35	52	133	53	75	18	164	184	871
Eastern Gotland Sea (North)	T8	3.9	0.4	3.2	2.3	23	40	33	23	34	80	41	50	17	107	106	564
Western Gotland Sea	T9	3.0	0.3	2.7	1.5	19	29	24	16	27	85	29	36	11	80	95	457

App. Table 3 *continued*

Sum (particulate + dissolved)	Transect	ACNLE	ACNE	FLE	ANT	PA	FLU	PYR	BAA	CHR	BBF	BKF	BAP	DBAHA	ICDP	BGHIP	ΣPAH_{sum}
										pg/L							
Kiel Bight/ Fehmarnbelt	T1	230	179	2115	42	3032	1224	487	55	147	136	55	57	18	119	109	8006
Mecklenburg Bight	T2	117	145	1719	42	1294	1423	540	66	217	154	58	41	15	99	92	6022
Arkona Sea	T3	118	147	1973	46	1432	1888	669	106	357	226	87	80	21	146	161	7456
Pomeranian Bight	T4	658	358	4050	101	4091	2695	1102	171	321	334	133	230	46	297	292	14880
Bornholm Sea	T5	88	109	1549	45	1257	1637	928	207	530	394	138	126	36	238	270	7550
Central Baltic Sea	T6	173	133	2144	46	2029	2216	923	190	509	360	136	135	35	235	222	9486
Eastern Gotland Sea (South)	T7	90	91	1296	44	1148	1507	720	162	418	306	120	115	26	190	210	6440
Eastern Gotland Sea (North)	T8	68	107	1213	28	1232	1314	654	125	367	286	100	86	23	133	131	5868
Western Gotland Sea	T9	46	79	922	26	876	976	496	99	298	202	79	59	15	95	110	4377

Naumann, M., Gräwe, U.,
Mohrholz, V., Kuss, J., Kanwischer, M.,
Feistel, S., Hand, I., Waniek, J.J.,
Schulz-Bull, D.E.:
Hydrographic-hydrochemical assessment of the Baltic Sea 2019

CONTENT

Leibniz-Institut für Ostseeforschung Warnemünde
IOW